Examination of stable oxygen isotope as a tree ring proxy of tropical ring-less trees

Wataru NAKAI

2019

Contents

General introduction

Tree rings have various information on the growing conditions. Tree rings, therefore, act as a proxy for climate such as temperature, precipitation, humidity, and so on. However, it is difficult to conduct tree ring research in tropical region because most tropical trees lack visible tree rings, or they form incomplete or irregular ring.

Some tree species in tropical region are reported to form visible growth rings despite poor seasonality in climate (Worbes 2002). It is, however, uncertain whether the rings are annual rings or not until they are confirmed to be formed annually by a certain method. Since tree species in tropical region form false rings (Bhattacharyya et al. 1992), it is necessary to confirm the observed ring-like structures are really annual rings. The process of annual ring detection needs two steps; (1) selecting indicators for annual ring, and (2) dating the indicators.

Growth dynamics of trees can be measured by monitoring radial growth or analyzing tree rings. Although radial growth of trees could be monitored in the same way by dendrometer band both in temperate and tropical region, the result could be used just for understanding seasonality of radial growth because the diameter change of trees contains the change of bark thickness and is not exact xylem growth. Moreover, the diameter prior to the start of monitoring could not be known and monitoring frequently is difficult if study sites are located at the remote place. On the other hand, tree ring analysis do not have such problems. However, as for trees without visible tree rings we have to detect tree rings before analysis, and we have to select appropriate tree ring indicator.

There are two types of tree ring indicator; visible indicator and invisible indicator. Visible indicators are wood anatomical features; for example, the change of size of wood fiber and thickness of cell wall, marginal parenchyma (Stahle et al. 1999; Abdul Azim and Okada 2014), the change of lumen area and density of vessels (Ohashi et al. 2014), and so on. Invisible indicators are elemental concentration such as calcium (Poussart et al. 2006), or stable carbon isotope ratio ($\delta^{13}C$) and oxygen isotope ratio ($\delta^{18}O$) (Poussart et al. 2004; Ohashi et al. 2009). Above all, $\delta^{18}O$ increasingly used as tree ring indicator. Since most of the tree ring indicators are formed by climatic stresses or specific to a certain species, these indicators are applicable to limited species or regions. On the other hand, since $\delta^{18}O$ in tree rings are controlled by source water , which is the water used for growing (McCarroll and Loader 2004), it could act as tree ring indicator for wide range of species.

Oxygen atoms of xylem cellulose come from source water. Precipitation is mixed with soil water and resulting source water is taken up by trees via roots. Source water becomes ^{18}O-enriched due to transpiration at leaf, and then is incorporated into carbohydrates by photosynthesis. Stable oxygen isotope ratio of leaf water at the evaporation site ($\delta^{18}O_e$) is expressed as follows:

$$\delta^{18}O_e = \delta^{18}O_s + \varepsilon^* + \varepsilon_k + (\delta^{18}O_v - \delta^{18}O_s - \varepsilon_k)e_a/e_i$$

where $\delta^{18}O_s$ is the stable oxygen isotope ratio of source water, ε^* is the fractionation factor related to liquid-vapor equilibrium, ε_k is the fractionation factor related to water diffusion through the stomata and leaf boundary layer, $\delta^{18}O_v$ is the stable oxygen isotope ratio of water vapor in the atmosphere, e_a

and e_i is the ambient and intercellular vapor pressures (McCarroll and Loader 2004). The values of ε^* and ε_k change depending on temperature. The leaf water become carbohydrates due to photosynthesis with +27‰ of fractionation, and carbohydrates become cellulose. When cellulose is synthesized from carbohydrates, part of oxygen atoms in carbohydrates exchange with xylem water. Assumed that the variations of ε^* and ε_k are negligible and $\delta^{18}O_v$ is in the isotopic equilibrium with $\delta^{18}O_s$ ($\delta^{18}O_v = \delta^{18}O_s - \varepsilon^*$), $\delta^{18}O$ of tree ring cellulose is mainly controlled by $\delta^{18}O_s$ and e_a/e_i, that is, $\delta^{18}O$ of precipitation and relative humidity. Since $\delta^{18}O$ of precipitation seasonally varies depending on various factors such as the amount of precipitation or the origin of water vapor (Ingraham 1998), the value probably varies even if the seasonality of temperature or precipitation is poor. If seasonal variation of precipitation $\delta^{18}O$ is successfully recorded in the xylem $\delta^{18}O$, seasonal variation of xylem $\delta^{18}O$ could be used as reliable tree ring indicator.

Intra-annual variation of $\delta^{18}O$ in tree rings has not been studied extensively yet. Most of the studies dealing with $\delta^{18}O$ in tree rings is focusing on the relationship between annual-ring $\delta^{18}O$ values and climatic factors such as precipitation and relative humidity (e.g. Nakatsuka et al. 2004; Liu et al. 2013; Johnstone et al. 2013; Colombaroli et al. 2016) or reconstruction of paleo climate (e.g. Sano et al. 2012; Bégin et al. 2015). Most of these studies are conducted in temperate region and case study in tropical region is insufficient, probably because lack of visible tree rings makes it difficult to identify when the xylem is formed. High resolution analysis, which means analysis of within-year $\delta^{18}O$ variation by subdividing each tree ring into small pieces, rarely conducted, probably because preparing a large number of samples is highly time- and labor-intensive work.

There are studies about intra-annual variation of $\delta^{18}O$ conducted in tropical region, and growth ring detection using seasonal variation of xylem $\delta^{18}O$ (e.g. Poussart and Schrag 2005; Pons and Helle 2011; Ohashi et al. 2016). However, $\delta^{18}O$ of precipitation in the same site as trees grew is not analyzed, and long year's mean of precipitation $\delta^{18}O$ collected in the closest GNIP (the Global Network of Isotopes in Precipitation) station is usually used. Moreover, if we analyze trees without visible tree rings, xylem $\delta^{18}O$ chronologies have to be dated with appropriate methods. Cambial marking with mechanical stimulation (Wolter 1968; Shiokura 1989) is usually used to study periodical xylem growth or growth amount in a certain period. However, if we use cambial marking, the sample trees need to be cut, and following research will be hampered. Radiocarbon dating method could point out when the xylem was formed, but the method does not have accuracy less than 1 year. Furthermore, cellulose, which is a single component in wood, is usually used when xylem $\delta^{18}O$ is analyzed but the extraction procedure is labor- and time-consuming especially when intra-annual variation of xylem $\delta^{18}O$ is studied because of the large number of subsamples.

Seasonal variation of $\delta^{18}O$ recorded in tree xylem is possibly used as a widely applicable tree ring proxy. However, to practically use the xylem $\delta^{18}O$ pattern as a tree ring proxy, several topics need to be studied. In this study, to test the applicability of xylem $\delta^{18}O$ pattern as a tree ring proxy, after the suitable preliminary treatment for xylem $\delta^{18}O$ analysis was examined, the following three topics are examined: (1) whether seasonal variation of source water $\delta^{18}O$ is recorded to xylem $\delta^{18}O$ of trees forms

visible growth rings, (2) the applicability of high voltage DC pulse cambial marking as a dating method, (3) applicability of growth ring detection for trees without visible growth rings using xylem $\delta^{18}O$ pattern. Finally, these topics are compared between seasonally dry forests and tropical rainforests.

In Chapter 1, the sample preparation method for isotope analysis was examined. The question addressed here is whether cellulose extraction is necessary or not for the annual ring detection in tropical ring-less trees. In Chapter 2, intra-annual variation of xylem $\delta^{18}O$ and seasonality in precipitation $\delta^{18}O$ were examined in seasonally dry forests in northeast Thailand in order to reveal annual cyclicity of xylem $\delta^{18}O$. In Chapter 3, applicability of DC pulse marking method was tested in seasonally dry forests in northeast Thailand and tropical rainforest in peninsular Malaysia and the results were compared between two sites. In Chapter 4, growth ring detection of trees without tree rings using $\delta^{18}O$, combined with DC pulse marking, was tested in seasonally dry forests in northeast Thailand. In Chapter 5, seasonality in precipitation $\delta^{18}O$, intra-annual variation of xylem $\delta^{18}O$, and growth ring detection using $\delta^{18}O$ were compared between seasonally dry forests and tropical rainforests.

Chapter 1 Sample preparation of ring-less tropical trees for $\delta^{18}O$ measurement in isotope dendrochronology

1.1 Introduction

Most trees in the tropical region do not have annual rings because the seasonality of climatic factors is less pronounced through the year. In trees that have anatomically visible growth rings, these rings can be used for dendrochronology with some verification method, such as cambial marking (Worbes 1995). However, in trees without visible rings, definition of the growth zone, which is the region between two adjacent growth boundaries, is needed before application of dendrochronological methods. In this case, the radial variation of anatomical features, such as vessel lumen size and frequency (Ohashi et al. 2014), chemical element concentration (Hietz et al. 2015), or isotope ratios (Poussart et al. 2004) have been used to define the growth zone.

The stable oxygen isotope ratio ($\delta^{18}O$) in tree-ring cellulose is mostly determined by $\delta^{18}O$ of source water (usually precipitation) and relative humidity during growth (Roden et al. 2000). Therefore, $\delta^{18}O$ in the tree-ring cellulose should vary along with the seasonal variation of $\delta^{18}O$ in precipitation and/or relative humidity even with the trees without visible boundaries. For example, Poussart et al. (2004) found that $\delta^{18}O$ variation of *Podocarpus neriifolius* in Thailand and *Samanea saman* in Indonesia was mainly caused by seasonal change in relative humidity. Ohashi et al. (2015) analyzed $\delta^{18}O$ of eight trees in Brazil and they attributed the seasonal variation in $\delta^{18}O$ of trees to $\delta^{18}O$ of precipitation.

Sample preparation in isotope dendrochronology, especially for a high-resolution analysis, is problematic. Dendrochronological studies using $\delta^{18}O$ in wood usually analyze cellulose, one of the three major chemical components in wood (McCarroll and Loader 2004). Each component (cellulose, hemicellulose, and lignin) of wood has its own $\delta^{18}O$ value (Wilson and Grinsted 1977), and the percentage of each component can be different at stem position or among individuals. Thus, several studies have tested the necessity of cellulose extraction in dendrochronological studies. Despite the variations in percentage and its $\delta^{18}O$ value among each wood component, whole wood samples show similar $\delta^{18}O$ trend as in the α-cellulose samples within a tree (Mischel et al. 2015), and what is more, whole wood samples including both sapwood and heartwood may exhibit better correlation with the climate factors than α-cellulose samples (Gori et al. 2013). There are two procedures to extract α-cellulose: extraction after dividing (Loader et al. 1997) and extraction before dividing (Kagawa et al. 2015). Each tree ring is subdivided into thin sections with radial thickness ranging from 25 μm (Poussart and Schrag 2005) to 60 μm (Pons and Helle 2011), depending on the growth rate, to detect annual rings based on the radial variation of $\delta^{18}O$. Therefore, the number of samples to be analyzed can be overwhelming, and the extraction step could be a major bottleneck, if the former procedure is selected. If the latter procedure is selected, the number of samples to be extracted becomes fewer, but the chemical treatment shrinks the sample lath and makes dividing difficult. Moreover, sampling resolution may become insufficient because samples cannot be divided into as finer subdivisions as in the former method.

In case of annual ring detection, if the radial variation of $\delta^{18}O$ trend in α-cellulose samples is the

same as the samples before extraction, the cellulose extraction step could be skipped and the time required for sample preparation would be reduced significantly. Most of the studies comparing the trend between bulk and α-cellulose deal with inter-annual variation. Szymczak et al. (2011) found that *Pinus nigra* from the island of Corsica exhibited a high correlation (r = 0.77) between α-cellulose and the whole wood. Weigt et al. (2015) analyzed five tree species (*Fagus sylvatica*, *Quercus robur*, *Picea abies*, *Abies alba*, and *Pseudotsuga menziesii*) in Germany and reported that the whole wood and the α-cellulose carried environmental signal at similar strengths. However, few studies have dealt with the intra-annual variation. For example, Pons and Helle (2011) compared the seasonal variation of $\delta^{18}O$ in the whole wood and α-cellulose of *Carapa guianensis* and *Goupia glabra* in central Guyana; the correlation was 0.55 and 0.77, respectively, and the $\delta^{18}O$ values of whole wood were almost parallel to that of α-cellulose.

Analysis at a high time-resolution is necessary for detecting seasonal variation of $\delta^{18}O$ in trees, and samples must be subdivided into thin sections with sufficient time-resolution. However, cellulose extraction is labor-intensive work, especially for a large number of samples. If this extraction step can be eliminated, the analytical time can be greatly reduced. Whether the $\delta^{18}O$ chronology of whole wood samples parallels to that of α-cellulose samples must be tested to determine the necessity of α-cellulose extraction. In this study, the author compared the radial variation of $\delta^{18}O$ before and after cellulose extraction to evaluate the necessity of extracting α-cellulose to detect annual rings from trees with no visible rings. Moreover, the author examined the optimum sampling interval of analytical samples that achieves sufficient time resolution to detect peaks in the radial variations of $\delta^{18}O$ values.

1.2 Materials and methods

1.2.1 Study site

The study was conducted in plantations of *Acacia auriculiformis* (AA) and *Eucalyptus camaldulensis* (EC), and a natural forest (FOII) in Sakaerat Silvicultural Research Station (14°28′06.1″N, 101°54′15.0″E), Nakhon Ratchasima Province, northeastern Thailand. Three sites (AA, EC, and FOII) were located within 1 km of each other, and there was little difference in climatic conditions among them. The air temperature was measured every hour during research period, and mean annual temperature was 22.1, 23.4, and 22.9 °C in 2011, 2012, and 2013, respectively. Annual precipitation was 1155, 1132, and 1419 mm in 2011, 2012, and 2013, respectively (Sakaerat Environmental Research Station 2016). Fig. 1.1 shows precipitation from September 2011 to December 2013. In this region, dry season usually starts in November and continues until April. Fig. 1.2 shows the monthly change in the stable oxygen isotope ratio (‰) of the precipitation in Bangkok (IAEA/WMO 2016), approximately 180 km southwest of Sakaerat. The $\delta^{18}O$ value of precipitation is increasingly negative from February to October, then increases until January. The lowest $\delta^{18}O$ value is observed at the end of the wet season.

1.2.2 Samples

One tree from each site, *A. auriculiformis* from AA (AA2-3), *E. camaldulensis* from EC (EC5-3), and *Celtis timorensis* tree from FOII (FOII11-3) was sampled in February 2014. Diameter at breast height (DBH) of

each tree was 22.7, 22.1, and 26.9 cm, respectively. Wood core samples (5 mm in diameter, 3–4 cm in length) were collected from the trunk at 1.3 m above the ground with an incremental borer. Radial growth of sampled species in each site was monitored with dendrometer bands every two weeks from September 2011 to December 2013 (Fig. 1.3). Trees tended to grow fast in the wet season and slow in the dry season.

1.2.3 Sample preparation

Serial tangential sections were prepared from each core samples at 0.2 mm thickness in the radial direction, starting from cambium, with a sliding microtome. The sections were placed in acetone for 30 minutes to remove the glue (cyanoacrylate adhesive) that was used to prevent breakage of the core during sectioning. Each circular section sliced from a core sample was divided along wood grain into two semicircular sections, both of which were located at the same radial and longitudinal positions, and were side-by-side tangentially. One half was used for bulk analysis (bulk sample) and the other was used for extraction (extracted sample). Holocellulose was prepared from the extracted samples, and then every other holocellulose section was selected to prepare α-cellulose section (Fig. 1.4).

1.2.4 Chemical treatment

The author followed the methodology described in Loader et al. (1997) for α-cellulose extraction. The author omitted extractive removal treatment because the author used sapwood whose extractive content is negligible. Firstly, lignin was removed with sodium chlorite solution. Samples were processed in a mixture of sodium chlorite (10 g), acetic acid (5 mL), and deionized water (350 mL) at 70 °C for one hour, after which samples were washed with deionized water. These steps were repeated four times and the final products were labeled as holocellulose. Secondly, half of the selected holocellulose samples were further treated with sodium hydroxide solution (17.5% wt/wt) at 80 °C for one hour to remove hemicellulose. Later, samples were washed with deionized water, and the final product was labeled as α-cellulose. Both holocellulose and α-cellulose sample were dried at 65 °C overnight. Dry weights of samples before and after the chemical treatments were measured and the yields of holocellulose and α-cellulose were calculated.

The author used a Teflon vessel (8 mm external diameter, 150 mm length) with a polyethylene filter (average pore size 40 μm) (Harada et al. 2014) or a glass tube (8 mm external diameter, 5 cm length) with glass wool as the reaction tube. The samples were put into the tubes and the tubes were placed in an airtight beaker. Extraction was conducted in a temperature-controlled oven.

1.2.5 Stable oxygen isotope analysis

A 100–200 μg portion of each sample was weighed and wrapped in a 7 mm × 7 mm silver sheet that was cut out from silver foil (150 mm × 150 mm, 4 μm thick, Nitto Kagaku Co Ltd., Nagoya, Japan). The oxygen isotope ratios were measured using a continuous flow isotope ratio mass spectrometer (Delta V Advantage; Thermo Finnigan, Bremen, Germany) coupled with a high-temperature combustion elemental analyzer (TC/EA; Thermo Finnigan, Bremen, Germany). Obtained results were expressed in delta (δ) notation in per mil (‰) units relative to Vienna standard mean ocean water (VSMOW). The oxygen isotope ratios of

samples were calibrated with Merck cellulose. Standards were measured every nine samples. Standard deviation (SD) of the repeated measurements of standards within a sequence was less than 0.34‰.

1.2.6 Data processing

The author obtained regression line between distance from cambium (explanatory variable) and $\delta^{18}O$ values (dependent variable) by fitting kernel regression. The author assumes that neighboring samples have close $\delta^{18}O$ values. The regression line can follow all data points because degrees of freedom can be same as the number of samples in kernel regression. To avoid the overfitting, penalization term was added to the fitting model.

Kernel ridge regression was used to detect any trend in seasonal variation in the sequential $\delta^{18}O$ values. Kernel ridge regression is ridge regression combined with the kernel method. Ridge regression is a regression analysis with regularization. Without regularization, parameters of linear regression are obtained by minimizing the residual sum of squares (the least square method). However, in ridge regression, the parameters are obtained by minimizing the residual sum of squares plus a penalty term for regularization which is the square of the L^2 norm of the parameter.

Given the explanatory variable $\boldsymbol{x} = (x_1, x_2, \dots, x_n)$ and the target variable $\boldsymbol{y} = (y_1, y_2, \dots, y_n)$, the kernel ridge regression assumes the following linear relationship between *x* and *y*:

$$y_i = k(x_i, \boldsymbol{x})\theta + \epsilon$$

where $k(x_i, \boldsymbol{x})$ is the kernel function, θ is the coefficient, and ϵ is the noise term. In this study, $\boldsymbol{x}$ is the distance from the cambium (mm) and $\boldsymbol{y}$ is $\delta^{18}O$ value (‰). θ is determined to minimize the residual sum of squares plus a penalty term:

$$\sum_{i=1}^{n} (y_i - k(x_i, \boldsymbol{x})\theta)^2 + \alpha \, \|\theta\|_2{}^2$$

where α is the regularization parameter ($\alpha \geq 0$). As for our data, the radial basis function (RBF) kernel was used as the kernel function:

$$k(x, x') = \exp(-\gamma \|x - x'\|^2), \gamma = \sigma^{-2}$$

where $\sigma > 0$. The parameter of RBF kernel γ and the regularization parameter α were selected by trying various sets of γ and α to minimize the mean square error calculated by the leave-one-out cross-validation. Kernel ridge regression was performed by "scikit-learn" (Pedregosa et al. 2011) in Python. $\delta^{18}O$ values were obtained for every 0.05 mm by kernel ridge regression. Later, the position of peaks was determined. Peaks smaller than the threshold value were ignored. The threshold value was determined based on the SD of standards. Thus, if SD was less than 0.34‰ then the threshold value was $3\sqrt{SD^2 + SD^2} \approx 1.44$ ‰.

The differences in peak positions between the bulk samples ($\boldsymbol{P_B}$) and extracted samples ($\boldsymbol{P_E}$) were evaluated by the root mean squared error (RMSE). By assuming that bulk samples and extracted samples have *n* peaks ($\boldsymbol{P_B} = (P_{B1}, P_{B2}, \dots, P_{Bn})$, $\boldsymbol{P_E} = (P_{E1}, P_{E2}, \dots, P_{En})$; P_{B1} and P_{E1} were the closest peaks to cambium), RMSE was defined as follows:

$$\mathrm{RMSE} = \sqrt{\frac{\sum_{i=1}^{n} (P_{Bi} - P_{Ei})^2}{n}}$$

1.3 Results

1.3.1 Offset of $\delta^{18}O$ values for extracted samples from bulk wood

The $\delta^{18}O$ values cyclically changed in both bulk wood and α-cellulose whereas the offset was almost constant across the radial position within an individual core (Fig. 1.5). The mean offset of $\delta^{18}O$ values of α-cellulose from bulk wood was 4.7±1.1‰ in AA2-3, 3.2±0.6‰ in EC5-3, and 3.1±0.8‰ in FOII11-3. The mean offset of $\delta^{18}O$ values of holocellulose from bulk wood was 2.2±1.8‰, -0.2±0.7‰, and 1.3±1.4‰ respectively. The yields (%) of holocellulose and α-cellulose were 76–84% and 40–47%, respectively (Fig. 1.6). The author omitted holocellulose from data analysis because the yield of holocellulose was too high and the offset was too low compared to Pettersen (1984) and Cullen and Macfarlane (2005), respectively.

1.3.2 Radial variation of $\delta^{18}O$

Cyclic changes in $\delta^{18}O$ values in the radial direction was observed in all trees, both from bulk wood and α-cellulose (Fig. 1.5). The trend in bulk wood was similar to that of α-cellulose, but the cycles were more conspicuous in bulk wood partly because of the higher time resolution. The correlation coefficient between α-cellulose and bulk wood was 0.83, 0.90, and 0.77 for AA2-3, EC5-3, and FOII-11-3, respectively.

The range of $\delta^{18}O$ variation (‰) was similar among samples except for α-cellulose of AA2-3 and bulk wood of FOII11-3 (Table 1.1). The range was wider in α-cellulose of AA2-3 and narrower in bulk wood of FOII11-3.

1.3.3 Number of peaks and their positions

Figure 1.7 indicates the positions of peaks detected based on predicted values by kernel ridge regression. Parameters and R^2 values for the regressions are listed in Table 1.2. In AA2-3, the peak located at 9.40 mm from cambium in α-cellulose was not detected in bulk wood (Fig. 1.7 (a)). In EC5-3, two peaks located at 6.45 mm and 10.80 mm from cambium in α-cellulose were not detected in bulk wood. In FOII11-3, all the peaks detected in α-cellulose were also detected in bulk wood. Regarding the peaks both in α-cellulose and bulk wood, the RMSE was 0.13, 0.13, and 0.57 for AA2-3, EC5-3, and FOII11-3, respectively. The mean cycle length of FOII11-3 was 3.76 mm for bulk wood and 3.67 mm for α-cellulose, being longer than that of AA2-3 (2.13 mm for bulk wood, 1.9 mm for α-cellulose) and EC5-3 (2.77 mm for both bulk wood and α-cellulose).

Predicted values by kernel ridge regression were also obtained using bulk wood with 0.2 mm sampling interval and detected peaks were compared with peaks of 0.4 mm-interval sample to examine the effect of the difference in sampling interval on peak detection (Fig. 1.8). In AA2-3, all the peaks detected in 0.2 mm-interval sample were also detected in 0.4 mm-interval sample (Fig. 1.8 (a)). In EC5-3, two peaks located at 6.70 mm and 10.75 mm from cambium were not detected in 0.4 mm-interval sample (Fig. 1.8 (b)). In FOII11-3, one peak located at 1.75 mm from cambium was not detected in 0.4 mm-interval sample (Fig. 1.8 (c)).

1.4 Discussion

1.4.1 Offset and correlation between bulk samples and α-cellulose samples

The offset values observed in this study were rather small, but within the range of values in Barbour et al. (2001), in which measured $\delta^{18}O$ values were from *Quercus* and *Pinus* species grown on a wide range of source water $\delta^{18}O$ values. In EC5-3, the offset values were smaller than the range (5.0–7.0 ‰) of other three *Eucalyptus* species (Cullen and Macfarlane 2005). This smaller offset was attributable to less lignin content (Fig. 1.6). More lignin content resulted in greater offsets because $\delta^{18}O$ of lignin is smaller than that of α-cellulose (Cullen and Macfarlane 2005). The lignin content in softwoods is greater than in hardwoods. The lignin content of tropical hardwoods tends to be greater than that of temperate hardwoods (Pettersen 1984). Therefore, if the offset values are compared within a genus, the offset values of tropical trees are expected to be larger than those of temperate trees of the same genus.

The offset for AA2-3 was larger than that of EC5-3 and FOII11-3 especially in the inner part (Fig. 1.5). This difference was probably caused by both the difference in the wood components ratio and in transpiration assuming that they used source water with the same $\delta^{18}O$ value (Roden et al. 2000). Leaf water $\delta^{18}O$ value becomes increasingly positive when evaporation rate increases, and the $\delta^{18}O$ is reflected in the $\delta^{18}O$ value of α-cellulose. Therefore, in the case of the inner part of AA2-3, The author assumes $\delta^{18}O$ values of α-cellulose were greater probably because of high transpiration at the time of the wood formation, whereas $\delta^{18}O$ values of bulk wood were not so enriched probably because of higher lignin content.

Correlation coefficients in this study (0.83, 0.90, and 0.77 for AA2-3, EC5-3, and FOII-11-3, respectively) were relatively higher than the values reported in previous studies. As for intra-annual variation, Pons and Helle (2011) studied *Carapa guianensis* Aublet and *Goupia glabra* Aublet in central Guyana. They reported that correlation coefficients were 0.55 and 0.77, respectively, which were lower than those from this study. As for inter-annual variation, Battipaglia et al. (2008) compared $\delta^{18}O$ in late wood of *Fagus sylvatica* and *Acer pseudoplatanus* in bulk wood and α-cellulose. They reported that the correlation coefficients were lower than those of this study for *F. sylvatica* (0.46) and insignificant for *A. pseudoplatanus*. As far as ratios of wood components stay constant across different years of wood formation, $\delta^{18}O$ variation of whole wood is expected to be parallel to that of α-cellulose. However, in the case of dendrochronological samples over wider time span, wood components could have changed through time, and this could result in a weak correlation between whole wood and α-cellulose samples.

1.4.2 Effect of α-cellulose extraction on radial variation of $\delta^{18}O$

Although the peak positions of bulk wood were the same as those of α-cellulose in most cases, the peak detections sometimes failed. This failure is partly due to small radial growth rates or small amplitude of $\delta^{18}O$.

In AA2-3 and EC5-3, the number of peaks in bulk wood was fewer than that of α-cellulose (Fig. 1.7) because signal amplitudes in α-cellulose decreased in the bulk samples, or peak detection processes were affected by an outlier. In both cases, this would be solved by measuring the same samples multiple times or increasing sample size.

The failure of peak detection could happen if neighboring samples have a large difference in their

$\delta^{18}O$ values. The author needs to adjust parameters for kernel ridge regression or use other method to extract trend from data if such situation occurs. Moreover, before applying this method to detect growth ring, the author needs to test the validity of the method by using trees forming annual rings.

1.4.3 Effect of sampling resolution on radial variation of $\delta^{18}O$

Some peaks would not be detected if sampling interval are too wide. The number of peaks of 0.4 mm-interval sample were less than that of 0.2 mm-interval sample in EC5-3 and FOII11-3 because of insufficient sampling resolution to capture the peaks (Fig. 1.8). Annual increment of wood should be divided into sufficient number of subsamples in order to detect seasonally change of $\delta^{18}O$.

Optimal resolution for annual ring detection depends on growth rate. Pons and Helle (2011) reported that certainty of the annual ring detection was better at high resolution (60 μm) than at low resolution (200 μm). Ohashi et al. (2014) studied annual ring detection using vessel features (vessel frequency and mean vessel lumen area), and reported that approximately 40–60% of the annual-ring width was suitable for sampling resolution which is defined as the product of radial interval and filter length of moving average. In this study, optimal sampling resolution could be smaller than 0.2 mm when the author considers the growth rate estimated by the dendrometer monitoring.

1.4.4 Radial variation of $\delta^{18}O$ and its potential for annual ring detection

Seasonality in $\delta^{18}O$ values of precipitation was reflected in $\delta^{18}O$ values of tree xylem in most cases (Fig. 1.5), but sometimes it was absent. The mean cycle length of FOII11-3 was larger than those of AA2-3 and EC5-3 (Fig. 1.7) However, the annual increment based on dendrometer monitoring showed smaller values than those of other two tree species (Fig. 1.3). Therefore, seasonality in $\delta^{18}O$ values recorded in the xylem was not completely reflected because of low signal amplitude or insufficient sampling resolution.

The three studied species tended to grow fast in the wet season and slow in the dry season (Fig. 1.3), and the change in the $\delta^{18}O$ values of precipitation during the growing season was recorded in tree xylem. However, if the growing season was very short, the amount of change in the $\delta^{18}O$ values of precipitation would be very small and the amplitude should be also very small.

The author needs to cross-check the $\delta^{18}O$-dated tree age by other methods such as cambial marking (Ohashi et al. 2009) or radiocarbon dating (Worbes 1995) to verify the annual nature of the cycle in the $\delta^{18}O$ values in tree xylem. Another way to verify the annual nature is cross-dating using high correlation of $\delta^{18}O$ values among trees that grew in the same environment (Nakatsuka et al. 2004). Another possibility would be cross-dating the $\delta^{18}O$ chronology of the ring-less tropical tree by comparing with the $\delta^{18}O$ chronology of the tree forming annual rings such as teak (*Tectona grandis*). Moreover, the seasonality in the $\delta^{18}O$ values of precipitation should be monitored in the study site.

1.5 Summary

The author compared radial variation of $\delta^{18}O$ values in tropical trees with no distinct annual rings before and after cellulose extraction to examine the necessity of α-cellulose extraction for tropical dendrochronology.

Cyclic variations in $\delta^{18}O$ values in the radial direction were observed in three tree species for both bulk wood and α-cellulose samples. Correlations between bulk wood and α-cellulose were high in every species, and the offset was almost constant across the radial position. Thus, the author concluded that α-cellulose extraction is unnecessary for annual ring detection. Moreover, appropriate sampling resolution, depending on the growth rate is necessary for effective peak detection.

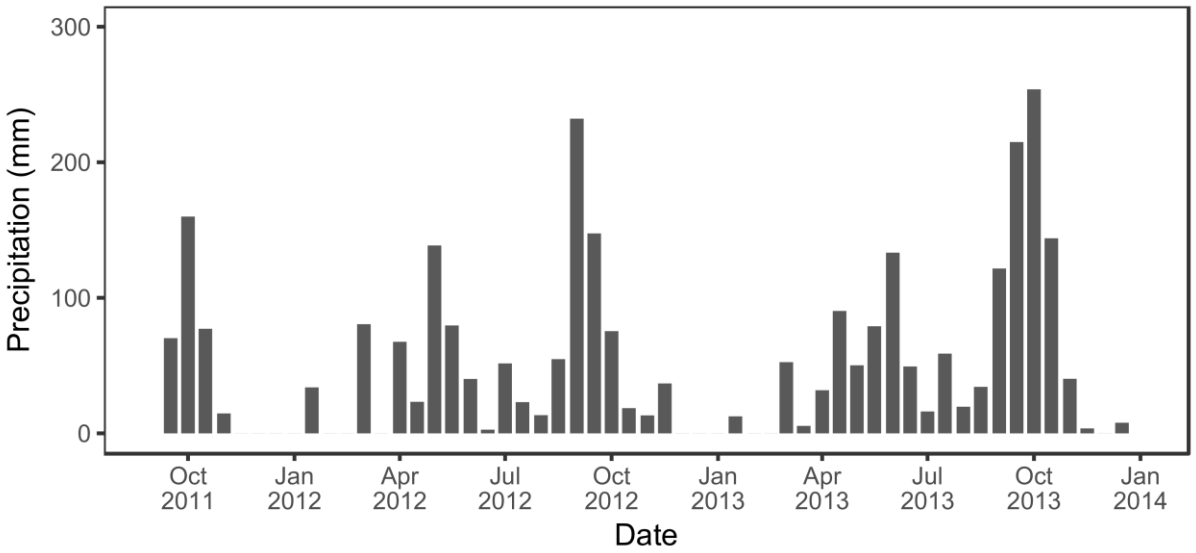

Fig. 1.1 Precipitation (mm) in study site from September 2011 to December 2013. The data are plotted every two weeks.

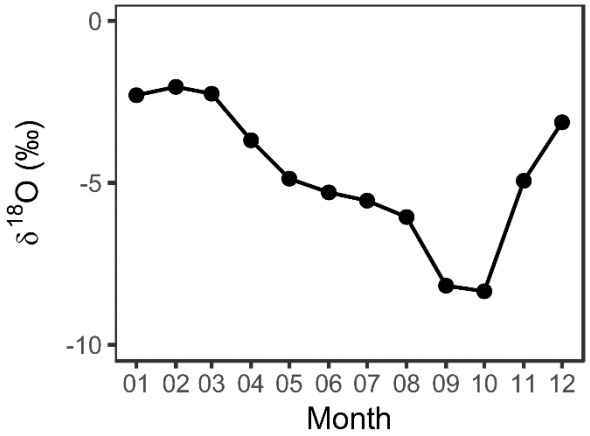

Fig. 1.2 Stable oxygen isotope ratio of precipitation in Bangkok. The data are the means from 1968 to 2014, obtained from the Global Network of Isotopes in Precipitation (IAEA/WMO 2016)

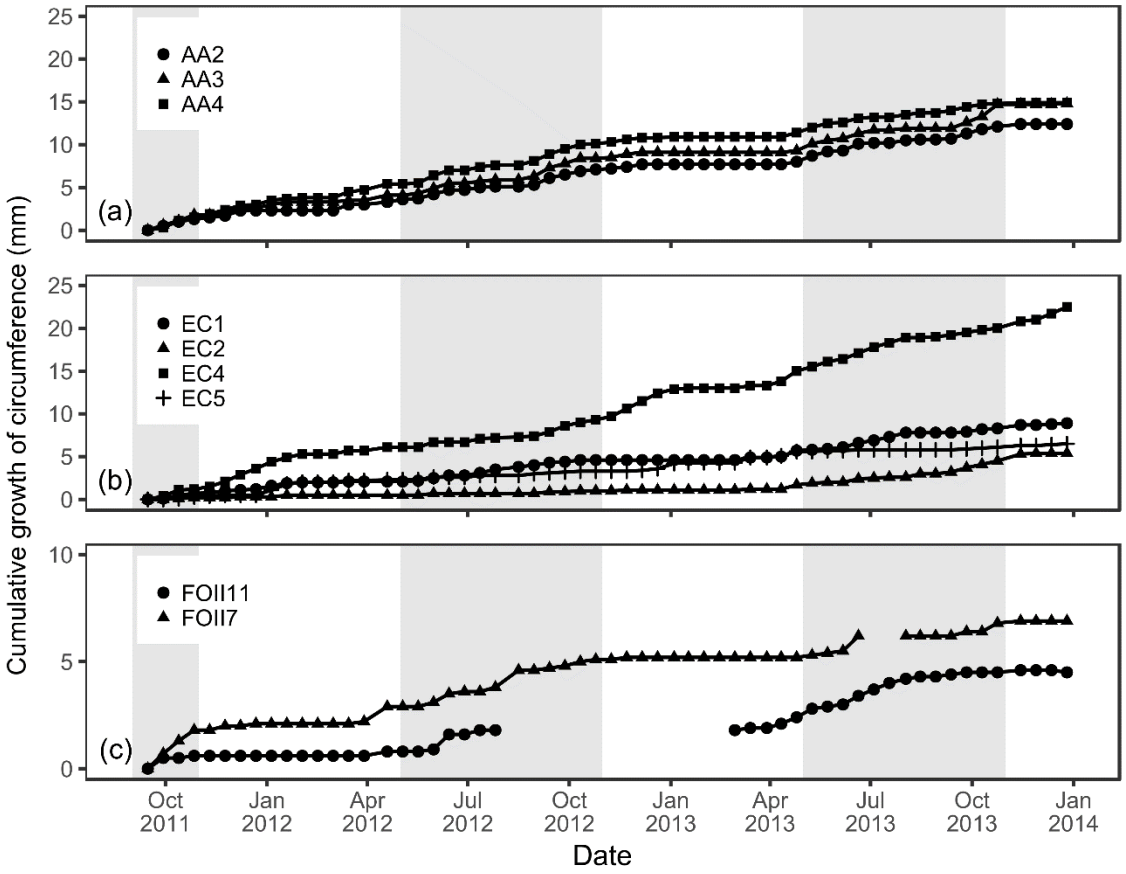

Fig. 1.3 Cumulative growth of circumference in (a) *Acacia auriculiformis* (AA), (b) *Eucalyptus camaldulensis* (EC), and (c) *Celtis timorensis* (FOII11 and FOII7). Gray color indicates the wet season. Data were obtained every two weeks. Missing values were caused by the destruction of the devices by wild animals.

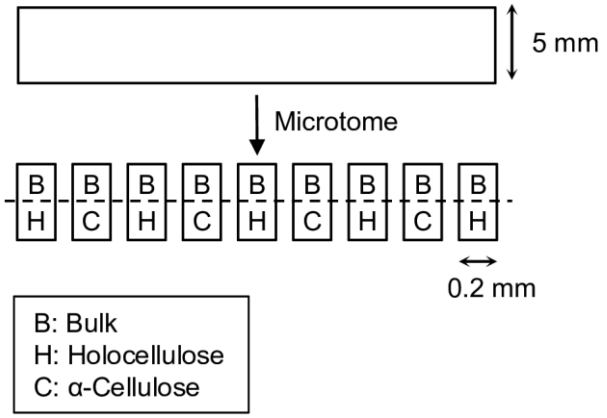

Fig. 1.4 Division of core samples. Each core was divided into 0.2 mm thick sections with a sliding microtome. The half of each section was analyzed as bulk wood. Holocellulose was prepared from the other half of each section, and α-cellulose was prepared from each sample of holocellulose.

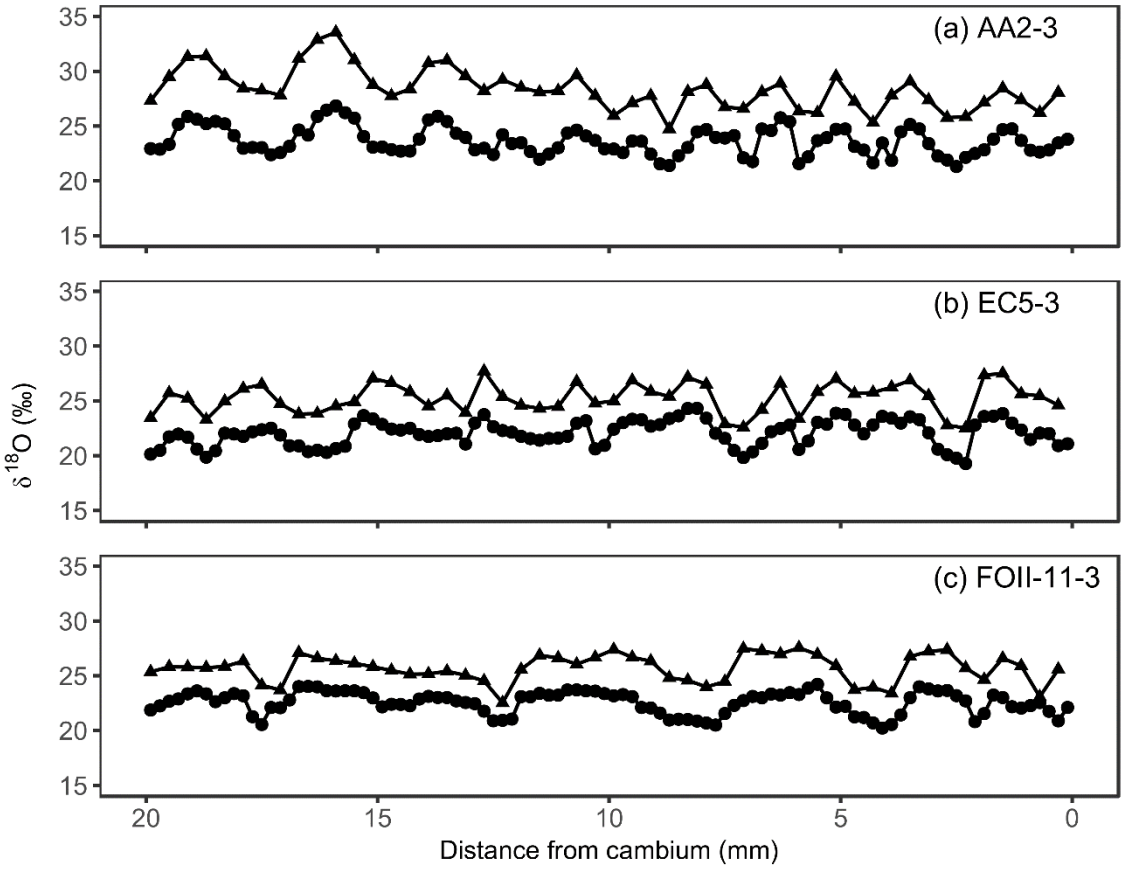

Fig. 1.5 Radial change of $\delta^{18}O$ values in bulk wood (filled circle) and α-cellulose (filled triangle).

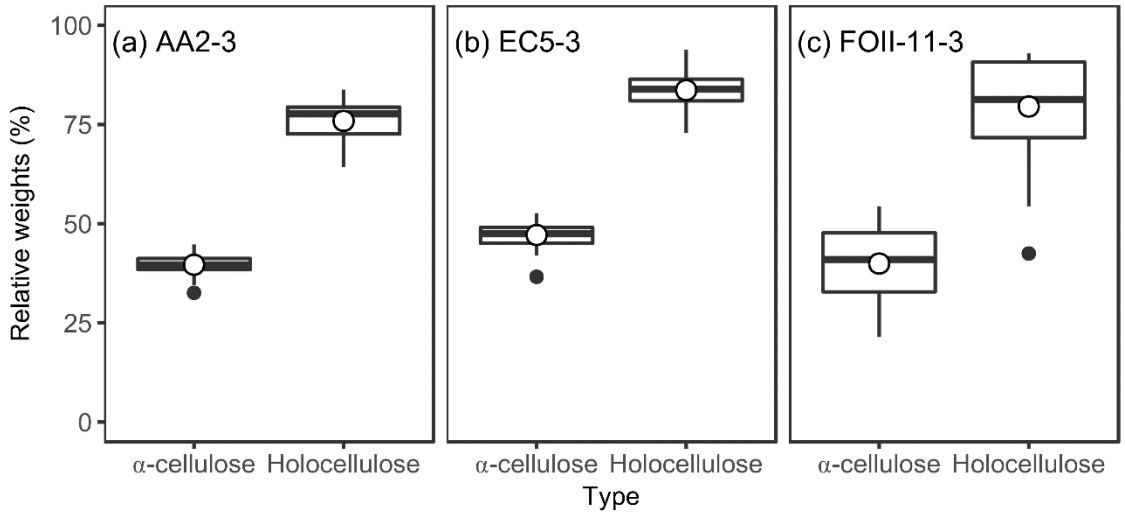

Fig. 1.6 Mass fraction of α-cellulose and holocellulose. Mean values are represented by a white circle.

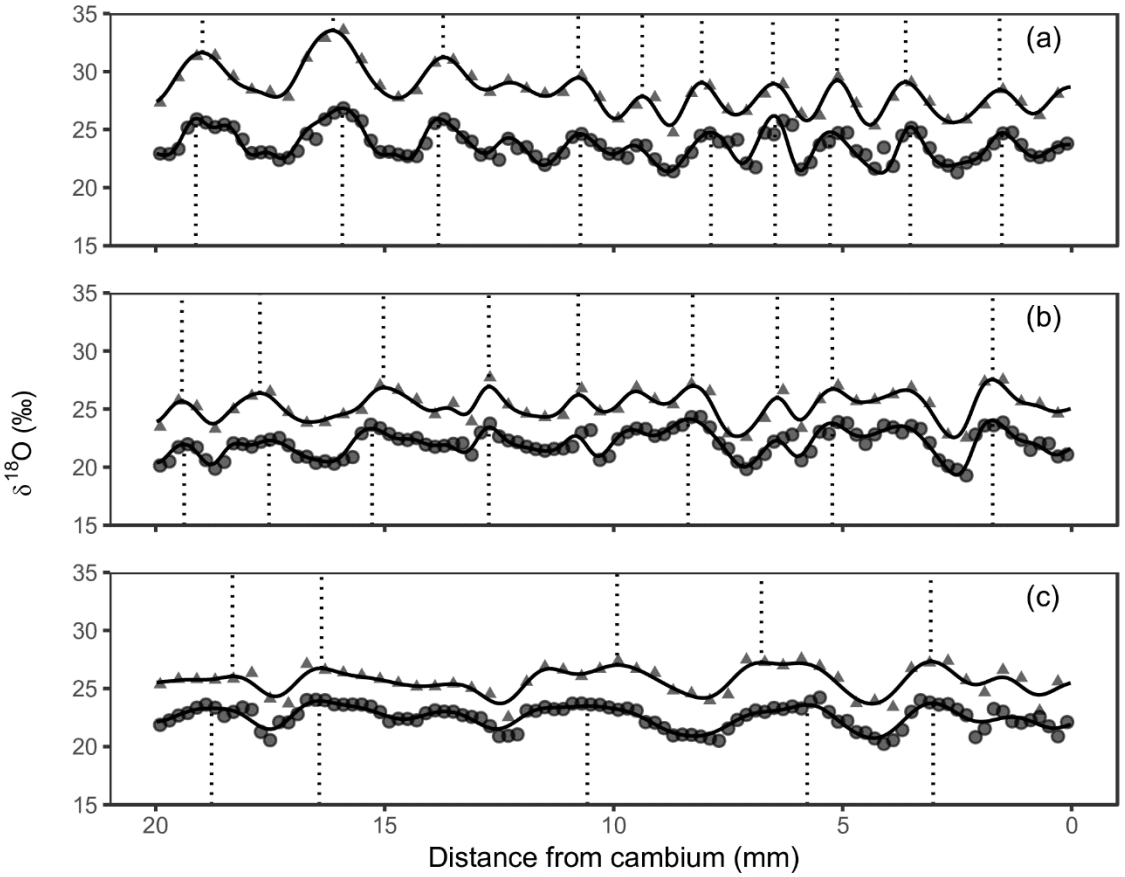

Fig. 1.7 The positions of peaks (dotted line) based on predicted values using kernel ridge regression (solid line). The filled triangle is the measured value of α-cellulose and filled circle is the measured value of bulk samples. Sampling interval is 0.4 mm. (a) AA2-3, (b) EC5-3, and (c) FOII11-3.

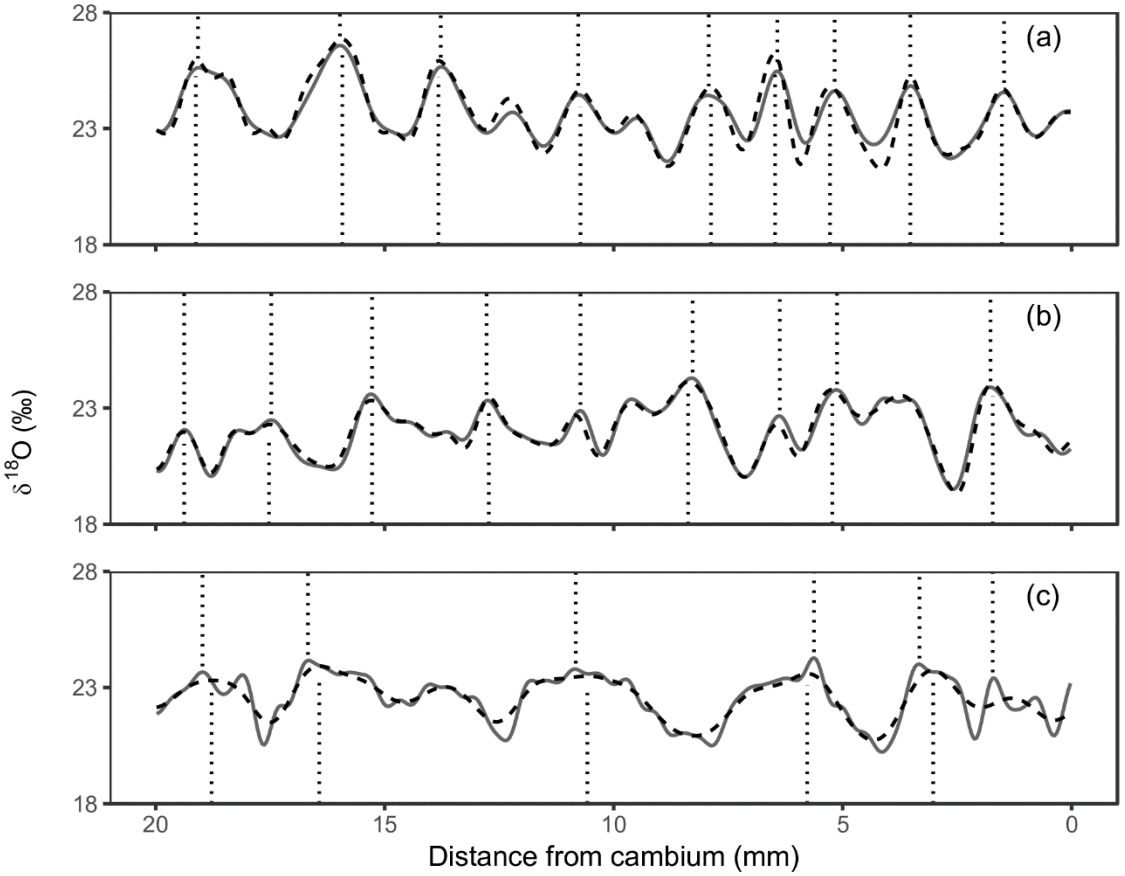

Fig. 1.8 Predicted values using kernel ridge regression. Sampling interval is 0.2 mm (solid) and 0.4 mm (dashed). Vertical dotted line is the positions of peaks based on 0.2 mm sampling interval (top) and 0.4 mm (bottom). (a) AA2-3, (b) EC5-3, and (c) FOII11-3.

Table 1.1 Mean, SD, and range of $\delta^{18}O$ values (‰).

Sample ID	Type[1]	Mean (‰)	SD (‰)	Range (‰)
AA2-3	B	23.65	1.27	5.53
	C	28.37	1.87	8.83
EC5-3	B	22.06	1.16	5.04
	C	25.27	1.37	5.19
FOII11-3	B	22.55	1.02	3.99
	C	25.68	1.25	5.02

[1]B: bulk; C: α-cellulose.

Table 1.2 Parameters and R^2 value of kernel ridge regression.

Sample ID	Type[1]	Interval (mm)	γ	α	R^2
AA2-3	B	0.2	7.61	0.5	0.905
		0.4	7.11	0.00003051	1.0
	C	0.4	3.56	0.0312	0.988
EC5-3	B	0.2	7.61	0.156	0.941
		0.4	7.11	0.125	0.977
	C	0.4	7.11	0.25	0.935
FOII11-3	B	0.2	7.61	0.000488	0.994
		0.4	3.56	0.5	0.875
	C	0.2	3.56	0.5	0.842

[1]B: bulk; C: α-cellulose.

Chapter 2 Intra-annual variation of stable oxygen isotope ratio of *Tectona grandis* in northeastern Thailand

2.1. Introduction

The value of stable oxygen isotope ratio ($\delta^{18}O$) of xylem cellulose is determined mainly by that of source water that trees absorb (McCarroll and Loader 2004), and the source water is usually represented by precipitation. So, if intra-annual variation of precipitation $\delta^{18}O$ have clear cyclicity, the variation would be recorded in the annually formed xylem. However, it is difficult to show radial variation of xylem $\delta^{18}O$ have annual cyclicity when the tree does not have visible growth rings.

Trees grown in one site use the same source water for photosynthesis and resulted xylem $\delta^{18}O$ would show a similar trend among trees (Nakatsuka et al. 2004). Thus, if trees with tree rings are available in the same site and their xylem $\delta^{18}O$ show annual cyclicity, the relationship would be applicable to the trees without visible growth rings in the site.

Tectona grandis (Lamiaceae) is a ring-porous and deciduous hardwood tree species naturally growing in the tropical forests of India, Myanmar, Thailand and Laos (Huang et al. 2015). Since it forms visible growth rings, *T. grandis* is often used for dendrochronological studies in the tropical region. For example, Pumijumnong et al. (1995) constructed ring-width chronology of *T. grandis* covering 1911 to 1990 in northern Thailand and concluded that the growth is positively correlated with rainfall during the first half of the wet season (April to June). Ram et al. (2008) found significant positive relationship of moisture index and rainfall during the monsoon months as well as on the annual scale with tree-ring width variations of teak in central India. They concluded that the teak tree-ring chronologies can be used as high-resolution proxy for past precipitation and moisture level in the environment.

In addition to ring-width analysis, isotope analysis, especially that of oxygen, has been applied to teak. Probably because of its climate-dependent nature, intra-annual variation in xylem $\delta^{18}O$ of *T. grandis* have different trends among study sites. In central India, $\delta^{18}O$ showed one negative peak within one tree ring (Managave et al. 2010). On the other hand, $\delta^{18}O$ shows opposite trend in southern India, probably because of different contribution to source water by southwest monsoon or northwest monsoon precipitation (Managave et al. 2011). Furthermore, *T. grandis* in northwest Thailand had different $\delta^{18}O$ variation within tree ring year by year, corresponding to different $\delta^{18}O$ variation of monthly precipitation year by year (Muangsong et al. 2016).

These results show that intra-annual variation of xylem $\delta^{18}O$ in *T. grandis* has a seasonal pattern, which is largely determined by the $\delta^{18}O$ variation of local precipitation. Thus, if we could confirm an annual cyclic variation of xylem $\delta^{18}O$ in trees with annual rings, we could expect the similar variation in the trees with no visible growth rings. In order to evaluate $\delta^{18}O$ variation within tree ring, $\delta^{18}O$ variation of precipitation in study site should be examined at the same time.

In this chapter, the author examined annual trend in $\delta^{18}O$ of precipitation and whether the trend is recorded in $\delta^{18}O$ of xylem. *Tectona grandis*, forming visible annual rings, was used to show the annual variation in $\delta^{18}O$ of its xylem. Bulk wood was analyzed because cellulose extraction is not necessary for the

purpose of annual ring detection (Nakai et al. 2018).

2.2. Materials and methods

2.2.1. Study site

Rain samples were collected at the Sakaerat Environmental Research Station (SERS; 14°30'37.0"N, 101°55'51.4"E), Nakhon Ratchasima Province, northeastern Thailand. Annual temperature was 22.6 °C, and annual precipitation was 1081 mm (1969–2017; Sakaerat Environmental Research Station 2018). Rainy season usually starts in May and continues until October (Fig. 2.1). Wood samples were collected at Wang Nam Kiao Forestry Student Practicing Station of the Faculty of Forestry, Kasetsart University (WNKFSPS; 14°29' N, 101°56' E) in Nakhon Ratchasima Province, northeastern Thailand. Since WNKFSPS is located within 3 km apart from SERS, the climate condition of WNKFSPS is assumed to be the same as that of SERS.

2.2.2. Samples

Rain samples were collected with a polyethylene funnel (9 cm in diameter) and a polyethylene container (5 L) twice a month, on the 1st and the 16th, since May 2015. The device for rain collection had a mechanism of preventing collected water from evaporating. After the weight was measured a part of collected samples (50 mL) was stored for isotope analysis.

Seven *Tectona grandis* were sampled in March 2015 to examine within-tree variation of $\delta^{18}O$. Two wood core samples (5 mm in diameter) were collected at 1.3 m above the ground from opposite direction for each tree with an increment borer. The length of core was about the half of diameter of each tree. Short wood core samples (3–4 cm in length; one core for each tree) were also collected in September 2016 and December 2017 to examine the effect of precipitation on xylem $\delta^{18}O$.

2.2.3. Sample preparation

After all wood cores were cross-dated, five cores were prepared for stable isotope analysis (Table 2.1). Serial tangential sections (0.05 mm thick) were prepared from each core sample in the radial direction, from cambium to pith, with a sliding microtome. The sections were placed in acetone for 15 minutes to remove the glue (cyanoacrylate adhesive) that was used to prevent breakage of the core during sectioning. Sections were then oven-dried at 65°C overnight.

2.2.4. Stable isotope analysis

Rain samples were filtered with syringe filters (pore size < 0.22 μm) before isotope analysis to remove coarse dust. Stable oxygen and hydrogen isotope ratios of rain samples were analyzed with isotopic water analyzer (Picarro L2120-i or L2130-i; Picarro inc., CA, USA) at the Research Institute for Humanity and Nature (RIHN). Each sample was measured six times and three of six measurements were averaged. Obtained results were expressed in delta (δ) notation in per mil (‰) relative to Vienna standard mean ocean water (VSMOW). Standard deviation of repeated measurements of samples was under 0.3‰. After stable oxygen ($\delta^{18}O$) and

hydrogen (δ^2H) isotope ratios were determined, the deuterium excess (d) values were calculated by the following equation (Dansgaard 1964):

$$d = \delta^2H - 8\,\delta^{18}O$$

to evaluate the fractionation processes of $\delta^{18}O$ and δ^2H in precipitation. The relationship between δ^2H and $\delta^{18}O$ in precipitation around the world is often described as $\delta^2H = 8\,\delta^{18}O + 10$ (the global meteoric water line; GMWL) and the d value of GWML is 10 (Ingraham 1998).

A 0.1–0.2 mg portion of each wood section was weighed and wrapped in a 7 mm × 7 mm silver sheet that was cut out from silver foil (150 mm × 150 mm, 0.004 mm thick, Nitto Kagaku Co Ltd., Nagoya, Japan). When the sample had a wide ring width, some sections were skipped because the number of sections was too large. The oxygen and carbon isotope ratio were measured using a continuous flow isotope ratio mass spectrometer (Delta V Advantage or Delta Plus; Thermo Finnigan, Bremen, Germany) coupled with a high-temperature combustion elemental analyzer (TC/EA; Thermo Finnigan, Bremen, Germany) at the Center for Ecological Research (CER) and the Research Institute of Humanity and Nature (RIHN). Obtained results were expressed in delta (δ) notation in per mil (‰) relative to Vienna standard mean ocean water (VSMOW) for oxygen or Pee Dee Belemnite (PDB) for carbon. The oxygen and carbon isotope ratio of samples measured with Delta V Advantage were calibrated with Merck cellulose. The oxygen isotope ratio of the samples measured with Delta Plus was calibrated by Merck cellulose, IAEA601, and USGS54 and the carbon isotope ratio was calibrated with CERKU-01, 02, 03 and 04 (Tayasu et al. 2011) and USGS54. Standard deviation of the repeated measurements of standards within a sequence was less than 0.5‰.

2.2.5. Data processing

Relationship between stable isotope ratio (explanatory variable) and distance from cambium (dependent variable) was analyzed by kernel ridge regression (details are in Nakai et al. 2018). Then each tree ring was evenly divided into 10 points and corresponding values of stable isotope ratio were obtained using regression line.

For evaluating within- and among-tree correlation of xylem $\delta^{18}O$, Pearson correlation coefficient was calculated. For within-tree correlation, $\delta^{18}O$ of two cores (TG0301 and TG0302) collected from tree TG03 were used. For among-tree correlation, cores from three trees (TG01, TG03 and TG07) were used, and mean value of correlation coefficients between all possible combinations of two cores were calculated. Three cores (TG0301, TG0302, and TG0304) of TG03 were averaged.

2.3. Results

2.3.1. Seasonal variation of $\delta^{18}O$ of precipitation

Precipitation $\delta^{18}O$ decreased through one year, and after the dry period on December, $\delta^{18}O$ showed more positive value before the dry period (Fig. 2.2). The distribution of precipitation had one or two peaks, spring (May–June) and summer (September). Monthly weighted mean of $\delta^{18}O$ of precipitation became more negative in September (Fig. 2.3). The differences between maximum and minimum of monthly weighted mean of $\delta^{18}O$ from 2015 to 2018 were 8.23, 9.85, 9.63, and 5.60 (‰) respectively.

The equation for the regression line from δ^2H to $\delta^{18}O$ (the local meteoric water line; LMWL) was $\delta^2H = 7.43\,\delta^{18}O + 4.73$ (Fig. 2.4). Both the slope and the intercept were smaller than those of the global meteoric water line (8.0 and 10.0, respectively). The deuterium excess values were seasonally varied (Fig. 2.5). The d values tended to be more negative in rainy season and more positive in dry season, especially in 2017 and 2018.

2.3.2. Inter-annual variation of $\delta^{18}O$ and $\delta^{13}C$

Both $\delta^{18}O$ and $\delta^{13}C$ values of *T. grandis* showed cyclic changes in radial direction (Fig. 2.6). The range of $\delta^{18}O$ values was wider than that of $\delta^{13}C$; up to 9‰ in $\delta^{18}O$ and under 5‰ in $\delta^{13}C$. Xylem $\delta^{18}O$ usually increased during the early part in a tree ring, and then decreased during the late part. The positions of negative peaks of $\delta^{18}O$ almost corresponded to the position of the ring boundaries, whereas $\delta^{13}C$ showed positive peaks at the beginning of tree ring and then decrease. While $\delta^{18}O$ values fluctuate within a limited range keeping almost a constant value, $\delta^{13}C$ values gradually increased in TG0302, decreased in TG0304 and TG0704.

2.3.3. Intra annual variation of $\delta^{18}O$

$\delta^{18}O$ values seasonally varied within a year (Fig. 2.7). The variation of $\delta^{18}O$ in one tree ring was similar within one tree (TG03) and among three trees. TG0301 and TG0302, collected from the same tree (TG03) in March 2015, showed high correlation, except for the year 2009 (Fig. 2.8). TG0304, also collected from TG03, showed a similar variation of $\delta^{18}O$ with TG0301 and TG0302 in 2014 (Fig. 2.7). Correlation among trees was high except for the years 2009 and 2013 (Fig. 2.9). The ring width of TG0704 from 2013 to 2016 was too narrow and the number of samples in each ring was not enough to judge the cyclicity of $\delta^{18}O$. Although the annual variation pattern of xylem $\delta^{18}O$ was slightly different year by year, within- and among-tree correlations were observed for most of the years analyzed.

2.4. Discussion

2.4.1. Annual trend in $\delta^{18}O$ of precipitation

$\delta^{18}O$ of precipitation showed a common variation during the research period; decreasing from February to September and then increasing to the next January (Fig. 2.2). There seems to be a common seasonal pattern every year and, if so, this annual cyclicity in $\delta^{18}O$ of precipitation is a desirable condition for tree ring detection. This pattern is probably because vapor source for precipitation is different among seasons. In Bangkok, about 300 km southwest of Sakaerat, the vapor source for precipitation in summer (from June to September) and precipitation in winter (from November to next April) come from different region; summer precipitation come from ocean and winter precipitation come from the mixing of the continental air mass and oceanic moisture (He et al. 2006). The decrease in September was partly because of amount effect, which is negative correlation between the $\delta^{18}O$ value and the amount of rain (Dansgaard 1964). Thus, both $\delta^{18}O$ value and amount of precipitation will be the factors affecting xylem $\delta^{18}O$ value.

2.4.2. Relationship between $\delta^{18}O$ of precipitation and $\delta^{18}O$ of xylem

Within-ring variation of xylem $\delta^{18}O$ was characterized by (1) increasing trend at the beginning of ring boundaries, and (2) decreasing trend towards the next year's ring boundaries (Fig. 2.6). The former is probably due to more positive $\delta^{18}O$ value of precipitation at the beginning of rainy season or enrichment of ^{18}O in soil water by evaporation during dry season, and the latter is probably due to the decreasing trend of precipitation $\delta^{18}O$ during rainy season.

Precipitation $\delta^{18}O$ showed more positive value at the beginning of the rainy season during the research period (Fig. 2.3) and resulting xylem $\delta^{18}O$ would have more positive value at the beginning of each year's growth. Furthermore, source water, which is mixture of soil water and precipitation, would evaporate during dry season resulting in ^{18}O enrichment before it is taken up by trees. *T. grandis* in Indonesia also showed increase of xylem $\delta^{18}O$ at the beginning of the growth boundaries and this trend was attributable to ^{18}O enrichment of soil water during dry season (Schollaen et al. 2013). The increasing trend at the beginning of each year's growth is also attributable to the use of stored carbohydrates. Krepkowski et al. (2013) confirmed by the ^{13}C pulse labeling experiment that *Podocarpus falcatus* (evergreen coniferous species) in Ethiopia uses stored carbohydrate for three years. Moreover, Helle and Schleser (2004) suggested that the rise of xylem $\delta^{13}C$ at the early wood of deciduous ring-porous trees is caused by usage of stored carbohydrate. When xylem is formed with stored carbon, a part of carbon-bound oxygen exchange with xylem water and the ratio of exchanged oxygen atoms is affected by the aridity such as precipitation or relative humidity (Cheesman et al. 2017). Nabeshima et al. (2018) studied intra-annual variation of hydrogen isotope ratio (δD) and $\delta^{18}O$ of *Quercus crispula*, a deciduous ring-porous species, and concluded that while the ratio of exchanged oxygen atom is constant in the late wood, the ratio changes in the early wood with increasing of the supply of current photosynthetic sugars with heavy isotope ratio. *T. grandis* is also a deciduous ring-porous species and uses the stored carbon at xylem formation before leafing, which is indicated as the rapid rise of $\delta^{13}C$ across ring boundary typically observed in TG0301 and TG0302 (Fig. 2.7). Increasing trend of $\delta^{18}O$ at the beginning of current year xylem formation is attributable to the same physiological process.

The decreasing trend of $\delta^{18}O$ is attributable mainly to the decreasing trend of precipitation $\delta^{18}O$ from May to September (Fig. 2.3). There is usually a lot of rain from May to September (Fig. 2.1) and *T. grandis* would grow actively using precipitation whose $\delta^{18}O$ value has decreasing trend in the growing season. Taken together, the up and down cycle of xylem $\delta^{18}O$ within a tree ring would be caused by the cyclic variation in precipitation $\delta^{18}O$ and the rotation of dry and rain season.

2.4.3. Correlation of xylem $\delta^{18}O$ within or among trees

Correlation of xylem $\delta^{18}O$ between cores collected from opposite direction (180°) was high except for 2009 (Fig. 2.8). This relationship is advantageous over analysis using tree ring width because *T. grandis* sometimes forms false rings (Palakit et al. 2012). Correlation of xylem $\delta^{18}O$ among trees was high except for 2009 and 2013 (Fig. 2.9). In 2009 the amount of precipitation in September was very small (Fig. 2.10). The false ring of *T. grandis* would be formed by the drought followed by wet weather during the growing season (Palakit et al. 2012). So, it is possible that small amount of precipitation on September would change the radial

growth pattern within a tree. The fitted line had no negative peaks at the position of tree ring in 2013, but raw data had (Fig. 2.6). This means abrupt change of $\delta^{18}O$ was ignored as an outlier when fitting was applied and analyzing more samples around the position of tree ring at 2013 would improve correlation among trees.

Once growth boundaries are detected based on xylem $\delta^{18}O$ chronology, radial growth increment could be easily calculated, and conventional tree ring analysis could be applied. However, to fully utilize intra-annual variation of $\delta^{18}O$, the way to average multiple xylem $\delta^{18}O$ chronologies would be needed. Since within-tree correlation and among-tree correlation are good, master chronology considering intra-annual variation of trees growth would be created if the number of samples are enough. To extend this approach to trees without visible growth ring, the way to detect peaks objectively is needed. In any case, more number of trees or species is needed to advance tropical dendrochronology using $\delta^{18}O$.

2.5. Summary

$\delta^{18}O$ of precipitation has a deceasing trend from spring to summer in the period from 2015 to 2018 and this seems to be a typical pattern in northeast Thailand. Xylem $\delta^{18}O$ of *T. grandis* showed annual cyclicity and the variation within a tree ring seems to be similar within tree and among trees. Xylem $\delta^{18}O$ of *T. grandis* had negative peaks at ring boundaries and the decreasing part of $\delta^{18}O$ at the following part of tree ring would reflect the decreasing trend of precipitation $\delta^{18}O$. Thus, radial cycle of xylem $\delta^{18}O$ could be interpreted as one year's growth of trees in this study site.

Table 2.1 Description of $\delta^{18}O$-analyzed samples

Tree	Core	DBH (cm)	Sampling date	Start	End
TG01	4	43.4	December 2017	2009	2017
TG03	1	41.1	March 2015	2006	2014
	2		March 2015	2006	2014
	4		December 2017	2014	2017
TG07	4	37.1	December 2017	2010	2017

Start is the year of oldest tree ring, and End is the year of most recent tree ring.

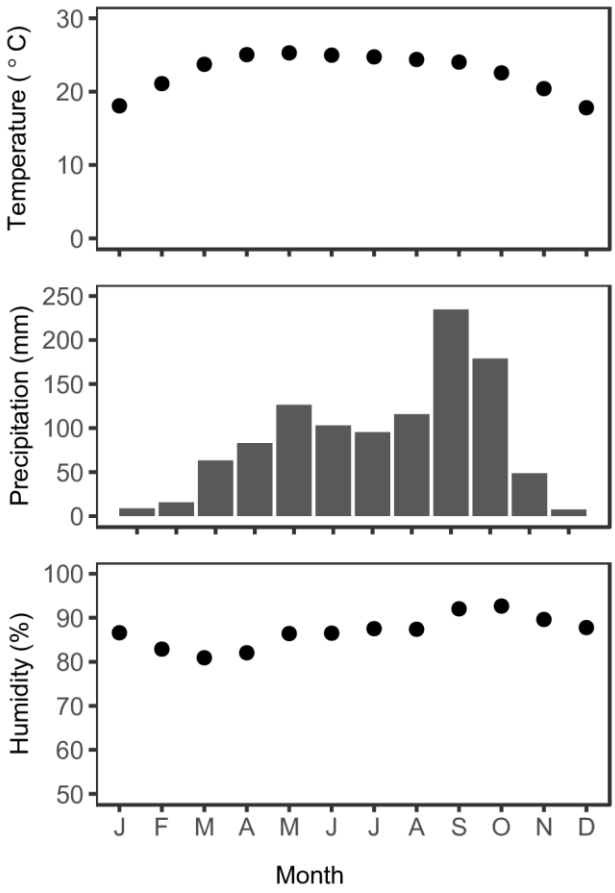

Fig. 2.1 Mean temperature (top), precipitation (middle), and humidity (bottom) of Sakaerat Environmental Research Station (SERS) from 1969 to 2017.

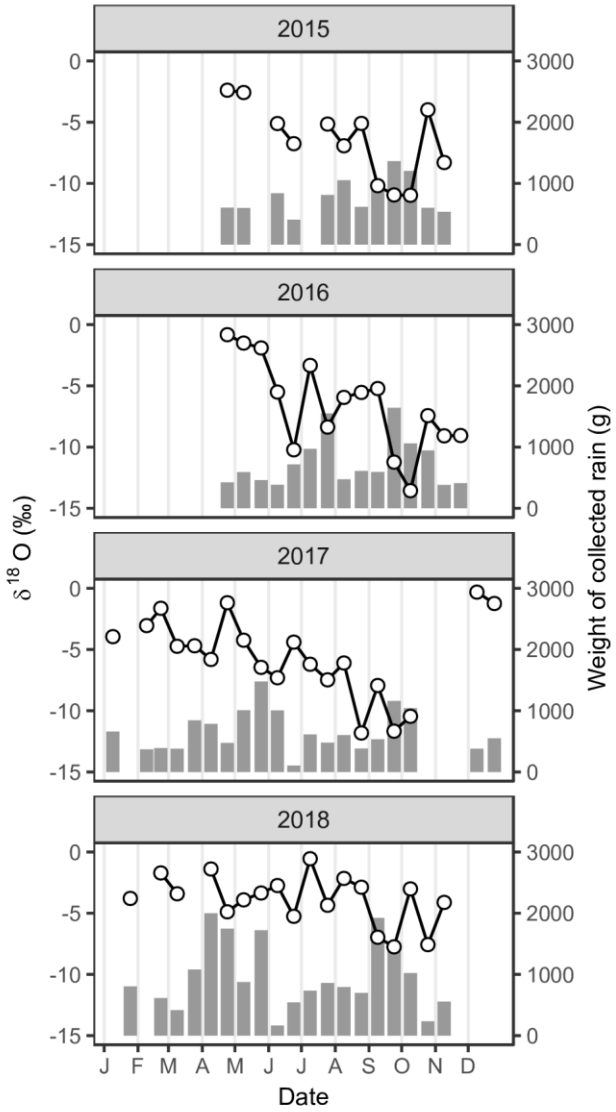

Fig. 2.2 $\delta^{18}O$ of precipitation (circle) and weight of collected rain sample (bar) from May 2015 to November 2018. Samples were collected on the 1st and the 16th every month. The data are plotted between two consecutive collection date. Missing values are because of no rain, except for the data on April 1st, 2018. Only the weight was plotted for the sample collected on April 1st, 2018 because the sample was lost before analysis.

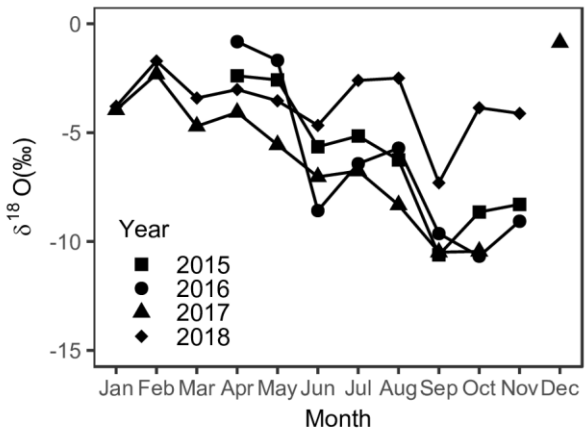

Fig. 2.3 Monthly change of precipitation $\delta^{18}O$. The values of each month were weighted by collected amount and shown as mean values.

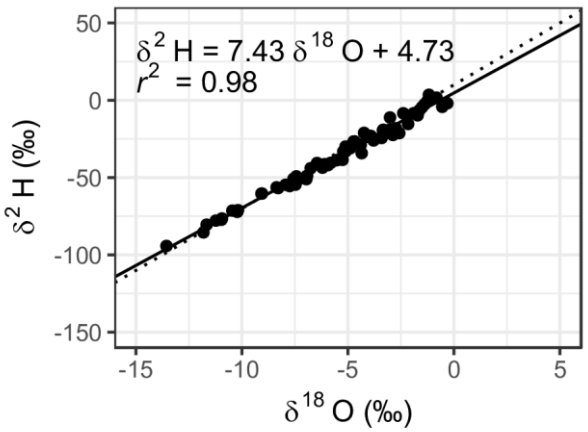

Fig. 2.4 The relationship between δ^2H and δ^{18}O in precipitation. A dotted line is the linear regression line ($\delta^2\mathrm{H} = 7.43\ \delta^{18}\mathrm{O} + 4.73$; local meteoric water line) and a solid line is the global meteoric water line ($\delta^2\mathrm{H} = 8\ \delta^{18}\mathrm{O} + 10$)

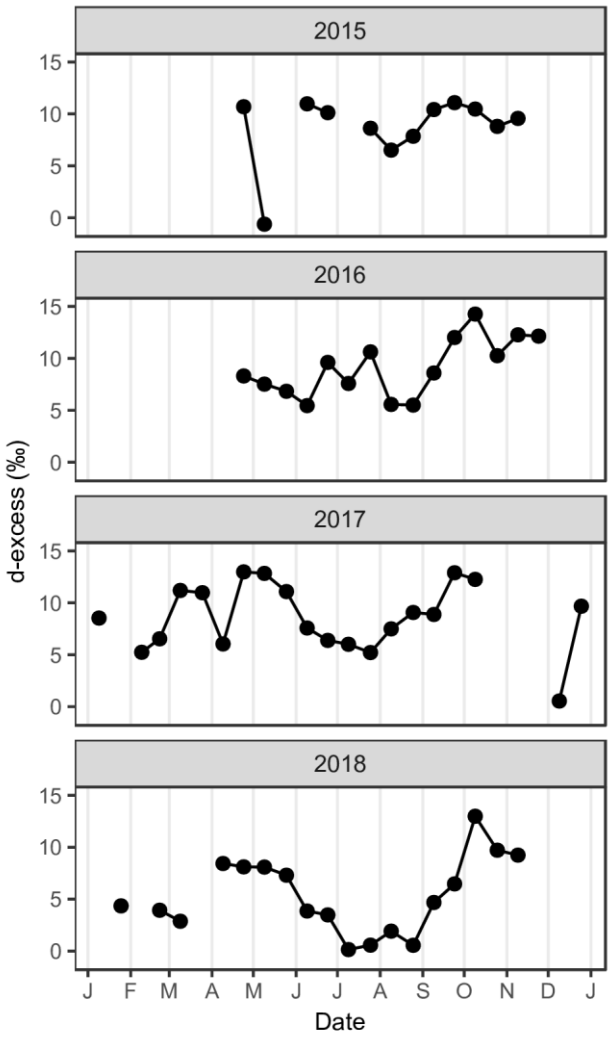

Fig. 2.5 The deuterium excess (d-excess) values of rain sample in SERS from May 2015 to November 2018. Samples were collected on the 1st and the 16th every month. The data are plotted between two consecutive collection date. Missing values are because of no rain, except for the data on April 1st, 2018, which was lost before analysis.

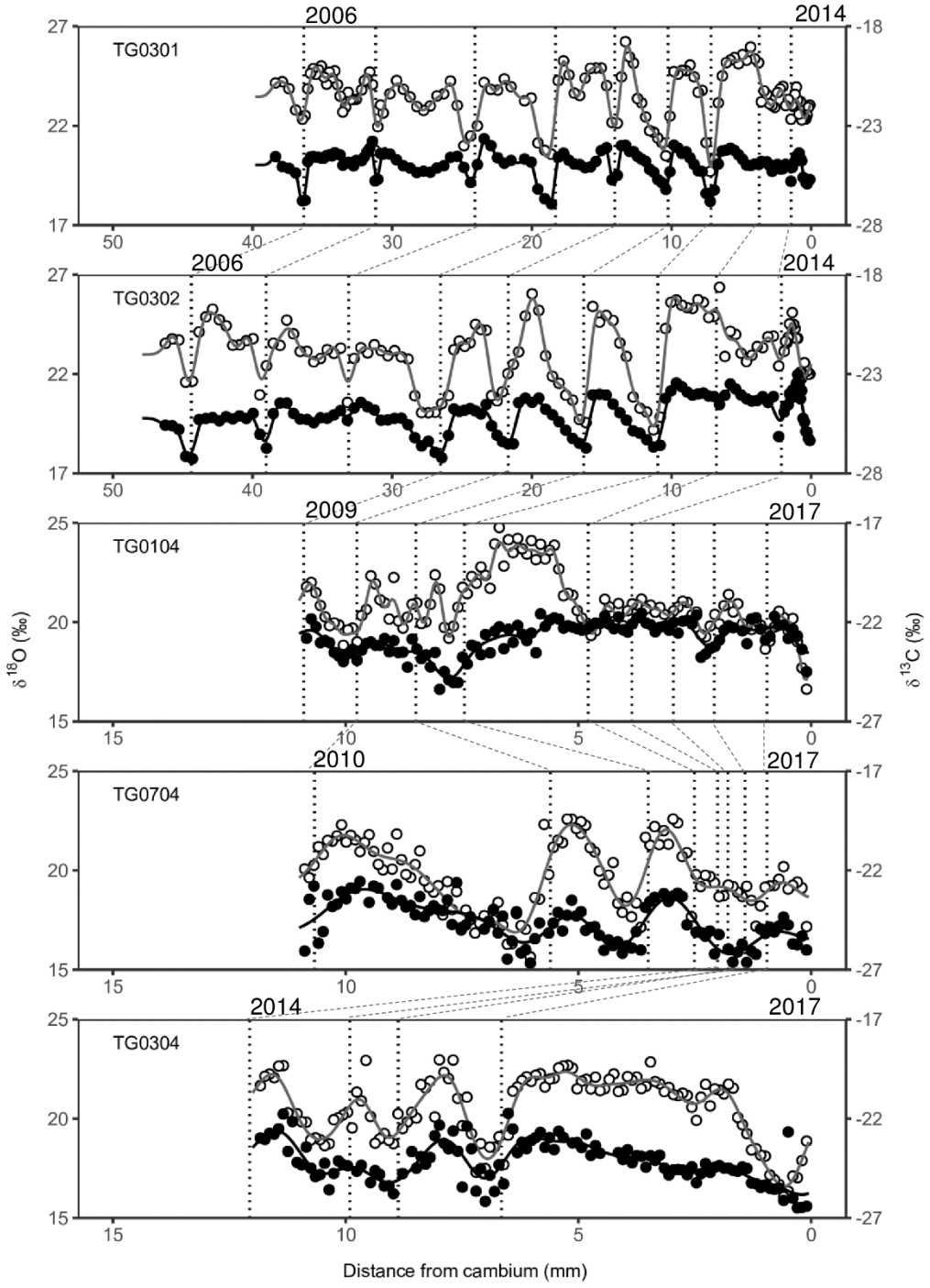

Fig. 2.6 $\delta^{18}O$ (raw: open circle; fitted: gray line) and $\delta^{13}C$ (raw: filled circle; fitted: black line) of xylem (*T. grandis*). TG0301, TG0302, and TG0304 were collected from same tree. TG0301 and TG0302 were collected in March 2015 and the outermost tree ring was produced in 2014. TG0104, TG0304, and TG0704 were collected in December 2017 and the outermost tree ring was produced in 2017. Vertical dotted lines are the position of ring boundaries.

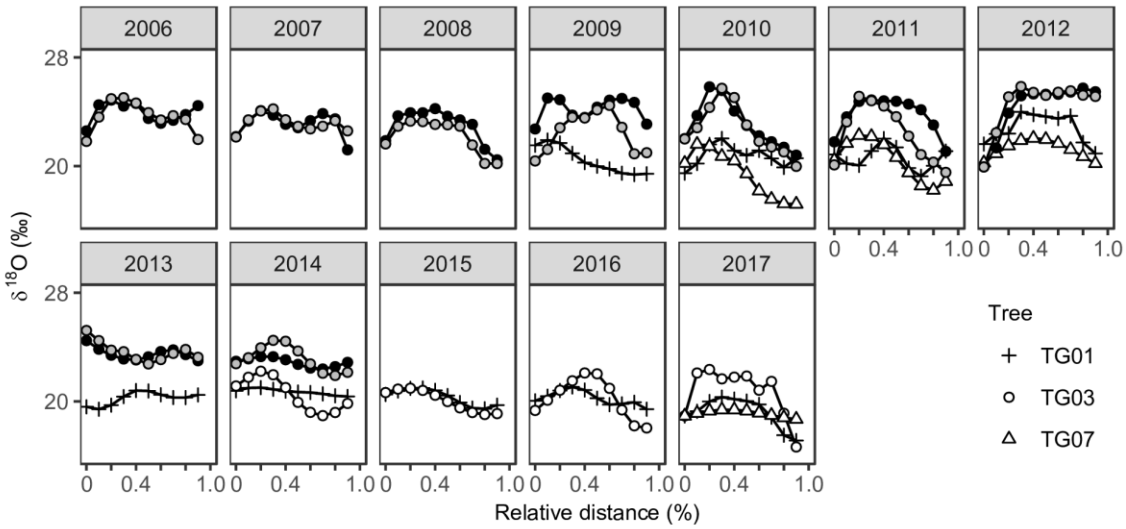

Fig. 2.7 Intra-annual variation of xylem $\delta^{18}O$. Values are plotted against relative distance from growth ring boundaries. For tree TG03, black circle is TG0301, gray circle is TG0302, and white circle is TG0304. Tree rings from 2013 to 2016 in TG0704 were not used because the ring width was too narrow.

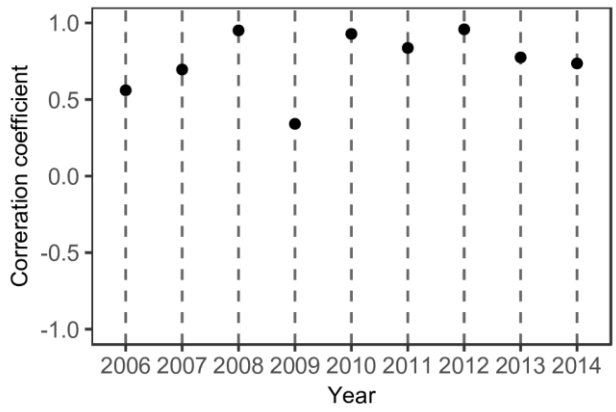

Fig. 2.8 Within-tree correlation of xylem $\delta^{18}O$ in *T. grandis*. Two cores (TG0301 and TG0302) collected from tree TG03 were compared.

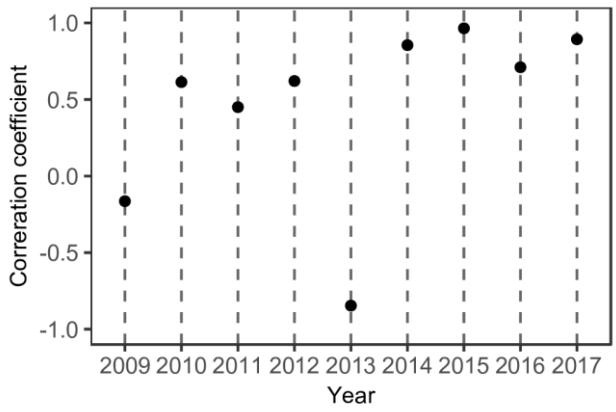

Fig. 2.9 Among-tree correlation of xylem $\delta^{18}O$ in *T. grandis*. Each value is the mean of correlation coefficients for possible pairs of different trees. Cores collected from one tree were averaged. Tree rings from 2013 to 2016 in TG0704 were not used because the ring width was too narrow.

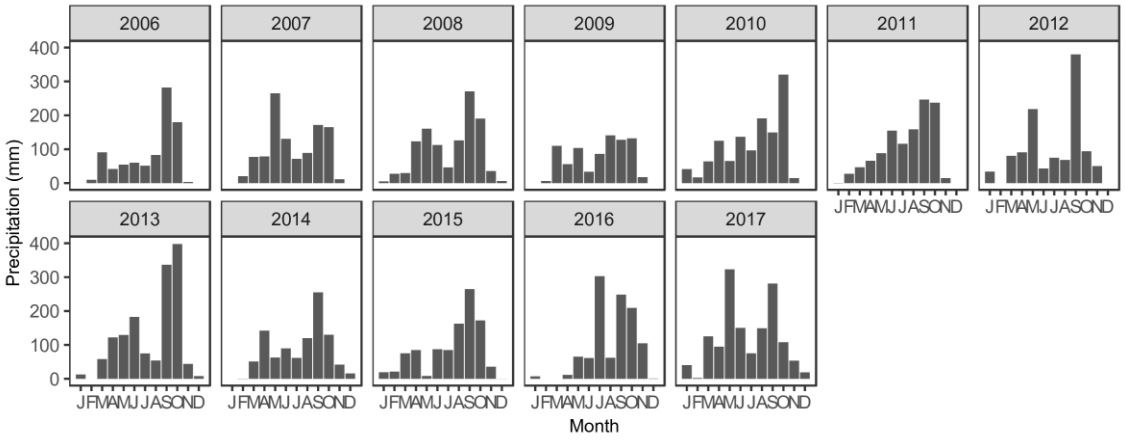

Fig. 2.10 Monthly precipitation in SERS from 2006 to 2017.

Chapter 3 Application of high-voltage DC pulse to ring-less trees for cambial marking

3.1. Introduction

Cambial marking (Wolter 1968; Shiokura 1989) is a simple method for estimating periodical wood formation. The cambium is injured mechanically, and the scars produced work as time markers. While the position of scars tells us xylem formation after marking, these scars also causes some problems. The marking often induces the formation of excessive traumatic tissue around the scars, causing error in determining xylem increment after marking. In addition, marking positions have to be changed for repeated application to avoid interactions of the neighboring wound tissues (Sass et al. 1995). These problems make it difficult to estimate annual growth accurately because radial growth rate is different by direction. In this study, the author tested cambial marking by electric stimulation instead of mechanical stimulation to solve the problems of the conventional marking method.

The effect of electric stimulation on xylem formation was studied for coniferous trees by Imagawa and Ishida (1981) and for broad-leaved trees by Imagawa and Ishida (1983). Imagawa and Ishida (1981) studied reaction of *Abies sachalinensis* to electric stimulation under several conditions changing magnitude of voltage (1.5, 12, 135 and 337.5 V), direction of electrodes (horizontal and vertical), distance between electrodes (1, 3, 5, 6 and 40 cm), and duration of stimulation (5 seconds, 10 minutes, 1 hour and 2 hours). As a result, they found radially crushed cells aligned tangentially and concluded that a stimulation at 135 V for 5 seconds applied to electrodes inserted 6 cm apart vertically could inscribe mark to xylem successfully. Imagawa and Ishida (1983) applied electric stimulation at 154 V for 5 seconds to *Alnus japonica* and *Cinnamomum camphora*. They found radially crushed cells aligned tangentially. The crushed cells were wood fibers which had thin wall. They also found ray parenchyma cells extended in shape and crushed vessels. Furthermore, they found that normal cells were produced after marking, meaning that electric stimulation did not kill the cambium and the influence was temporally.

Since influenced region is very small and the influence is temporal, the marking by electric stimulation has an advantage over the marking by mechanical stimulation. However, the condition of marking, especially magnitude of electricity and duration of stimulation, needs to be optimized to minimize influenced region and to apply marking on same position repeatedly.

In this chapter, the author tested applicability of high-voltage DC pulse marking to trees with no rings in tropics. The study was conducted in a seasonally dry forest and a tropical rainforest. Tree growth in the former is more seasonal than those in the latter, and the difference is favorable to compare trees' response to the marking under different growing conditions.

3.2. Materials and methods

3.2.1. Study site

For seasonally dry forests, neighboring two sites, the Sakaerat Silvicultural Research Station (SSRS; 14º28′ 06.1″N, 101º54′15.0″E) and the Sakaerat Environmental Research Station (SERS; 14°30'37.0"N,

101°55'51.4"E), Nakhon Ratchasima Province, Northeast Thailand were selected (Fig. 3.1). Two plots of dry evergreen forests (FOI and FOII) are selected from SSRS. A dry dipterocarp forest and a dry evergreen forest are selected from SERS. Mean annual temperature and annual precipitation was 23.0 °C and 1169 mm (2011–2017) (Sakaerat Environmental Research Station 2018). In this region, rainy season usually starts in May and continues until October (Fig. 3.2).

For a tropical rainfores, a secondary disturbed lowland dipterocarp forest in Ayer Hitam Forest Researve (AHFR, 3º1′ N, 101º39′ E), Selangor, Malaysia, was selected (Fig. 3.1). Mean annual temperature and annual precipitation was 27.8 °C and 2536 mm (2006–2015, Kuala Lumpur) (National Climatic Data Center 2017). Monthly precipitation is usually more than 100 mm all year round (Fig. 3.2).

3.2.2. Sample trees

Seven trees (four species) were selected from FOI and eight trees (seven species) were selected from FOII in SSRS (Table 3.1). All of them are canopy or sub-canopy species and evergreen. Thirteen trees (seven species) were selected from the dry evergreen forest and 5 trees (one species: *Irvingia malayana*) were selected from the dry dipterocarp forest in SERS (Table 3.2). All of them are canopy species and evergreen except *I. malayana*, which has short leaf life span (< 1 year) and is classified as semi-deciduous (Ishida et al. 2014). Five trees (five species), all of which are Dipterocarpaceae, were selected from AHFR (Table 3.3).

3.2.3. High voltage DC pulse marking

High voltage DC pulse marking was conducted with a custom-designed apparatus (Hokusetsu Systems, Sakai, Osaka, Japan), which was driven by 8 AA batteries. Two stainless steel nails of 1.2 mm thick and 25 mm long were used as electrodes. The nails were inserted into each tree stem at about 1.3 m height, and DC pulse in 0.5 seconds at 500 V was applied. Samples were collected from middle of electrodes with an increment borer of 5 mm in diameter in both sites.

DC pulse was applied once to electrodes inserted 5 cm apart in longitudinal direction for trees of SRRS and SERS on each day of marking. As for trees of SSRS, DC pulse marking was applied five times; May 2011, September 2011, February 2012, February 2013, and August 2013. Thus, DC pulse marking was applied 4 times to trees collected in August 2013 and the marking was applied 5 times to trees collected in February 2014. As for trees of SERS, DC pulse marking was applied in March 2015.

The distance between electrodes was 5 cm or 7 cm for trees of Ayer Hitam and DC pulse was applied once or twice to electrodes on each day of marking (Table 3.3). DC pulse marking was applied two times; October 2014 and March 2016.

3.2.4. Sample preparation

Sample cores (5 mm in diameter) were extracted with an increment borer. Transverse sections in 20–30 μm thick were cut using a sliding microtome and double stained with safranine and fast green, or safranine and alcian blue. Each section was observed microscopically under a compound microscope (Olympus BX50) to examine tissues affected by DC pulse marking.

3.3. Results

3.3.1. Responses of trees to DC pulse markings in SSRS and SERS

Marks produced by DC pulse marking were observed in three trees out of 15 trees in SSRS; one of *Hopea ferrea* (FOI-9), *Garcinia cowa* (FOII-3), and one of *Celtis timorensis* (FOII-11). *G. cowa* had all five marks (Fig. 3.4), but *H. ferrea* had one mark (Fig. 3.3) and *C. timorensis* had two marks (Fig. 3.5). Tissues affected by DC pulse marking were different among trees, and different among five markings. In *G. cowa*, deformed ray parenchyma was observed at the 1st (May 2011) and the 2nd (September 2011) marks (Fig. 3.4 a, b); thin walled wood fiber, most of which was crushed, was observed at the 3rd (February 2012), the 4th (February 2013); and the 5th (August 2013) marks (Fig. 3.4 b, c, d), and crushed vessel was observed at 4th mark (Fig. 3.4 d). In *C. timorensis*, deformed ray parenchyma and thin walled wood fiber were observed at both marks (Fig. 3.5 a, b). Although *C. timorensis* lacks three marks, it had growth rings at 8.1 mm, 2.7 mm, and 1.63 mm from the cambium (Fig. 3.6). Judging from the position of growth ring boundaries, these two marks might be formed by the 1st (May 2011) and the 2nd (September 2011) markings. In *H. ferrea*, deformed ray parenchyma was observed (Fig. 3.3). The mark in *H. ferrea* could not be dated because other four marks were not observed.

Marks produced by DC pulse marking were observed in three trees out of 13 trees in SERS; one *Hopea ferrea* (DEF2), *Carallia brachiata*, and one *Irvingia malayana* (IM4). These marks were produced in March 2015. In *H. ferrea*, deformed ray parenchyma was observed (Fig. 3.7). In *C. brachiata*, small diameter vessels were observed in core collected from the middle point of two electrodes, and crushed vessel was observed in core collected above the upper electrode (Fig. 3.8 a, b). In *I. malayana*, deformed ray parenchyma was observed, and small diameter vessels aligned tangentially (Fig. 3.9).

3.3.2. Responses of trees to DC pulse markings in AHFR

The 1st marking was applied in October 2014 and the 2nd marking was applied in March 2016. Marks produced by DC pulse marking were observed all samples except for *Dipterocarpus verucucus*. As for *Shorea acuminata*, marks observed in SA4-1 (7-cm electrode spacing, 500 V, 1 time; Fig. 3.10 a, b) and SA4-2 (7-cm electrode spacing, 500 V, 2 times; Fig. 3.10 c, d) and cell deposit was observed under both marking condition. Axial resin canals were aligned tangentially with cell deposits in some marks (Fig. 3.10 a, b, and d). SA4-3 (5-cm electrode spacing, 500 V, 2 times) was not analyzed because of wounded tissues caused by electrode insertion. As for *Shorea macroptera*, deformed ray parenchyma was observed in SM3-1 (7-cm electrode spacing, 500 V, 1 time; Fig. 3.11) but was not observed in SM3-2 (7-cm electrode spacing, 500 V, 2 time). SM3-3 (5-cm electrode spacing, 500 V, 2 times) was not analyzed because of wounded tissues caused by electrode insertion. *Shorea parvifolia* had cell deposits on the 1st mark, and deformed ray parenchyma and small diameter vessels on the 2nd mark (Fig. 3.12). *Shorea leprosula* also had cell deposits on the 1st mark, and deformed ray parenchyma and small diameter vessels on the 2nd mark (Fig. 3.13).

3.4. Discussion

3.4.1. Difference in responses to DC pulse marking between seasonally dry forest and tropical rainforest

Responses of xylem tissue to DC pulse marking could be interpreted as follows. Cells forming secondary wall stop further formation by electric stimulation, resulted in thin walled cells. Because these thin walls are mechanically weak, they will be crushed by expansion of newly formed cells. Cambial initials seem not to die by DC pulse, but cells subsequently differentiated have abnormal features such as small diameter vessels, deformed ray parenchyma, and cell deposit in lumens. As for *Shorea* spp. (Dipterocarpaceae) axial resin canals were formed. Judging from these responses, the position of the cambial zone was considered to be the outer side of the thin walled tissues and crushed cell zone, where deformed ray parenchyma started to appear.

DC pulse marking successfully inscribed marks only in three trees in SSRS and in three trees in SERS. Even in the trees successfully marked, all marks were not observed in *H. ferrea* and *C. timorensis*. On the other hand, DC pulse markings successfully inscribed marks in all trees except for *D. verucucus* in AHFR. This difference was probably caused by difference in climate. The successfulness of marking by electric stimulation is affected by the condition of cambial activity (Imagawa and Ishida 1981). Monthly precipitation in AHFR is always more than 100 mm, whereas that in Sakaerat (SSRS and SERS) is below 100 mm in dry season lasting from November to April. Moreover, some marking in Sakaerat was carried out during short rain period. So, marking to some trees did not inscribe mark probably because xylem production of the tree was not active at the time of marking.

Three types of marks were observed in trees in Sakaerat; deformed ray parenchyma, thin walled wood fiber, and crushed vessels. Same kind of marks were also observed in the study conducted in temperate region (Imagawa and Ishida 1983), but the marks in this study were harder to identify because the extent of influence was small or influenced tissues were not aligned tangentially.

In AHFR, cell deposit was observed in *S. acuminata*, *S. parvifolia*, and *S. leprosula* (Figs. 3.10, 3.12, and 3.13). Although Imagawa and Ishida (1983) reported deposits were observed in vessel or paratracheal parenchyma cells, those of trees in AHFR seems to be distributed wider in radial direction. *S. acuminata* showed traumatic axial resin canals tangentially aligned. Some *Shorea* spp. species show axial resin canals in a concentric line under normal growing condition (Ogata et al. 2008), and this feature is not common in trees in temperate region. Although axial resin canals were formed without stimulation by DC pulse, axial resin canals at the marked position (Fig. 3.10 a, b, and d) were judged to be produced by DC pulse marking because traumatic resin canals were sometimes observed after cambial pinning (Nobuchi et al. 1995). In addition, axial resin canals observed in Fig. 3.10 (a, b, and d) are surrounded by the cells including deposits in their lumen. Axial resin canals observed in Fig. 3.10 (c) are not surrounded by the deposit-containing cells and located bellow the deposits zone. The marks of sample trees in AHFR were easier to recognize than that in Sakaerat. This is probably because cambial activity of trees in AHFR was more active through a year than that in Sakaerat.

3.4.2. Difference in responses to different intensity of DC pulse marking

In AHFR, different marking condition, 7-cm electrode spacing but applying DC pulse once or twice, were compared. In *S. acuminata*, cell deposits and axial resin canals were observed in both one-time and two-time of application (Fig. 3.10). No marks were observed in *S. macroptera* with two-time of application. Therefore, under the condition of 7-cm electrode spacing and 500 V of DC pulse, one-time of application might be enough to inscribe marks in the xylem, but uncertainty is remained about suitable condition. If marking intensity (applying voltage, applying time and electrode spacing) is enough, influenced tissues would be formed at the middle position of two electrodes because tissues influenced by electric stimulation distribute around the electrodes (Imagawa 1985). The suitable intensity of electric stimulation of trees in SERS (5 cm electrodes spacing) should be weaker than that of trees in AHFR (7-cm electrode spacing), but this needs more examination. The condition of marking should be improved considering both suitable intensity of electric stimulation and activity of xylem formation.

3.5. Summary

The applicability of high-voltage DC pulse marking was tested to trees with no distinct growth rings in tropics. The response to marking was compared between seasonally dry forest (Sakaerat) and tropical rainforest (AHFR). The trees in AHFR was more sensitive to DC pulse marking than those in Sakaerat probably because cambial activity was more active through a year in AHFR than in SERS. The tissues produced by marking were almost similar to those reported in previous studies, but some reaction might be specific to some species. Although the condition of marking still has room for improvement and more case study is needed, DC pulse marking method are applicable to trees in seasonally dry forest and tropical rainforest.

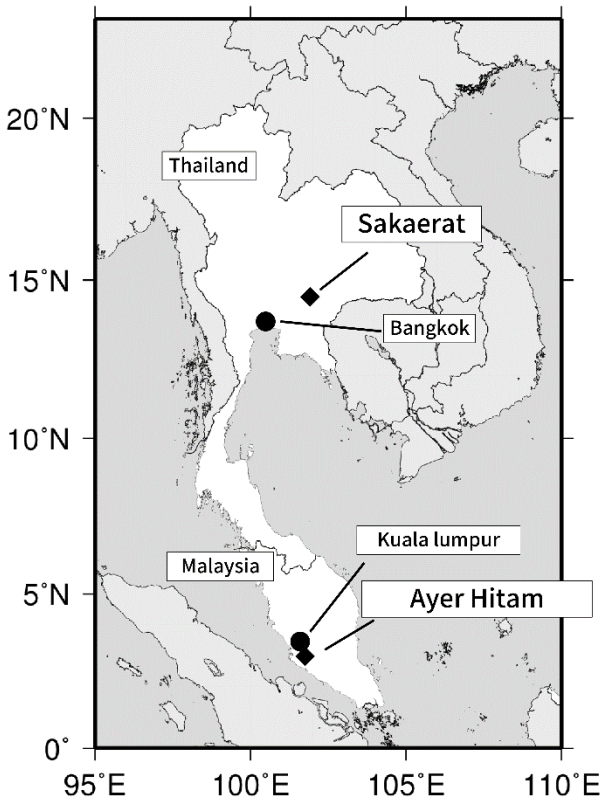

Fig. 3.1 Locations of study sites

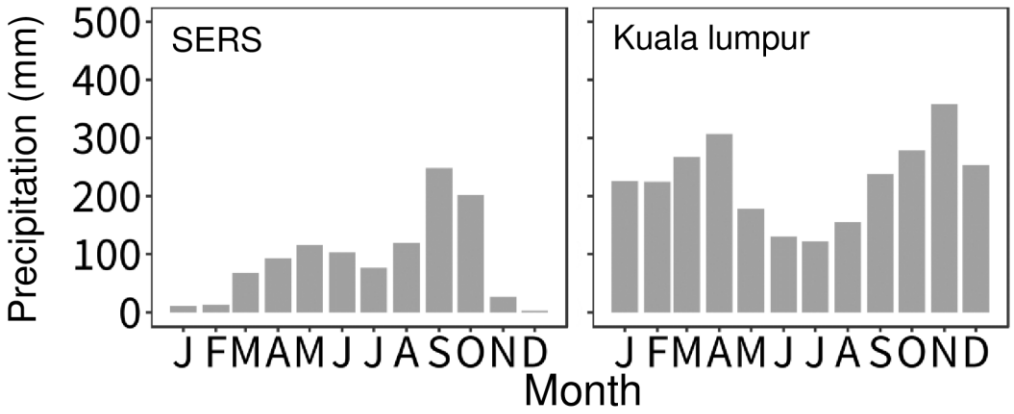

Fig. 3.2 Monthly precipitation in SERS and Kuala Lumpur (2006–2015)

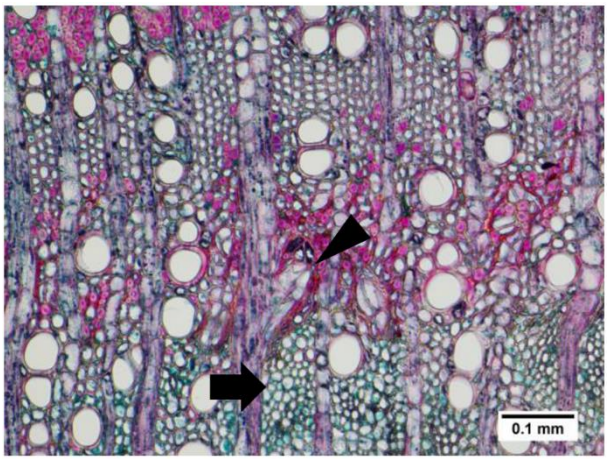

Fig. 3.3 Transverse secton of *Hopea ferrea* (FOI-9) in SSRS at 4.5 mm from cambium. Black arrowhead is deformed ray parenchyma and black arrow indicates thin walled wood fiber produced by DC pulse marking. Bark side is top direction.

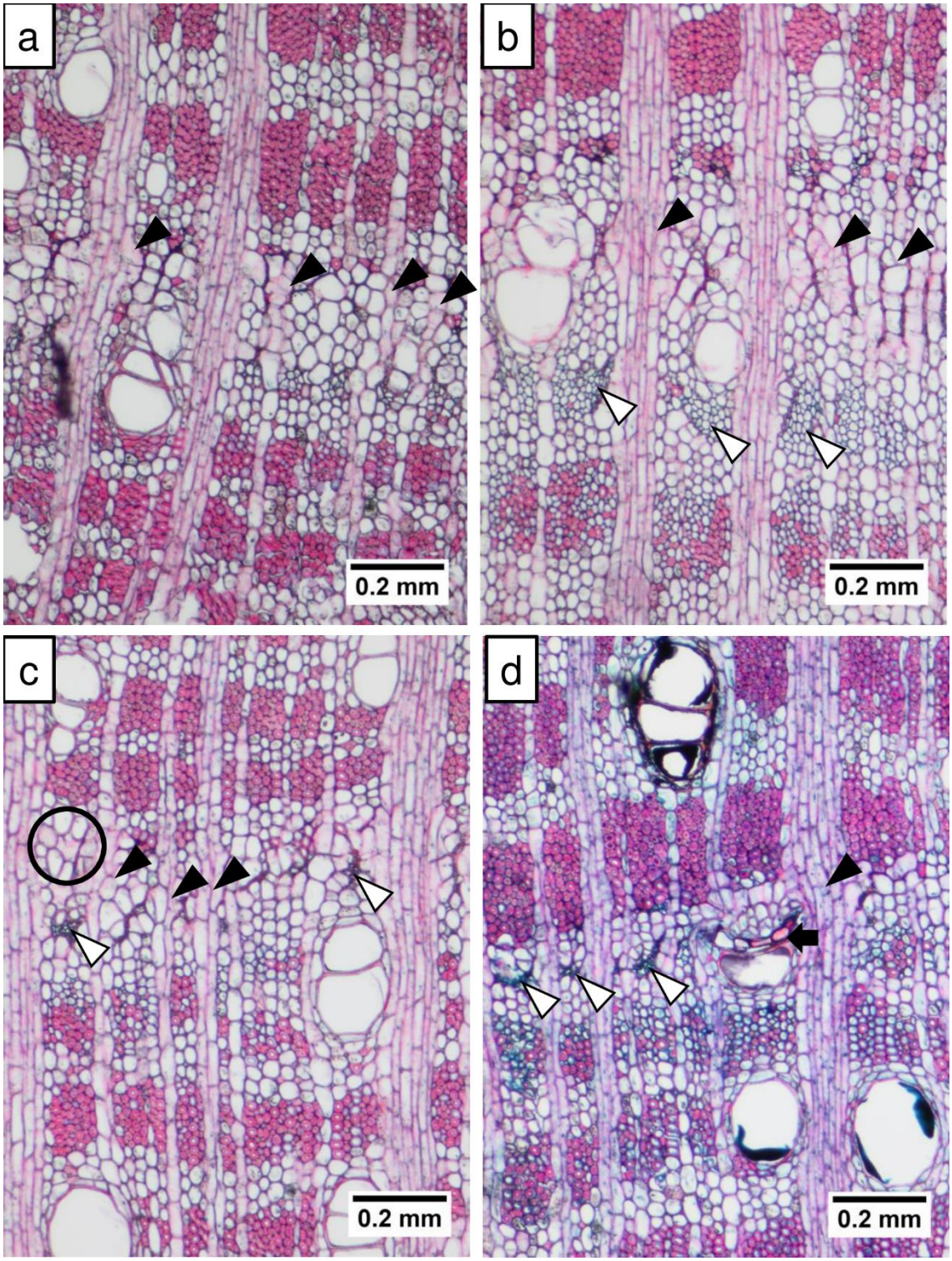

Fig. 3.4 Transverse sections of *Garcinia cowa* (FOII-3) in SSRS at 9.5 mm (a), 8.1 mm (b), 6.4 mm (c), 3.0 mm (d), and 1.1 mm (e) from cambium. Black arrowheads are deformed ray parenchyma, white arrowheads are thin-walled wood fiber, and black arrow is crushed vessel. Circle is axial parenchyma produced by DC pulse marking. Bark side is top direction. (Continue to next page)

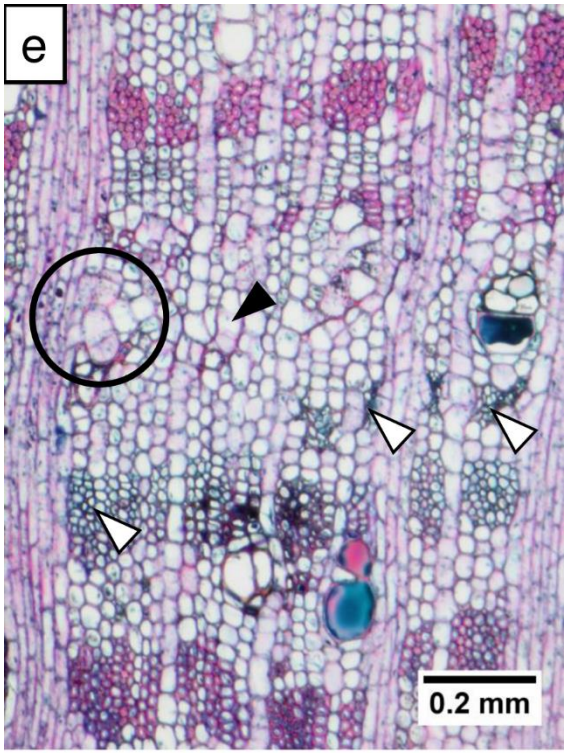

Fig. 3.4 (Cont.)

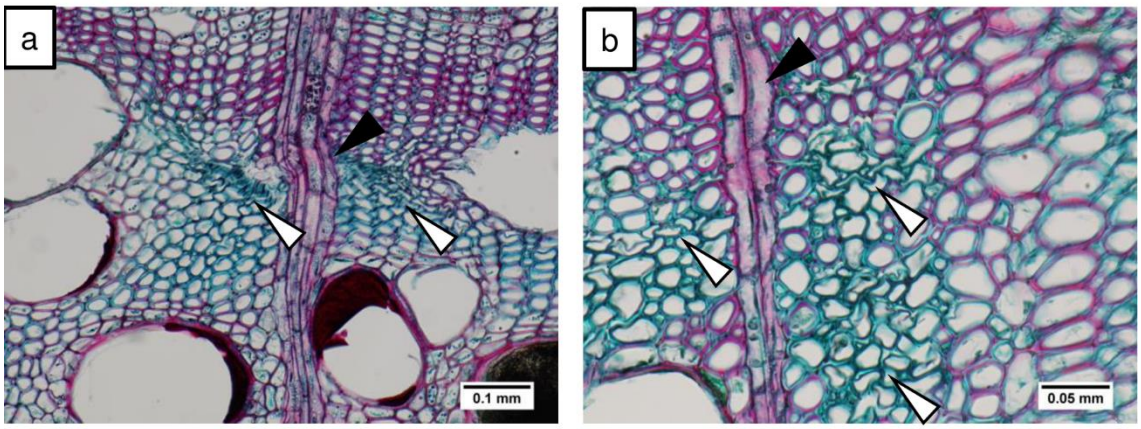

Fig. 3.5 Transverse sections of *Celtis timorensis* (FOII-11) in SSRS at 7.9 mm (a) and 3.9 mm (b) from cambium. Black arrowheads are deformed ray parenchyma and white arrowheads are crushed thin-walled wood fibers produced by DC pulse marking. Bark side is top direction.

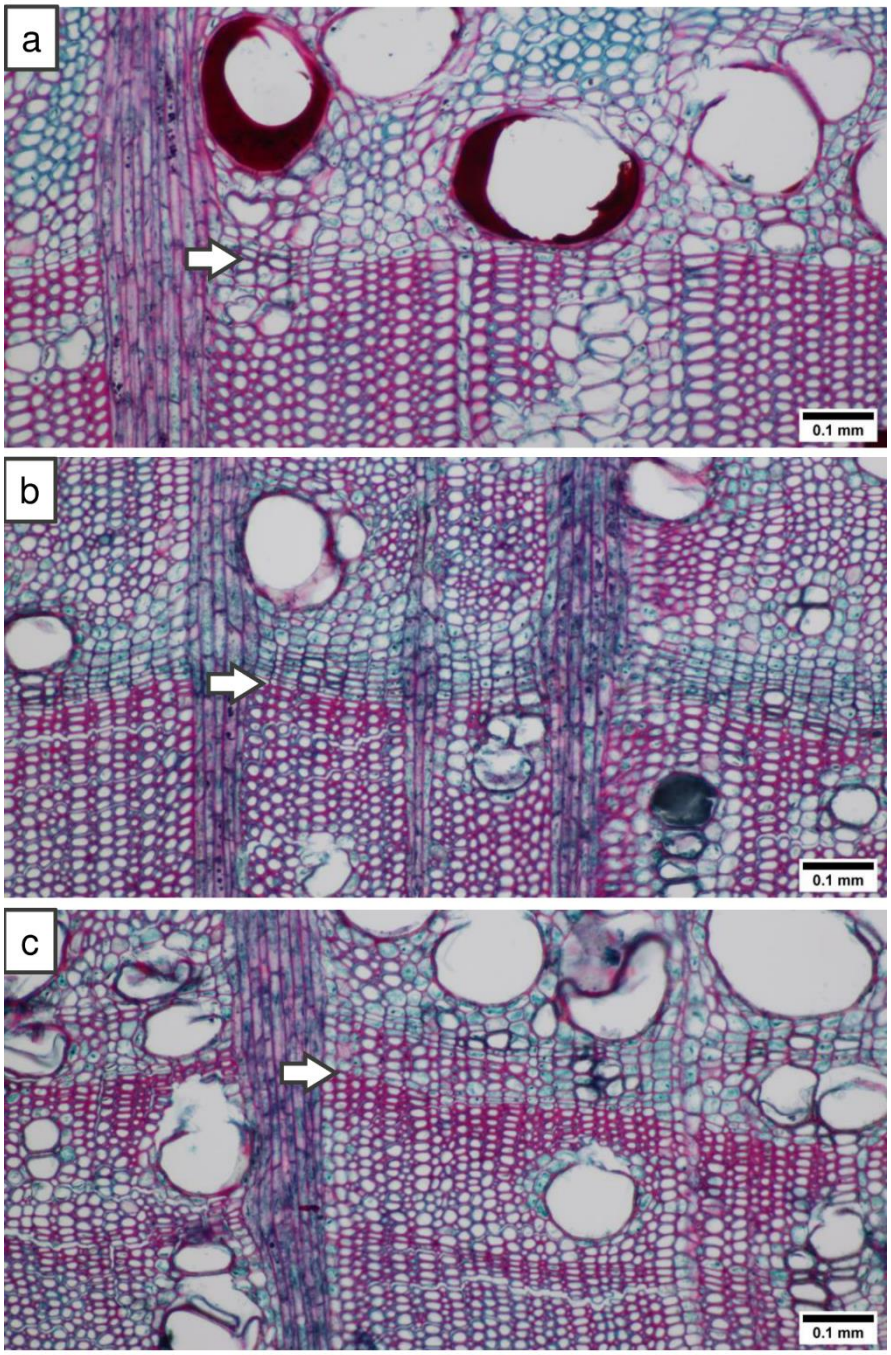

Fig. 3.6 Growth rings of *Celtis timorensis* (FOII-11) in SSRS observed at 8.14 mm (2011, a), 2.78 mm (2012, b), and 1.35 mm (2013, c) from cambium. White arrow indicates growth ring boundaries. Bark side is top direction.

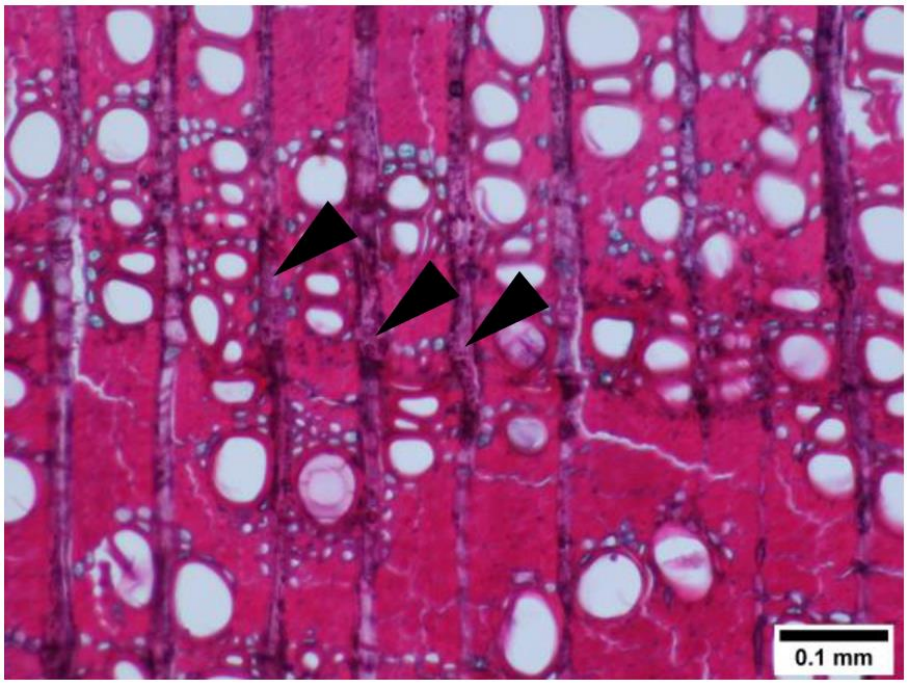

Fig. 3.7 Transverse section of *Hopea ferrea* (DEF2) in SERS. Black arrowheads indicate deformed ray parenchyma. Bark side is top direction.

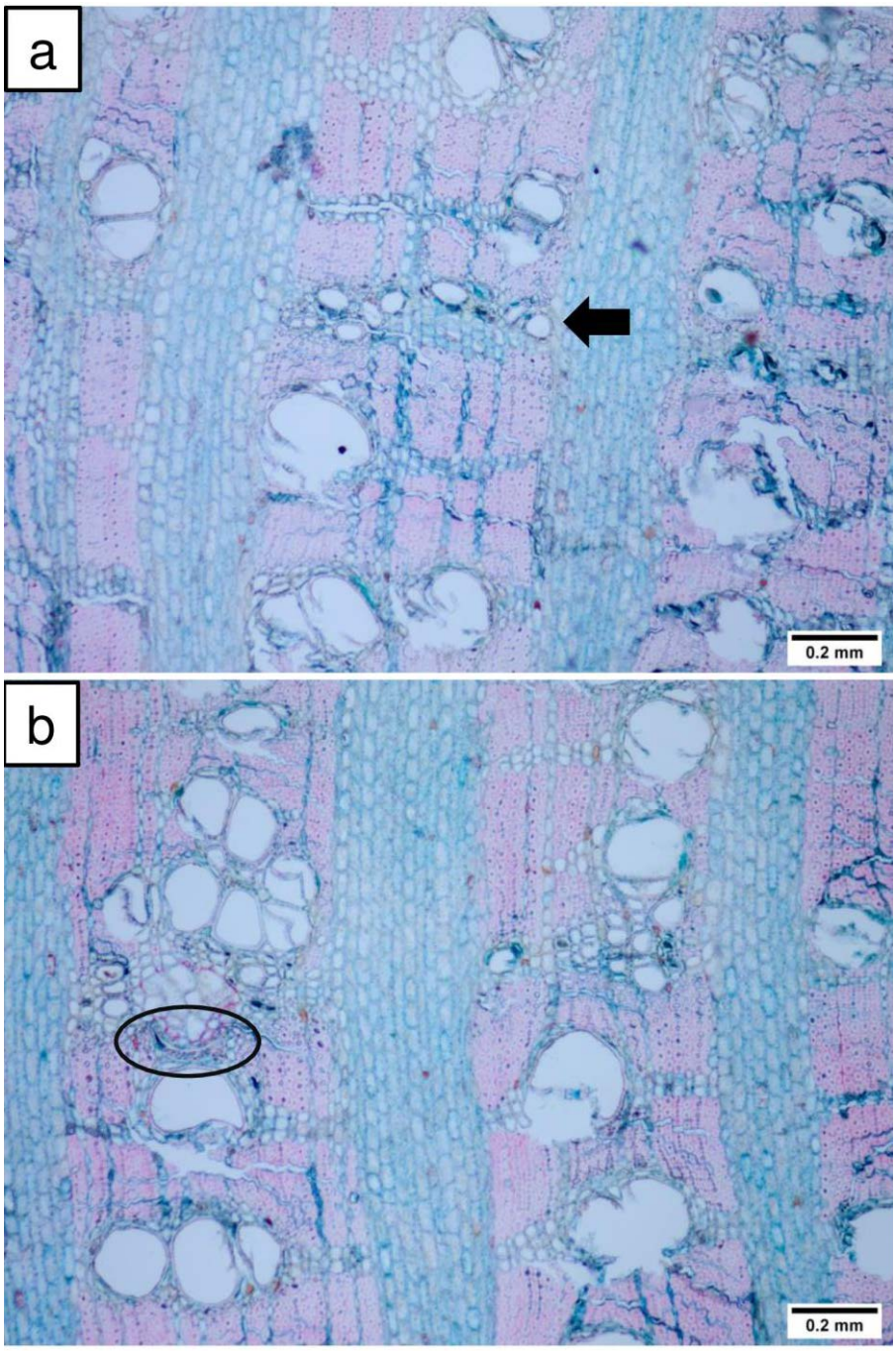

Fig. 3.8 Transverse sections of *Carallia brachiata* (DEF13) in SERS. (a) Traumatic tissue formed at 3.3 mm from the cambium in the core collected from middle of two electrodes. Black arrow indicates small diameter vessels. (b) Traumatic tissue formed at 2.8 mm from the cambium in the core collected from 10 mm above the upper electrode. Circle indicates crushed vessel. Bark side is top direction.

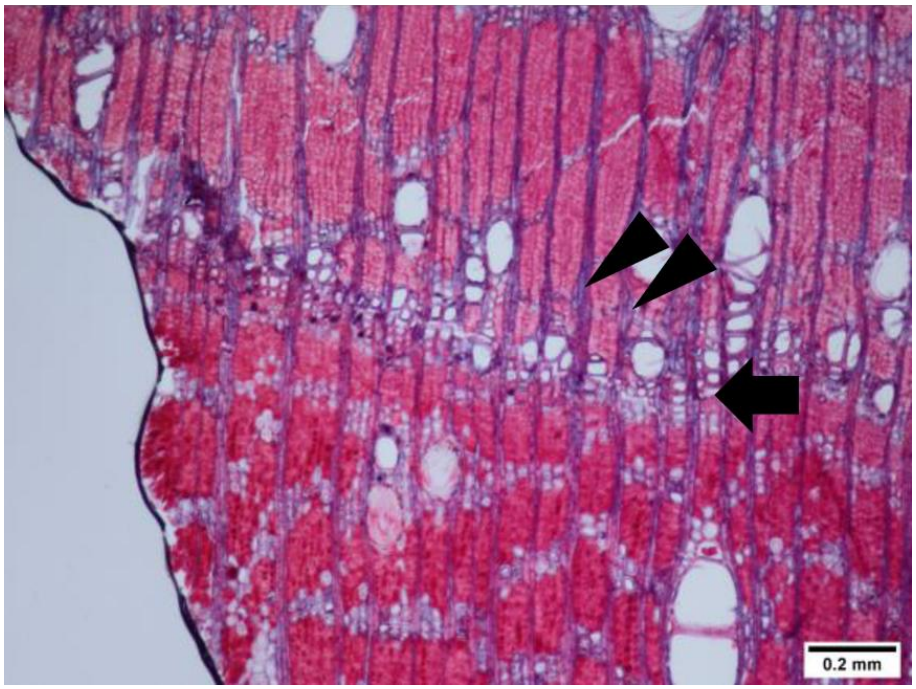

Fig. 3.9 Transverse section of *Irvingia malayana* (IM4) at 7.7 mm from cambium. Black arrowheads indicate deformed ray parenchyma. Bark side is top direction. Black arrow indicates small diameter vessels.

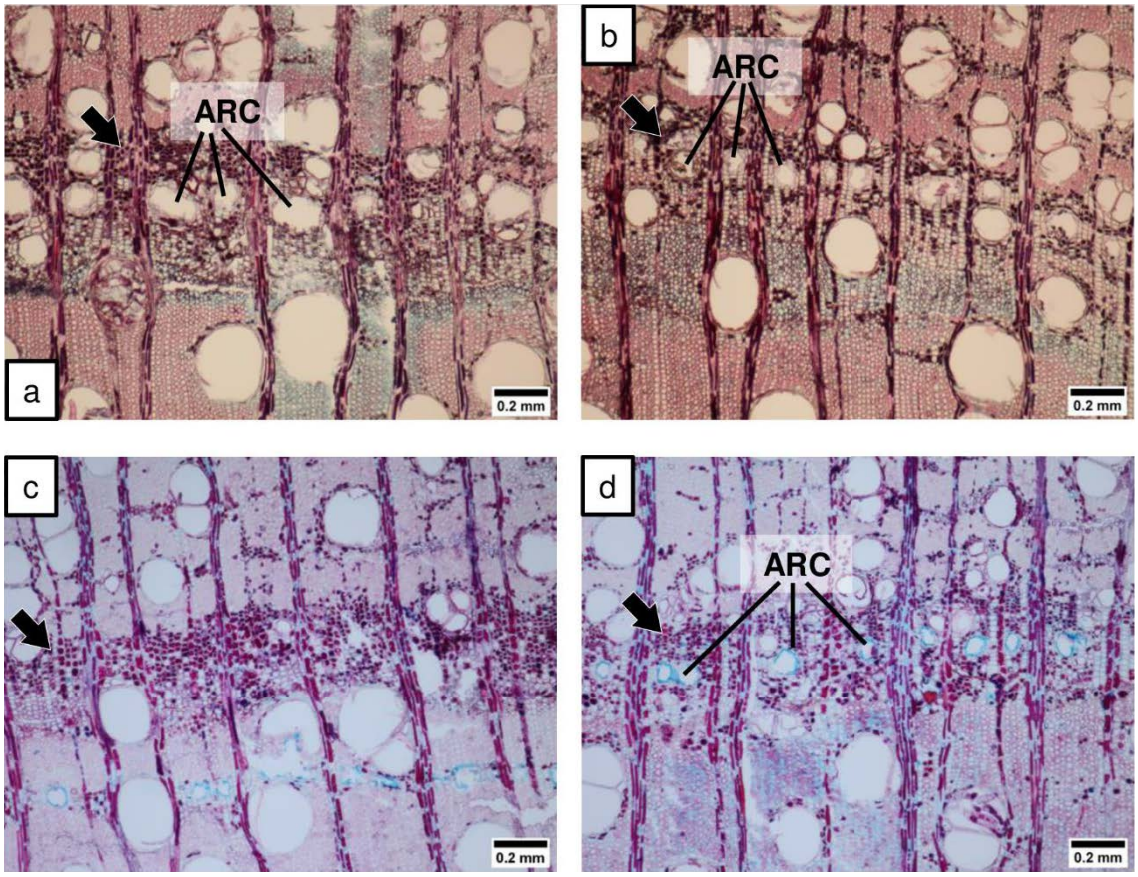

Fig. 3.10 Transverse section of *Shorea acuminata* (SA4) in AHFR collected in December 2016 (SA4-1; a and b), November 2017 (SA4-2; c and d). (a and c) mark produced in October 2014. (b and d) mark produced in March 2016. Electrodes were inserted 7 cm apart and 500 V of DC pulse was applied one time for SA4-1 (a and b) and two times for SA-4-2 (c and d) on each marking. Black arrows indicate cell deposit (a, b, c, and d). ARC indicate axial resin canals surrounded by the cells including deposits. Note that cells including deposits are not observed around the resin canals formed before marking (c). Bark side is top direction.

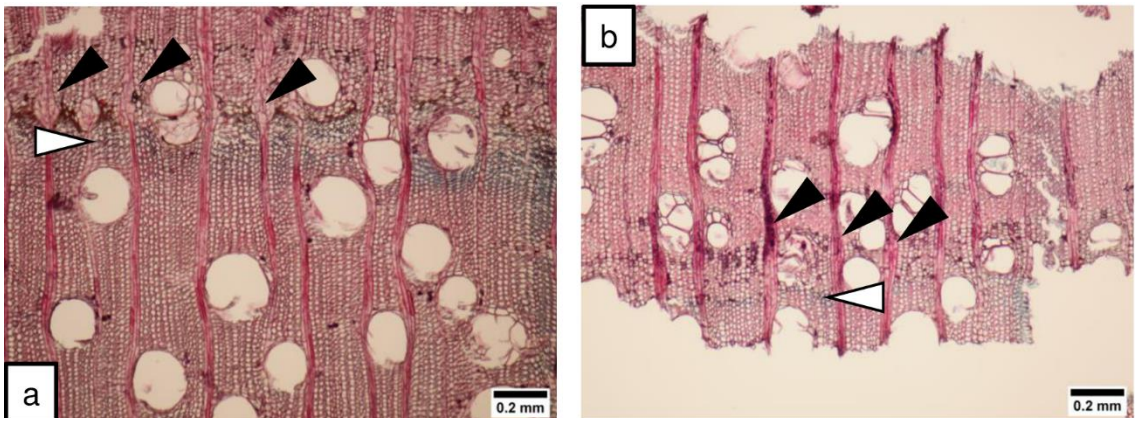

Fig. 3.11 Transverse section of *Shorea macroptera* (SM3) in AHFR collected in December 2016 (SM3-1; a, b), (a) mark produced in October 2014, (b) mark produced in March 2017. Electrodes were inserted 7 cm apart and 500 V of DC pulse was applied one time on each marking. Black arrowhead indicates deformed ray parenchyma and white arrowhead indicates thin walled wood fiber. Bark side is top direction.

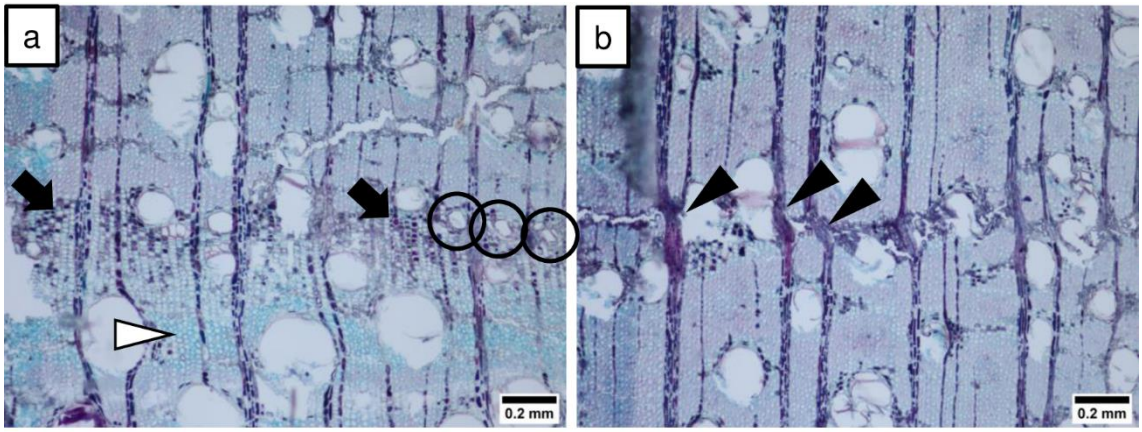

Fig. 3.12 Transverse section of *Shorea parvifolia* (SP2) in AHFR collected in December 2016 (SP2-1), (a) mark produced in October 2014, (b) mark produced in March 2016. Electrodes were inserted 7 cm apart and 500 V of DC pulse was applied one time on each marking. Black arrowheads indicate deformed ray parenchyma and white arrowheads indicate thin walled wood fiber, circles indicate small vessel, and black arrow indicate cell deposit. Bark side is top direction.

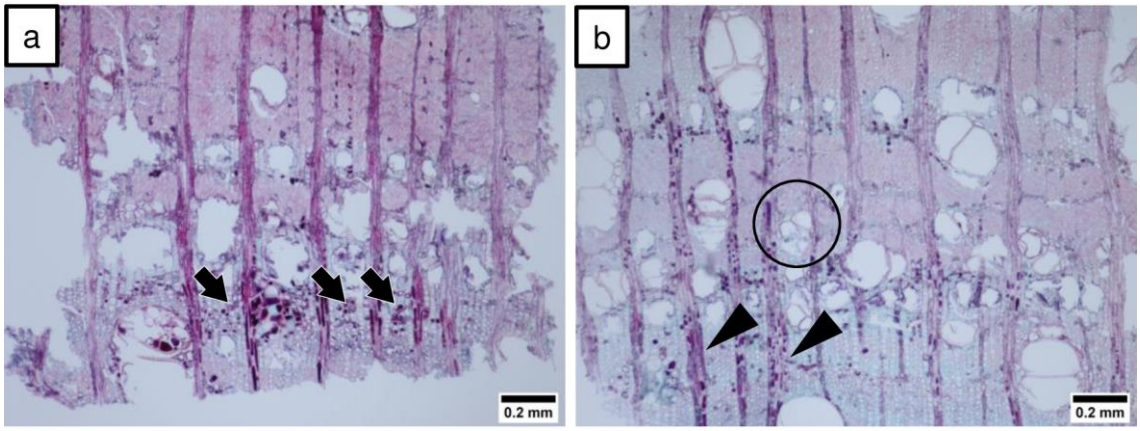

Fig. 3.13 Transverse section of *Shorea leprosula* (SL2) in AHFR collected in December 2016 (SL2-1), (a) mark produced in October 2014, (b) mark produced in March 2017. Electrodes were inserted 7 cm apart and 500 V of DC pulse was applied one time on each marking. Black arrowheads indicate deformed ray parenchyma, circle indicates small vessels, and black arrows indicate cell deposit. Bark side is top direction.

Table 3.1 Description of samples in SSRS

Tree	Core	Species (Family)	DBH (cm)	Condition	Date of marking	Collected
FOI-1	3	*Hydnocarpus ilicifolia* King (Achariaceae)	29.2	5cm, 500V, 1 time	May 2011, Sep 2011, Feb 2012, Feb 2013	Aug 2013
FOI-2	1	*Shorea henryana* (Dipterocarpaceae)	34.9	5cm, 500V, 1 time	May 2011, Sep 2011, Feb 2012, Feb 2013, Aug 2013	Feb 2014
FOI-3	1	*Walsura robusta* Roxb. (Meliaceae)	10.1	5cm, 500V, 1 time	May 2011, Sep 2011, Feb 2012, Feb 2013, Aug 2013	Feb 2014
FOI-4	1	*Hopea ferrea* (Dipterocarpaceae)	10.4	5cm, 500V, 1 time	May 2011, Sep 2011, Feb 2012, Feb 2013, Aug 2013	Feb 2014
FOI-5	3	*Hopea ferrea* (Dipterocarpaceae)	17.3	5cm, 500V, 1 time	May 2011, Sep 2011, Feb 2012, Feb 2013	Aug 2013
FOI-6	3	*Hopea ferrea* (Dipterocarpaceae)	25.7	5cm, 500V, 1 time	May 2011, Sep 2011, Feb 2012, Feb 2013	Aug 2013
FOI-9	1	*Hopea ferrea (Dipterocarpaceae)*	28.6	5cm, 500V, 1 time	May 2011, Sep 2011, Feb 2012, Feb 2013, Aug 2013	Feb 2014
FOII-1	3	*Shorea henryana (Dipterocarpaceae)*	12.0	5cm, 500V, 1 time	May 2011, Sep 2011, Feb 2012, Feb 2013	Aug 2013
FOII-3	1	*Garcinia cowa* Roxb. Ex DC. (Clusiaceae)	15.0	5cm, 500V, 1 time	May 2011, Sep 2011, Feb 2012, Feb 2013, Aug 2013	Feb 2014
FOII-4	3	*Vitex peduncularis* Wall. Ex Schauer (Lamiaceae)	34.7	5cm, 500V, 1 time	May 2011, Sep 2011, Feb 2012, Feb 2013	Aug 2013
FOII-5	1	*Walsura robusta* Roxb. (Meliaceae)	11.3	5cm, 500V, 1 time	May 2011, Sep 2011, Feb 2012, Feb 2013, Aug 2013	Feb 2014
FOII-7	1	*Celtis timorensis* Span (Cannabaceae)	32.5	5cm, 500V, 1 time	May 2011, Sep 2011, Feb 2012, Feb 2013, Aug 2013	Feb 2014
FOII-10	1	*Pterospermum acerifolium* (L.) Willd. (Malvaceae)	12.0	5cm, 500V, 1 time	May 2011, Sep 2011, Feb 2012, Feb 2013, Aug 2013	Feb 2014
FOII-11	1	*Celtis timorensis* Span (Cannabaceae)	26.9	5cm, 500V, 1 time	May 2011, Sep 2011, Feb 2012, Feb 2013, Aug 2013	Feb 2014
FOII-12	1	*Lithocarpus* sp. (Fagaceae)	28.8	5cm, 500V, 1 time	May 2011, Sep 2011, Feb 2012, Feb 2013, Aug 2013	Feb 2014

Table 3.2 Description of samples in SERS

Tree	Core	Species (Family)	DBH (cm)	Condition	Date of marking	Collected
DEF2	1	*Hopea ferrea* (Dipterocarpaceae)	27.4	5cm, 500V, 1 time	Mar 2015	Sep 2016
DEF4	1	*Hopea ferrea* (Dipterocarpaceae)	27.3	5cm, 500V, 1 time	Mar 2015	Sep 2016
DEF6	3	*Dehaasia candolleana* (Lauraceae)	25.9	5cm, 500V, 1 time	Mar 2015	Sep 2016
DEF8	2	*Hopea ferrea (Dipterocarpaceae)*	21.2	5cm, 500V, 1 time	Mar 2015	Sep 2016
DEF10	1	*Syzygium albiflorum* (Myrtaceae)	15.8	5cm, 500V, 1 time	Mar 2015	Sep 2016
DEF13	2	*Carallia brachiata* (Rhizophoraceae)	18.6	5cm, 500V, 1 time	Mar 2015	Nov 2017
DEF14	1	*Hydnocarpus ilicifolia* (Achariaceae)	30.2	5cm, 500V, 1 time	Mar 2015	Sep 2016
DEF15	1	*Aglaia elaeagnoidea* (Meliaceae)	17.3	5cm, 500V, 1 time	Mar 2015	Sep 2016
IM1	1	*Irvingia malayana* (Irvingiaceae)	47.6	5cm, 500V, 1 time	Mar 2015	Sep 2016
IM3	3	*Irvingia malayana* (Irvingiaceae)	25.7	5cm, 500V, 1 time	Mar 2015	Sep 2016
IM4	2	*Irvingia malayana* (Irvingiaceae)	33.2	5cm, 500V, 1 time	Mar 2015	Nov 2017
IM5	3	*Irvingia malayana* (Irvingiaceae)	26.3	5cm, 500V, 1 time	Mar 2015	Sep 2016
IM6	2	*Irvingia malayana* (Irvingiaceae)	25.4	5cm, 500V, 1 time	Mar 2015	Nov 2017

Table 3.3 Description of samples in AHFR

Tree	Core	Species	DBH (cm)	Condition	Date of marking	Collected
SM3	1	*Shorea macroptera* (Dipterocarpaceae)	34.1	7 cm, 500 V, 1 time	Oct 2014, Mar 2016	Dec 2016
	2			7 cm, 500 V, 2 times	Oct 2014, Mar 2016	Nov 2017
	3**			5 cm, 500 V, 2 times	Oct 2014, Mar 2016	Nov 2017
SP2	1	*Shorea parvifolia* (Dipterocarpaceae)	36.9	7 cm, 500 V, 1 time	Oct 2014, Mar 2016	Dec 2016
	2*			7 cm, 500 V, 2 times	Oct 2014, Mar 2016	Nov 2017
	3*			5 cm, 500 V, 2 times	Oct 2014, Mar 2016	Nov 2017
SA4	1	*Shorea acuminata* (Dipterocarpaceae)	38.3	7 cm, 500 V, 1 time	Oct 2014, Mar 2016	Dec 2016
	2			7 cm, 500 V, 2 times	Oct 2014, Mar 2016	Nov 2017
	3**			5 cm, 500 V, 2 times	Oct 2014, Mar 2016	Nov 2017
SL2	1	*Shorea leprosula* (Dipterocarpaceae)	51.3	7 cm, 500 V, 1 time	Oct 2014, Mar 2016	Dec 2016
	2*			7 cm, 500 V, 2 times	Oct 2014, Mar 2016	Nov 2017
	3*			5 cm, 500 V, 2 times	Oct 2014, Mar 2016	Nov 2017
DV3	1	*Dipterocarpus verucucus* (Dipterocarpaceae)	55.6	7 cm, 500 V, 1 time	Oct 2014, Mar 2016	Dec 2016
	2*			7 cm, 500 V, 2 times	Oct 2014, Mar 2016	Nov 2017
	3			5 cm, 500 V, 2 times	Oct 2014, Mar 2016	Nov 2017

Condition: distance between electrodes, voltage of electric stimulation, number of times DC pulse marking applied at one marking

* Samples not processed yet

** Samples not used because of wounded tissues caused by electrodes

Chapter 4 Cyclic variation of $\delta^{18}O$ in ring-less trees in northeastern Thailand

4.1 Introduction

In tropical region, dendrochronological analysis is limited to specific species because many species do not have visible annual rings (Worbes 2002). For developing tree ring study in tropical region, it is necessary to analyze trees with no visible annual rings. In this point of view, various approaches have been attempted to detect annual rings.

Annual ring detection requires two steps: (1) selection of growth indicator as tree ring proxy and (2) age determination of the growth indicator. For example, tree-ring like structure such as marginal parenchyma (Abdul Azim and Okada 2014), cyclic changes of vessel size and frequency (Ohashi et al. 2014), and fluctuation of stable carbon and oxygen isotope ratio (Poussart et al. 2004; Verheyden et al. 2004; Ohashi et al. 2009, 2016; Pons and Helle 2011) have been studied as a growth indicator. These growth indicators are dated by several methods such as cambial marking (Wolter 1968; Sass et al. 1995), radio-carbon dating (Kurokawa et al. 2003; Poussart and Schrag 2005), and monitoring of radial growth with dendrometer (Worbes 1999).

Cyclic change of stable oxygen isotope ratio ($\delta^{18}O$) is used in recent several studies in growth indicators (Poussart et al. 2004; Poussart and Schrag 2005; Pons and Helle 2011; Ohashi et al. 2016) because of the development of analytical instruments and the improvement of sample preparation. $\delta^{18}O$ value of xylem cellulose, one of the main components of wood, is mainly determined by oxygen isotopic composition of source water and relative humidity (Roden et al. 2000; McCarroll and Loader 2004). Thus, if these factors have seasonal variation, $\delta^{18}O$ values of wood are expected to show cyclic change, which are interpreted as annual rings.

Detecting growth ring based on the variation of $\delta^{18}O$ is not a straightforward way. Poussart et al. (2004) tried to detect growth ring of *Samanea saman* in Indonesia and *Podocarpus neriifolius* in Thailand, with radiocarbon dating method and a kind of marking method respectively. The number of $\delta^{18}O$ cycle agreed with radiocarbon age in both trees when they assigned the maximum and minimum of xylem $\delta^{18}O$ to the month when the relative humidity was minimum and maximum respectively. Poussart and Schrag (2005) studied growth ring detection of 11 trees in northern Thailand. The $\delta^{18}O$ cycles were dated with radiocarbon, and the maximum and minimum of xylem $\delta^{18}O$ were assigned to the month when the relative humidity was minimum and maximum respectively. Growth ring was successfully detected for 7 trees from 11 trees, but 4 trees did not have clear cycle of $\delta^{18}O$. Ohashi et al. (2016) tested annual ring detection using $\delta^{18}O$ about *Eschweilera coriacea*, *Iryanthera coriacea*, and *Protium hebetatum* in Amazon, Brazil. The boundaries of tree rings were assigned to the maximum of $\delta^{18}O$ because the month when $\delta^{18}O$ of precipitation show maximum was the same as the month sample trees started to growth. The year counted based on $\delta^{18}O$ cycle agreed with the year radiocarbon showed in some *E. coriacea* and *P. hebetatum* but did not agreed in two *E. coriacea* and *I. coriacea* probably because of missing ring, or wedging rings. Since $\delta^{18}O$ in plant tissue is determined largely by climate and rarely by physiological process, it is a promising tool to detect periodical changes of xylem formation especially in seasonal climates.

In this chapter, the author tested applicability of annual ring detection using $\delta^{18}O$ variation of xylem. Considering the results in Chapter 2, the author assumes; (1) trees in seasonally dry forests start radial growth at certain season and stop, (2) the positions of negative peaks of $\delta^{18}O$ correspond to the positions of xylem formed at the beginning of radial growth. Variation of xylem $\delta^{18}O$ was examined for trees in seasonally dry forests and annual cyclicity was tested by dating based on the cambial marking.

4.2 Materials and methods

4.2.1 Study site

Neighboring two sites are selected in seasonally dry forests as study sites; Sakaerat Silvicultural Research Station (SSRS; 14º28′ 06.1″N, 101º54′15.0″E) and Sakaerat Environmental Research Station (SERS; 14°30'37.0"N, 101°55'51.4"E), Nakhon Ratchasima Province, Northeast Thailand (Fig. 3.1). Fig. 4.1 shows temperature (˚C), relative humidity (%), and precipitation (mm) from January 2011 to December 2017. Mean annual temperature and annual precipitation was 23.0 °C and 1169 mm (2011–2017). In this region, rainy season starts usually in May and continues until October. Fig. 4.1 also shows monthly change of stable oxygen isotope ratio (‰) of precipitation in SERS (2015–2017). The $\delta^{18}O$ value show decreasing trend from the start of rainy season to the end of rainy season.

4.2.2 Sample trees

Three trees were selected from SSRS; *Celtis timorensis*, *Garcinia cowa*, and *Hopea ferrea* (Tables 3.1 and 4.1). All of them were evergreen. Radial growth of the trees in SSRS was monitored with dendrometer bands every two weeks from September 2011 to December 2013 (Fig. 4.2). Wood core samples were collected on February 2014 with an increment borer (5 mm in inner-diameter). Two trees were selected from SERS; *Carallia brachiata* and *Irvingia malayana* (Tables 3.2 and 4.1). *C. brachiata* is evergreen and *I. malayana* is evergreen or partly deciduous (Gardner et al. 2000). Wood core samples were collected on November 2017 with incremental borer which was 5 mm in inner-diameter.

4.2.3 High-voltage DC pulse marking

High-voltage DC pulse marking was applied five times to trees in SSRS and one time to trees in SERS. Two stainless nails (1.2 mm thick, 25 mm long) were used as electrodes. The electrodes were inserted into each tree stem at about 1.3 m height and the distance between them were 5 cm in vertical direction. DC pulse (0.5 seconds, 500 V) was applied with the device designed for cambial marking (Hokusetsu Systems, See Chapter 3) on May 2011, September 2011, February 2012, February 2013, and August 2013 in SSRS and on March 2015 in SERS.

4.2.4 Stable isotope analysis

After sections were cut for microscopic observation, cores were divided into 0.05 mm in radial direction from cambium and every two sections were used for isotope analysis. Bulk samples were analyzed because radial variation patterns are similar between bulk wood and cellulose (Loader et al. 2003; Cullen and

Grierson 2006; Szymczak et al. 2011; Nakai et al. 2018). Some samples were placed in acetone for 30 minutes to remove the glue (cyanoacrylate adhesive) that was used to prevent breakage of the core during sectioning. Divided sub-samples were dried overnight at 60 °C and 100–200 μg were weighed. Then, sub-samples were wrapped in a silver foil (7 mm × 7 mm, 4 μm thick, Nittokagaku Co Ltd.).

As for samples in SSRS, stable isotope analysis was conducted with a continuous flow mass spectrometer (Thermo Fisher MAT 252) coupled to a high-temperature pyrolysis system (Hekatech HTO) with Costech Xero-blank 100 position auto-sampler at the Forestry and Forest Products Research Institute. Before loaded into auto-sampler, samples were dried overnight in a vacuum-oven at 70 °C to reduce moisture (Kagawa et al. 2015). Two standards, Merck cellulose and IAEA-C3 cellulose, were used to calibrate stable oxygen isotope ratio. Stable carbon isotope ratio was calibrated by IAEA-C3 cellulose. Standard deviation of the repeated measurements of the standards within a sequence was smaller than 0.15 ‰. As for samples in SERS, stable isotope analysis was conducted with a continuous flow isotope ratio mass spectrometer (Delta Plus; Thermo Fisher Scientific, Waltham MA, USA) coupled with a high-temperature combustion elemental analyzer (TC/EA; Thermo Fisher Scientific, Waltham MA, USA) at the Center for Ecological Research (CER). Three standards, Merck cellulose, IAEA601, USGS54 were used to calibrate stable oxygen isotope ratio. Stable carbon isotope ratio was calibrated by CERKU-02, 04, 06 and 07, all of which were prepared in CER (Tayasu et al. 2011), and USGS54. Results were shown using δ notation in per mil units (‰) with respect to the internationally accepted reference materials for stable oxygen isotope (Vienna standard mean ocean water; VSMOW) and stable carbon isotope (Pee dee belemnite; PDB).

4.3 Results

4.3.1 Seasonality of radial growth and position of marks formed by DC pulse marking

G. cowa, *C. timorensis*, and *H. ferrea* in SSRS started radial growth on April 2012 and stop on November and start again on next April (Fig. 4.2). Thus, these trees started radial growth just before the rainy season and continue until the end of rainy season (Fig. 4.1).

Tissues affected by DC pulse markings were described in Chapter 3 in detail. As for samples in SSRS, five marks by DC pulse marking were observed in *G. cowa*, two marks were observed in *C. timorensis*, and one mark was observed in *H. ferrea*. *H. ferrea* had a mark at 4.5 mm from cambium (Fig. 3.3), *G. cowa* had marks at 9.5, 8.1, 6.4, 3.0, and 1.1 mm from cambium (Fig. 3.4), and *C. timorensis* had marks at 7.9 and 3.9 mm from cambium (Fig. 3.5). Five marks observed in *G. cowa* correspond to the marking in May 2011, November 2011, February 2012, February 2013, and August 2013.

Both *C. brachiata* and *I. malayana* had a mark formed by DC pulse marking in March 2015. *C. brachiata* had small vessels at 3.3 mm from cambium in core collected from the middle point of the two electrodes (Fig. 3.8 a). Crushed vessel was also observed at 2.8 mm from cambium in core collected from the above side of electrodes (Fig. 3.8 b). *I. malayana* had deformed ray parenchyma at 7.7 mm from cambium (Fig. 3.9).

4.3.2 Radial variations of $\delta^{18}O$ and $\delta^{13}C$

Fig. 4.3 shows radial variation of $\delta^{18}O$ and $\delta^{13}C$ in trees in SSRS collected on February 2014. $\delta^{18}O$ in *G. cowa* and *C. timorensis* showed clear up-down cycles (Fig. 4.3; b, c) but in *H. ferrea*, cyclic change was not observed in this measured region. Compared to $\delta^{18}O$, $\delta^{13}C$ did not show clear cyclic change. All three trees show increasing trend at the outermost part.

Radial variation of $\delta^{18}O$ and $\delta^{13}C$ in trees in SERS collected on November 2017 are in Fig. 4.4. Both *C. brachiata* and *I. malayana* showed clear up-down cycles. Both trees show increasing trend at the outermost part.

4.4 Discussion

4.4.1 Annual ring detection using stable isotope

In chapter 2, precipitation $\delta^{18}O$ and xylem $\delta^{18}O$ of *Tectona grandis* showed following trend: (1) precipitation $\delta^{18}O$ decreased from April to September (2) xylem $\delta^{18}O$ had negative peaks at the positions of growth ring boundaries. Based on these two results, decreasing trend of $\delta^{18}O$ in the later part of each year's growth of *T. grandis* would correspond to the growth from April to September. As for trees without rings in SSRS, monitoring radial growth with dendrometer band showed that *H. ferrea G. cowa*, and *C. timorensis* actively grew from April to November (Fig. 4.2), which was overwrapped with rainy season (Fig. 4.1). So, the author assumed that as for trees without visible growth rings, xylem whose $\delta^{18}O$ had decreasing trend was formed from April to November, that is, rainy season of each year. This assumption does not contradict to the result of *G. cowa*. At the positions of marks by the first marking (May 2011), the third marking (February 2012), and the forth marking (February 2013), $\delta^{18}O$ had positive peaks, and at the positions of marks by the second marking (September 2011) and fifth marking (August 2013) $\delta^{18}O$ had negative peaks (Fig. 4.3; b). Moreover, two marks of *C. timorensis* would be produced by first and second marking. Therefore, the cycle of one increasing and one decreasing could be interpreted as the growth ring in case of *C. timorensis* and *G. cowa*. As for *H. ferrea*, because there was no cyclic change *G. cowa* and *C. timorensis* had and only one mark was observed, $\delta^{18}O$ variation could not be interpreted as growth ring. It is possible that $\delta^{18}O$ values of *H. ferrea* shown in Fig. 4.3 was the outermost part formed after last marking only, because radial increment of *H. ferrea* was about 2 times higher than *G. cowa* and *C. timorensis* (Fig. 4.2) and analyzed length was shorter than that of other two tree.

As for samples in SERS, the mark produced by the marking on March 2015 located at the position of positive peak of $\delta^{18}O$ both in *C. brachiata* and *I. malayana*. The $\delta^{18}O$ increased at the outermost part, and there were three cycle of decreasing and increasing from the mark to the cambium. So, the tree ring of these two trees could be detected by counting the number of $\delta^{18}O$ cycle because the number of cycles from the position of mark to the cambium was equal to the number of years from the date of marking to the date of sample collection.

4.4.2 Correlation of radial variation in stable isotope ratios within tree or among trees

Although the variation of $\delta^{18}O$ could not be dated because no marking applied, judging from growth ring

(Fig. 4.5), correlation of $\delta^{18}O$ between two radii seems to be similar (Fig. 4.6), same as *T. grandis*. Among trees in SSRS and SERS, radial variation of $\delta^{18}O$ had one decrease within a year and the trend of outermost region was similar among trees collected on the same month. So, the values of $\delta^{18}O$ of xylem seem to be controlled by same factor, such as $\delta^{18}O$ of source water or relative humidity.

4.5 Summary

$\delta^{18}O$ of trees without growth rings showed cyclic change. Considering monitoring results of radial growth and positions of marks produced by DC pulse marking, trees started growing in April and continued until November, and decreasing trend of precipitation $\delta^{18}O$ was recorded in xylem $\delta^{18}O$. Since the variation of xylem $\delta^{18}O$ seemed to be similar within tree and among trees in the same site, the xylem $\delta^{18}O$ seem to be controlled by the same factor, such as $\delta^{18}O$ of source water or relative humidity. Therefore, $\delta^{18}O$ can be used as proxy for growth ring in this region which has clear wet and dry season.

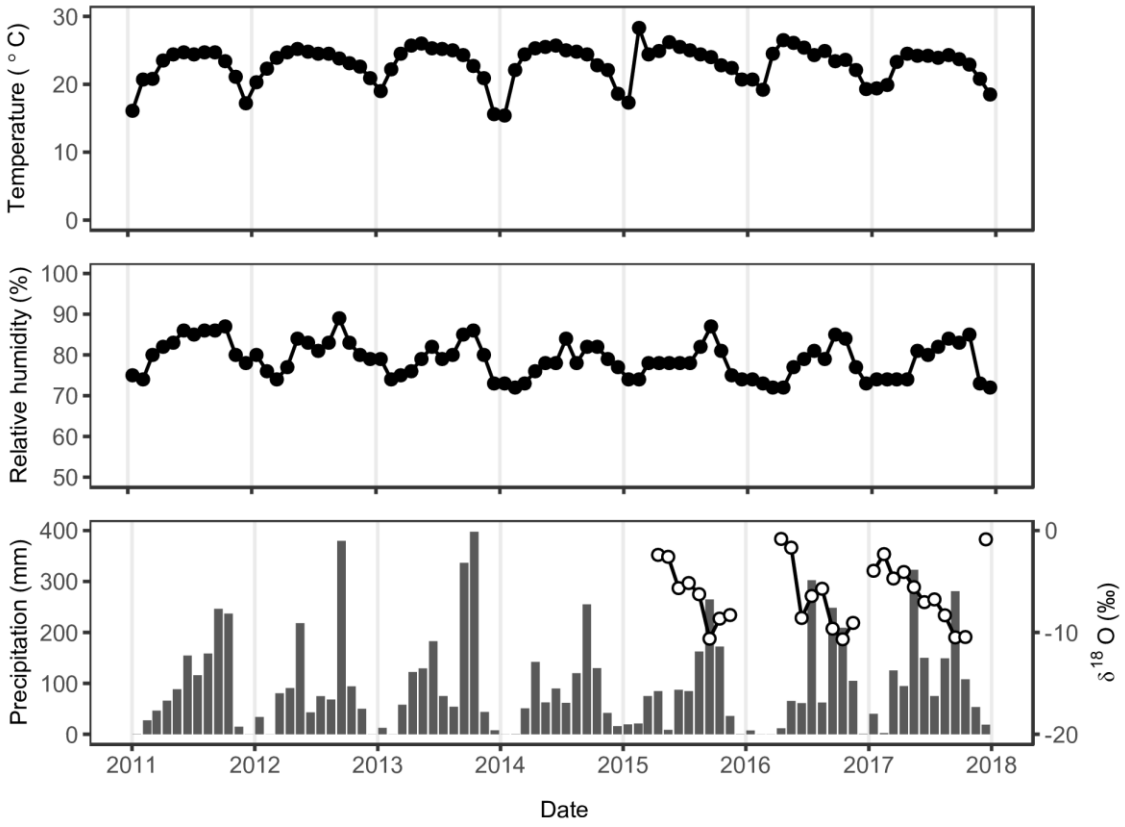

Fig. 4.1 Temperature, relative humidity, precipitation and $\delta^{18}O$ of precipitation of SERS from 2011 to 2017. The precipitation for $\delta^{18}O$ analysis was collected biweekly and the values were shown as monthly mean weighted by collected amount.

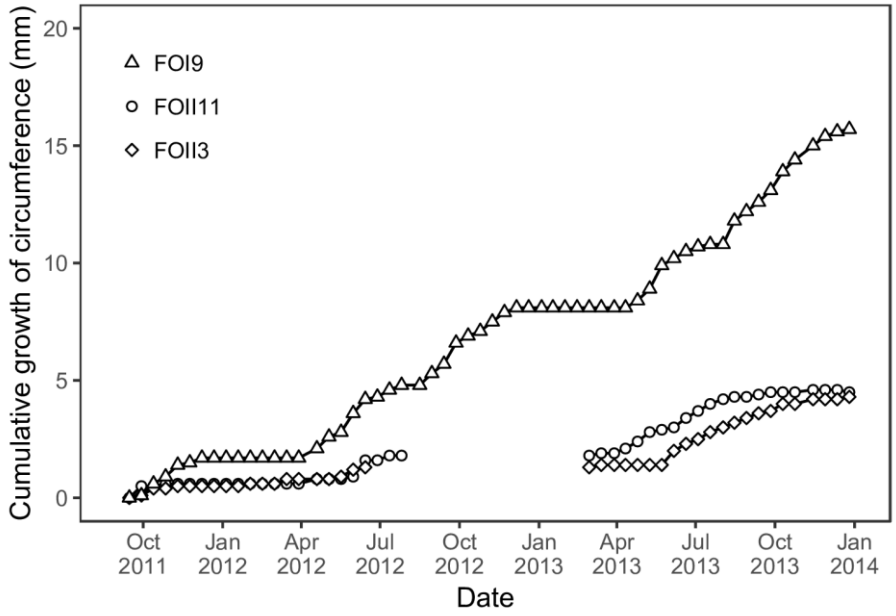

Fig. 4.2 Cumulative growth of circumference in *C. timorensis* (FOII11), *G. cowa* (FOII3), *H. ferrea* (FOI9) collected in SSRS. Data were obtained every two weeks. Missing values were caused by the destruction of the devices by wild animals.

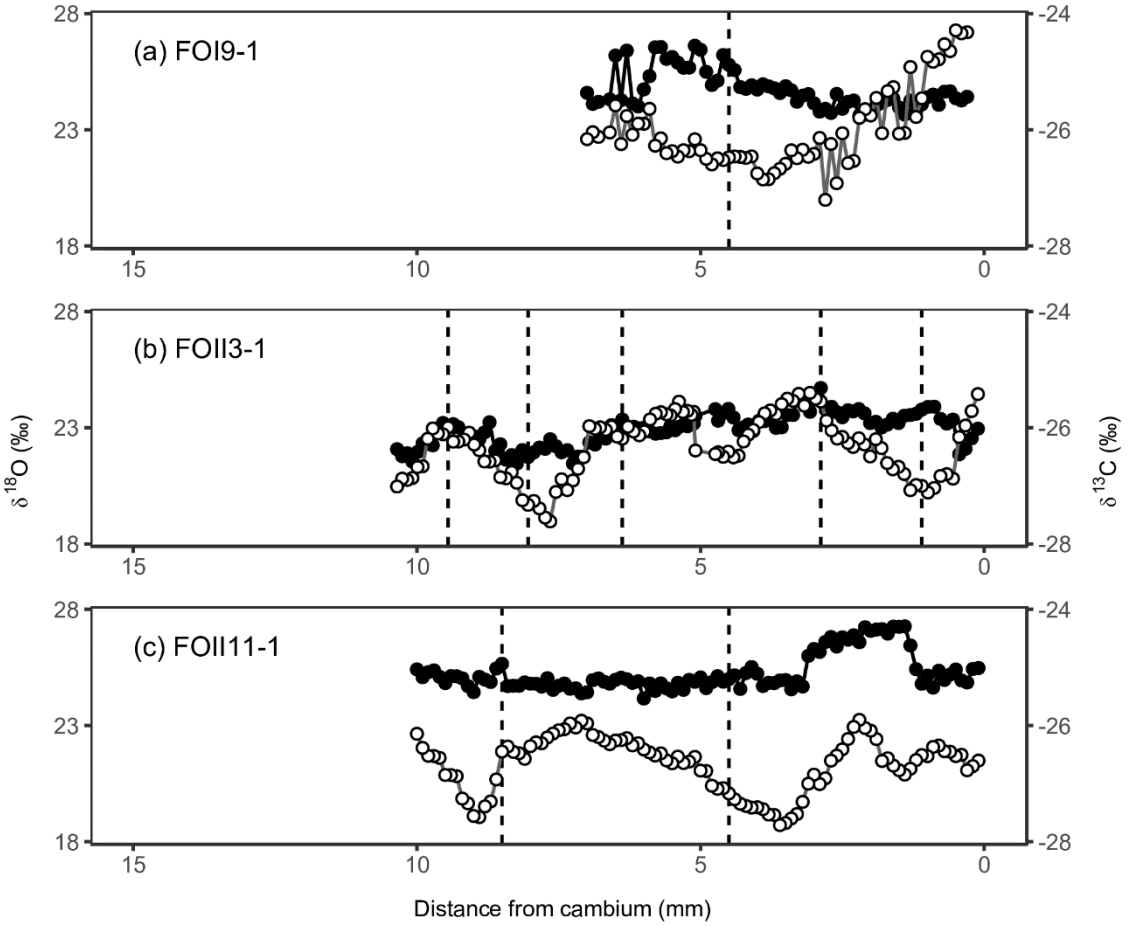

Fig. 4.3 Radial variation of stable carbon (filled circle) and oxygen (open circle) isotope ratio of *Hopea ferres* (FOI9-1, a), *Garcinia cowa* (FOII3-1, b), and *Celtis timorensis* (FOII11-1, c) in SSRS. Vertical dashed lines are the positions of tissues produced by DC pulse markings. Samples were collected on February 2014.

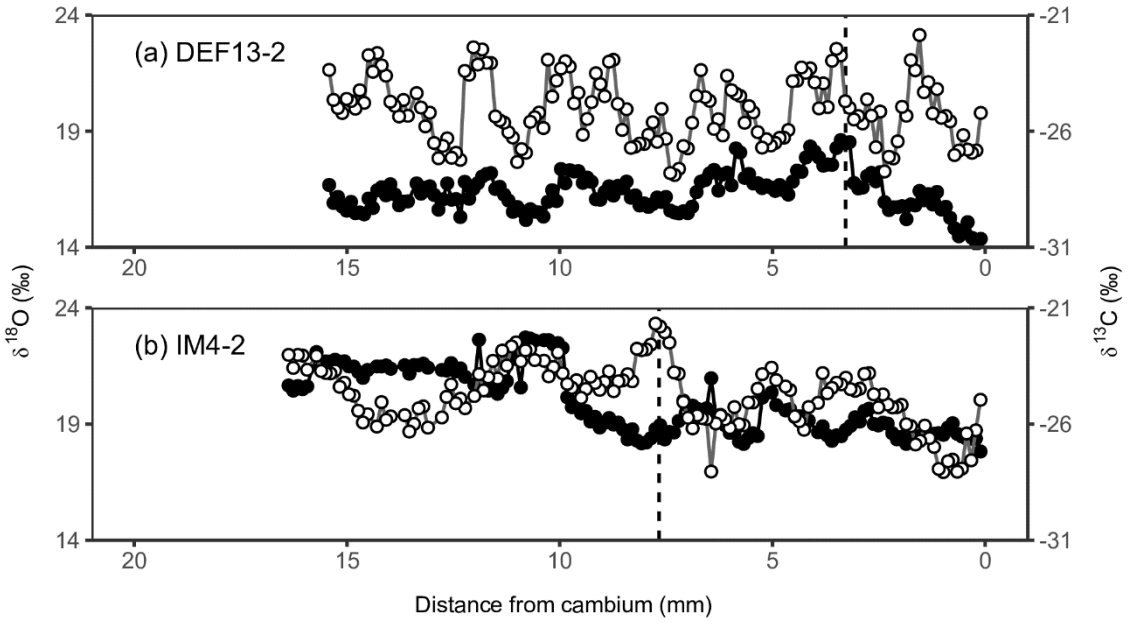

Fig. 4.4 Radial variation of stable carbon (filled circle) and oxygen (open circle) isotope ratio of *Carallia brachiata* and *Irvingia malayana* in SERS. A vertical dashed line is the position of tissues produced by DC pulse marking (March 2015). Samples were collected on November 2017.

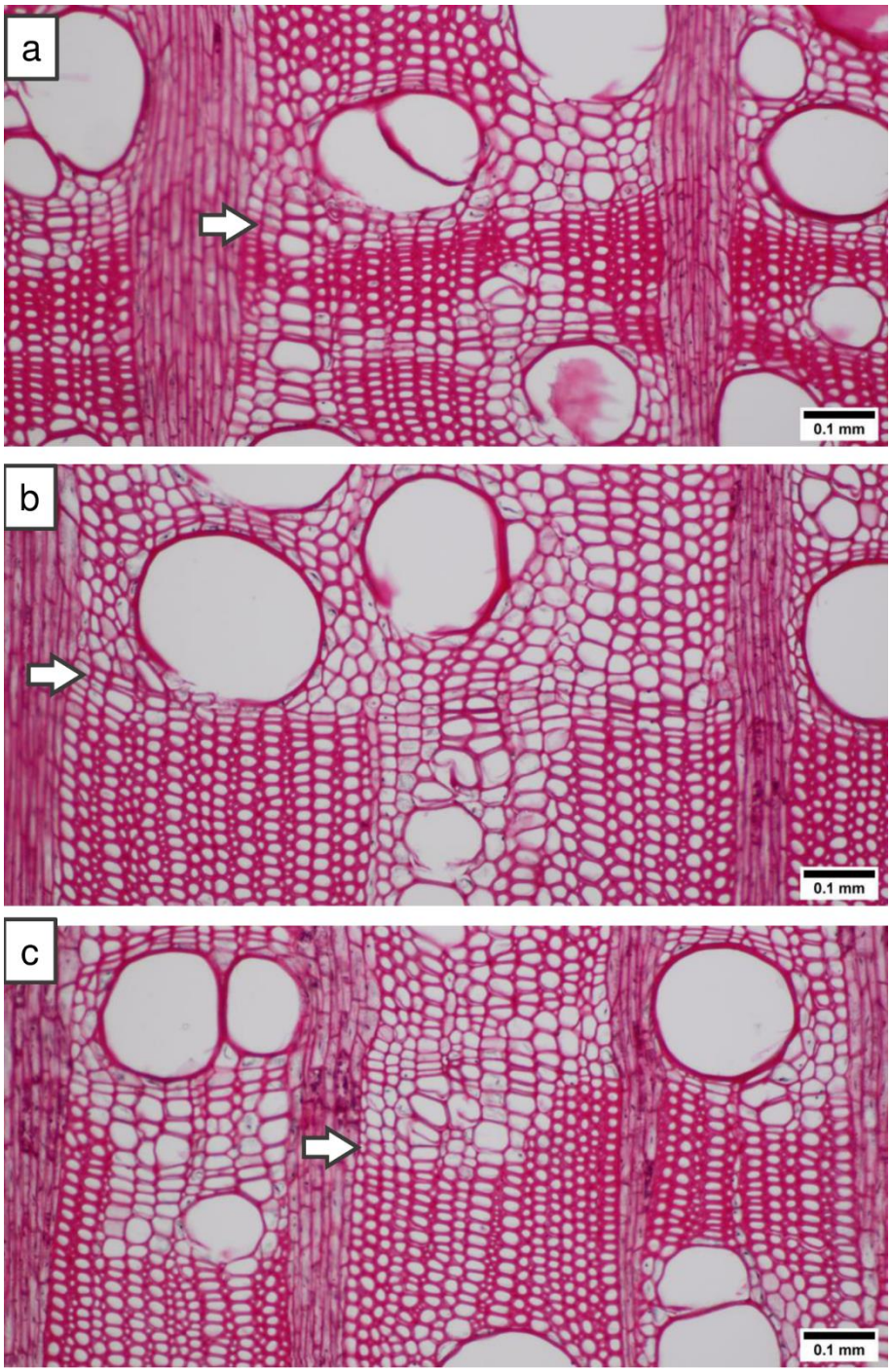

Fig. 4.5 Growth ring boundary of *Celtis timorensis* (FOII-11-3) in SSRS observed at 5.73 mm (2011, a), 3.53 mm (2012, b), and 1.82 mm (2013, c) from cambium. White arrow indicates growth ring boundary. Bark side is top direction.

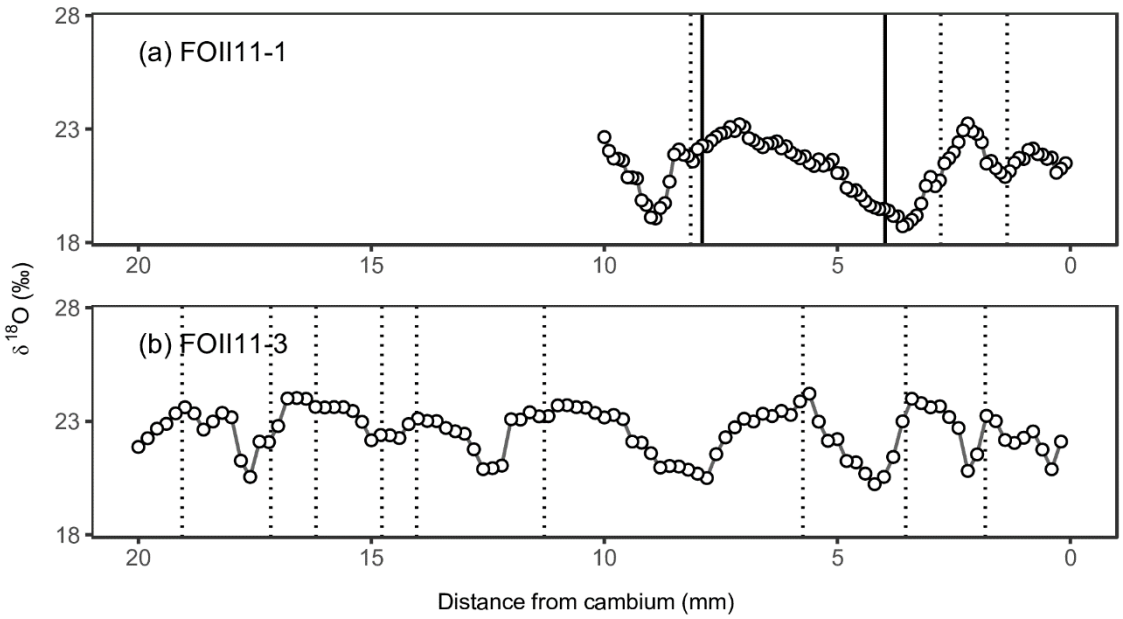

Fig. 4.6 Radial variation of stable oxygen isotope ratio of *C. timorensis*. (a) Sample collected from middle of electrodes (This study). (b) Sample collected from the same tree at same height as (a) but opposite direction (Nakai et al. 2018). Vertical solid lines are the position of tissues by DC pulse markings, and vertical dotted lines are the position of growth ring boundaries. Measured interval was 0.1 mm (a) and 0.2 mm (b) respectively.

Table 4.1 Sample trees

Site	Sample name	Species (Family)	DBH (cm)	Marking date	Sampling date
SSRS	FOI-9	*Hopea ferrea* (Depterocarpaceae)	28.6	May 2011, Sep 2011, Feb 2012, Feb 2013, Aug 2013	Feb 2014
	FOII-3	*Garcinia cowa* (Clusiaceae)	15.0	May 2011, Sep 2011, Feb 2012, Feb 2013, Aug 2013	Feb 2014
	FOII-11	*Celtis timorensis* (Cannabaceae)	26.9	May 2011, Sep 2011, Feb 2012, Feb 2013, Aug 2013	Feb 2014
SERS	DEF13	*Carallia brachiata* (Rhizophoraceae)	18.6	Mar 2015	Nov 2017
	IM4	*Irvingia malayana* (Irvingiaceae)	33.2	Mar 2015	Nov 2017

Chapter 5 Comparison of xylem $\delta^{18}O$ variation between seasonally dry forests and tropical rainforests

5.1. Introduction

Since a distinct dry period is observed in seasonally dry forests in tropics, the trees growing in the region reduce or stop their growth. This rhythm induces a periodicity of xylem formation and produce growth rings in certain species. In contrast, tropical rainforests where seasonal differences in temperature and precipitation are weak, xylem formation of trees shows less periodicity, resulting in less species producing visible regular growth rings. For this reason, anatomical reports on annual rings in tropical trees have been restricted to the region in the seasonal climate, such as Thailand (Ohashi et al. 2009), and northern Peninsular Malaysia (Abdul Azim and Okada 2014; Ohashi et al. 2014) in Southeast Asia.

Recent advance of isotopic approach, however, has been promoting several attempts in tropical dendrochronology. Oxygen isotope ratio ($\delta^{18}O$) in xylem seems to provide more distinct climate signals than carbon isotope ratio ($\delta^{13}C$) (Poussart et al. 2004; Rozendaal and Zuidema 2011), but the application to the species in humid tropics is still scarce. For further application of $\delta^{18}O$ in tropical trees especially in less seasonal climate, we have to confirm what is the necessary condition.

Since $\delta^{18}O$ value of xylem cellulose is determined mainly by that of source water, usually represented by precipitation, and relative humidity, growth ring detection would be possible if $\delta^{18}O$ of precipitation have clear annual cycle in study sites. Ohashi et al. (2016) tested annual detection using $\delta^{18}O$ in Amazon, Brazil, where climate is tropical rainforests and $\delta^{18}O$ of precipitation have clear annual cycle, and successfully detected growth ring in some species.

Peronema canescens (Lamiaceae) is a ring-porous and deciduous hardwood tree species and forming growth rings. *P. canescens* in Peninsular Malaysia is reported to form growth ring annually (Abdul Azim and Okada 2014). In western Java, Indonesia, inter-annual variation of $\delta^{18}O$ of *P. canescens* showed good correlation between trees and would be affected by external climatic factor such as precipitation, temperature, sunlight hour, and relative humidity (Harada et al. 2017).

In this chapter, the author examined the seasonality in precipitation $\delta^{18}O$ and intra-annual variation of xylem $\delta^{18}O$ using *Peronema canescens* growing in less seasonal climate. The author tested the applicability of annual ring detection to trees without visible growth rings in tropical rainforests in Peninsular Malaysia and the results were compared with those in seasonally dry forests.

5.2. Materials and methods

5.2.1. Study site

As study site of less seasonal climate, a tropical rainforest in Ayer Hitam Forest Reserve, Selangor, Malaysia (AHFR, 3°1' N, 101°39' E) was selected. Wood samples were also collected at Bukit Hari, Forest Research Institute Malaysia, Selangor, Malaysia (BHFRIM, 3°14' N, 101°38' E), which is located about 25 km north of AHFR.

Sakaerat environmental research station, Nakhon Ratchasima Province, northeastern Thailand

(SERS; 14°30'37.0"N, 101°55'51.4"E) was selected as study site of seasonally dry forest. Wood samples were also collected in Wang Nam Kiao Forestry Student Practicing Station of the Faculty of Forestry, Kasetsart University (WNKFSPS; 14°29' N, 101°56' E) in Nakhon Ratchasima Province, northeastern Thailand, which is 3 km apart from SERS. Figures 5.1 and 5.2 show temperature, relative humidity, and precipitation during research period in SERS and AHFR.

5.2.2. Samples

Rain samples were collected with a polyethylene funnel (9 cm in diameter) and a polyethylene container (5 L) at AHFR twice a month, on the 1st and the 16th, from March 2016 to November 2017. The device for rain collection had a mechanism of preventing collected water from evaporating. A part of collected samples (50 mL) was stored for isotope analysis after weight was measured. Wood core samples of eight *Peronema canescens* were collected at BHFRIM on December 2016. Two wood core samples (5 mm in diameter) of *P. canescens* were collected at 1.3 m above the ground from opposite direction for each tree with an increment borer. The length of core was about the half of a diameter of each tree. Wood core samples (5 mm in diameter) of *Shorea acuminata* and *Shorea macroptera* were first collected on December 2016 at AHFR with an increment borer for anatomical examination. Wood core samples of the same species were collected for isotope analysis on November 2017 (Chapter 3, Table 3.3).

Samples in seasonal dry forests were described in Chapters 2 and 4. Rain samples were collected twice a month, on the 1st and the 16th, since May 2015. Wood core samples of *Tectona grandis* were collected at WNKFSPS on March 2015. Wood core samples of *Carallia brachiata*, and *Irvingia malayana* were collected at SERS on November 2017.

5.2.3. DC pulse markings

High-voltage DC pulse marking was conducted with a custom-designed device (Hokusetsu Systems, Sakai, Osaka, Japan), which was driven by 8 AA batteries. Two stainless steel nails of 1.2 mm thick and 25 mm long were used as electrodes. DC pulse marking was applied to *C. brachiata*, and *I. malayana* on March 2015 in SERS. The condition of marking for samples in SERS were described in Chapter4.

In AHFR, DC pulse marking was applied on October 2014 and March 2016. Three pair of electrodes with different vertical distance were inserted to each tree. DC pulse (0.5 seconds at 500 V) was applied one or two times on each marking. The conditions of distance between electrodes and times of DC pulse applied were; 7 cm and one time, 7 cm and two time, and 5 cm and two time.

5.2.4. Sample preparation

Wood cores of *P. canescens* and *T. grandis* were cross-dated, and then, prepared for stable isotope analysis. As for other cores, thin tangential sections were cut with a sliding microtome and double stained with safranin and fast green or safranin and alcian blue for microscopic observation before isotope analysis.

Wood cores were divided into thin sections (0.05 mm thick in radial direction) from cambium with a sliding microtome. Samples were placed in acetone for 30 minutes to remove the glue (cyanoacrylate

adhesive) that was used to prevent breakage of the core during sectioning. Divided sub-samples were dried overnight at 60°C and 0.1–0.2 mg of each was used for isotope analysis.

5.2.5. Stable isotope analysis

Rain samples were filtered with syringe filter (pore size < 0.22 μm) before isotope analysis. Stable oxygen isotope ratio of rain samples was analyzed with isotopic water analyzer (Picarro L2120-i or L2130-i; Picarro inc., CA, USA) at the Research Institute for Humanity and Nature (RIHN). Each sample was measured six times and three of six measurements were averaged. Obtained results were expressed in delta (δ) notation in per mil (‰) relative to Vienna standard mean ocean water (VSMOW). Standard deviation of repeated measurements of reference water was under 0.3‰. After stable oxygen ($\delta^{18}O$) and hydrogen ($\delta^{2}H$) isotope ratios were determined, the deuterium excess (d) values were calculated by the following equation (Dansgaard 1964):

$$d = \delta^{2}H - 8\,\delta^{18}O$$

to evaluate the fractionation processes of $\delta^{18}O$ and $\delta^{2}H$ in precipitation.

Stable oxygen and carbon isotope ratio of wood samples were conducted with a continuous flow isotope ratio mass spectrometer (Delta V advantage or Delta Plus; Thermo Finnigan, Bremen, Germany) coupled with a high-temperature combustion elemental analyzer (TC/EA; Thermo Finnigan, Bremen, Germany) at the Center for Ecological Research (CER) and RIHN. Obtained results were expressed in delta (δ) notation in per mil (‰) relative to Vienna standard mean ocean water (VSMOW) for oxygen or Pee Dee Belemnite (PDB) for carbon isotope. Standard deviation of repeated measurements of samples was under 0.5‰.

5.2.6. Data processing

As for xylem $\delta^{18}O$ of *P. canescens* and *T. grandis*, relationship between stable isotope ratio (explanatory variable) and distance from cambium (dependent variable) was analyzed by kernel ridge regression (details are in Nakai et al. 2018). Then each tree ring was evenly divided into 10 points and corresponding values of stable isotope ratio were obtained using regression line.

For evaluating within-tree correlation of xylem $\delta^{18}O$, Pearson correlation coefficient was calculated. As for *P. canescens*, $\delta^{18}O$ of two cores (PC0401 and PC0402) collected from tree PC04 were used. As for *T. grandis*, $\delta^{18}O$ of two cores (TG0301 and TG0302) collected from tree TG04 were used (details are in Chapter 2).

5.3. Results

5.3.1. Seasonal variation of $\delta^{18}O$ of precipitation in AHFR

There was no common trend through the observation years in precipitation $\delta^{18}O$ in AHFR, also in the amount of precipitation (Fig. 5.3). In 2016, $\delta^{18}O$ decreased about 9‰ from March to June and then the value did not change until the end of the year. In 2017, $\delta^{18}O$ increased about 3‰ on February and stay constant until April. After that, the value decreased about 1‰ in April and about 3‰ in September. The amount of precipitation

is small (Figs. 5.2 and 5.3). The variation in monthly weighted mean of precipitation $\delta^{18}O$ was smaller in 2017. The ranges of monthly weighted mean of $\delta^{18}O$ in 2016 and 2017 were 7.11‰ and 4.68‰ respectively (Fig. 5.4).

The equation for the local meteoric water line in AHFR was $\delta^2H = 7.7\delta^{18}O + 10.77$. The slope was smaller than that of global meteoric water line, but the intercept was larger (Fig. 5.5). The deuterium excess values increased from the start of the year (March in 2016 and January in 2017) to May and kept almost constant until the end of the year (Fig. 5.6).

5.3.2. Radial variation of $\delta^{18}O$ and $\delta^{13}C$ of trees with rings in AHFR

Both $\delta^{18}O$ and $\delta^{13}C$ values of *P. canescens* showed cyclic changes in radial direction (Fig. 5.7). Although $\delta^{13}C$ showed rapid rise at the beginning of tree ring almost every year, $\delta^{18}O$ showed different pattern year by year. Each of $\delta^{18}O$ and $\delta^{13}C$ fluctuate within a limited range, but the range of $\delta^{18}O$ was wider than that of $\delta^{13}C$; up to 8‰ in $\delta^{18}O$ and under 4‰ in $\delta^{13}C$.

$\delta^{18}O$ values of *P. canescens* seasonally varied within a year (Fig. 5.8). Intra-annual variation of $\delta^{18}O$ was similar within a tree, but the correlation was very small or negative in some year (Fig. 5.9). Correlation of intra-annual variation in $\delta^{18}O$ between two cores collected from the same tree was good from 2008 to 2010 and from 2015 to 2016. However, the correlation was negative at 2013 and 2014.

5.3.3. Radial variation of $\delta^{18}O$ and $\delta^{13}C$ of ringless trees in AHFR

Fig. 5.10 shows radial variation of $\delta^{18}O$ and $\delta^{13}C$ of *S. acuminata* (SA4-2) and *S. macroptera* (SM3-2). The position of marks by DC pulse marking of SM3-2 were estimated based on the positions of marks of another core sample collected from the same tree on the same day (SM3-3), because no mark was observed. *S. acuminata* had two positive peaks between the first mark on October 2014 and the second mark on March 2016 (about 17 months of growth), and there was negative peak on the position of the second marking. After second mark, *S, acuminata* had two positive peaks (about 21 months of growth between the day of the second marking and the day sample collected). *S. macroptera* had five positive peaks between the first mark and the second mark. After second mark, *S. macroptera* had two positive peaks. Both *S. acuminata* and *S. macroptera* had decreasing trend at the outermost part.

5.4. Discussion

5.4.1. Seasonal variation in $\delta^{18}O$ of precipitation

The $\delta^{18}O$ values in precipitation in AHFR seems to be controlled by the amount of precipitation, rather than the origin of water vapor. The variation of monthly weighted mean of $\delta^{18}O$ in AHFR was less seasonal than that in SERS (Figs. 2.3 and 5.4,). On the other hand, the deuterium excess values show similar change both in 2016 and 2017 in AHFR but that in SERS showed less seasonal trend during study period (Figs. 2.5 and 5.6). The deuterium excess is an index of non-equilibrium condition and reflects the rate of evaporation of precipitation in the source area (Dansgaard 1964). Considering the monthly change of the deuterium excess values, the monthly change of the source of precipitation in AHFR would be the same every year, but the

monthly change of $\delta^{18}O$ would not be the same every year. The Peninsular Malaysia have two monsoonal seasons, north-east (November to March) and south-west (May to September), and precipitation in these two seasons should have different origin of vapor. However, in Pasoh, near the Kuala Lumpur, there was no difference in isotopic composition ($\delta^{18}O$ and $\delta^{2}H$) in precipitation between north-east and south-west monsoon and the amount of rainfall affected the $\delta^{18}O$ values (Marryanna et al. 2017). So, less periodicity in $\delta^{18}O$ in precipitation probably due to the less periodicity in the amount of rainfall.

5.4.2. Intra-annual variation in $\delta^{18}O$ of xylem

Xylem $\delta^{18}O$ in *P. canescens* radially varied and the pattern seemed to be similar between two cores collected from opposite direction of the same tree. However, correlation coefficients were very low in some year, especially in 2013 (Figs. 5.8 and 5.9). Trees in tropical rainforest often show different radial growth pattern among different direction, and sometimes form false ring or wedging ring. This also affects the value of $\delta^{18}O$. In Amazon, Brazil, age determined based on $\delta^{18}O$ pattern did not agree with the age determined by radiocarbon dating in some trees (Ohashi et al. 2016). To obtain reliable results, the age should be determined by cross-dating among several cores and among trees, or other method such as radiocarbon dating.

The within-ring variations of $\delta^{18}O$ in *P. canescens* were not constant every year (Fig. 5.7) although those in *T. grandis* in Thailand were similar every year (Chapter 2). This suggests that, in AHFR, $\delta^{18}O$ of xylem formed at a certain season would not show typical value every year and simple interpretation of $\delta^{18}O$ cycle as growth ring, for example interpreting the position of positive or negative peaks of $\delta^{18}O$ as position of growth boundaries, would be difficult. This is probably because of poor annual cyclicity in $\delta^{18}O$ of precipitation (Fig. 5.4). Precipitation $\delta^{18}O$ is affected by the amount of precipitation in this region (Marryanna et al. 2017), therefore, even if growth rings were formed almost same season every year, $\delta^{18}O$ of precipitation (and that of source water) would be different every year and resulting xylem $\delta^{18}O$ would be different. In case of *T. grandis* in Thailand, seasonal variation of $\delta^{18}O$ of precipitation seems to be constant every year, and alternate pattern of dry and rainy season would be controlling seasonality of tree growth. Compared to SERS, seasonal variation of xylem $\delta^{18}O$ was indistinct in AHFR because seasonality in precipitation $\delta^{18}O$ is poor and there is no distinct seasonality of dry and rainy period.

5.4.3. Annual ring detection of ring-less trees using $\delta^{18}O$

Xylem $\delta^{18}O$ had wider range of variation than that of $\delta^{13}C$, and this trend is the same as trees in Thailand. The number of years after marking agreed with the number of cycles between marks and cambium in *C. brachiata* and *I. malayana* in Thailand (Fig. 4.10). However, there was more than two cycle within a year in xylem $\delta^{18}O$ of *S. acuminata* and *S. macroptera* in AHFR. *S. acuminata* had two $\delta^{18}O$ peaks between 1st mark and 2nd mark (17 months), and two peaks between 2nd mark and cambium (20 months). On the other hand, *S. macroptera* had at least three peaks between 1st and 2nd marks, and two peaks between 2nd mark and cambium. Different pattern of xylem $\delta^{18}O$ probably because the way $\delta^{18}O$ incorporated into xylem cellulose is different between species, even if they located closely. Before precipitation is took up by trees, it is mixed with soil water and as a result, isotope ratio will be changed. Therefore, it is probable that each tree took up

soil water with different $\delta^{18}O$ because isotope composition of soil water is different by depth or topography (Gazis and Feng 2004), and the soil depth trees take up water would be different by trees. Moreover, a part of oxygen atoms of photosynthate, whose isotope ratio is enriched at leaves, would exchange with that of unenriched stem water before cellulose synthesis (Cheesman et al. 2017; Nabeshima et al. 2018) and the rate of exchange would be different between species. In order to interpret $\delta^{18}O$ pattern in xylem, various species should be analyzed with both dating method such as cambial marking or radiocarbon and phenological observation.

5.5. Summary

Precipitation $\delta^{18}O$ in AHFR showed poorer seasonality compared with that in SERS, and the pattern might not be constant every year. $\delta^{18}O$ variation seems to be similar within the same tree, but correlation was low in some years. *T. grandis* in SERS showed similar intra-annual variation of xylem $\delta^{18}O$, but *P. canescens* did not show any constant pattern during observed years. In case of trees without tree rings, *S. acuminata* and *S. macroptera* in AHFR showed different $\delta^{18}O$ pattern between xylems formed in the same period, but *C. brachiata* and *I. malayana* in SERS showed similar pattern. These contrasting difference between seasonally dry forest and tropical rainforest probably is because of both difference in seasonality of precipitation $\delta^{18}O$ and difference in seasonality of tree growth.

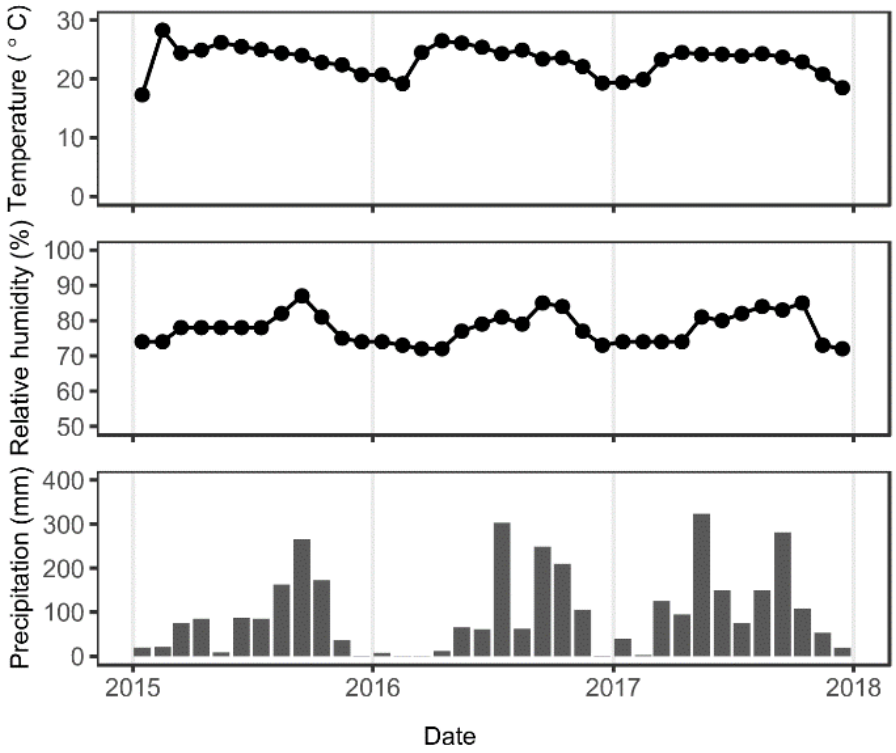

Fig. 5.1 Mean temperature, mean relative humidity, and total precipitation in SERS from January 2015 to December 2017.

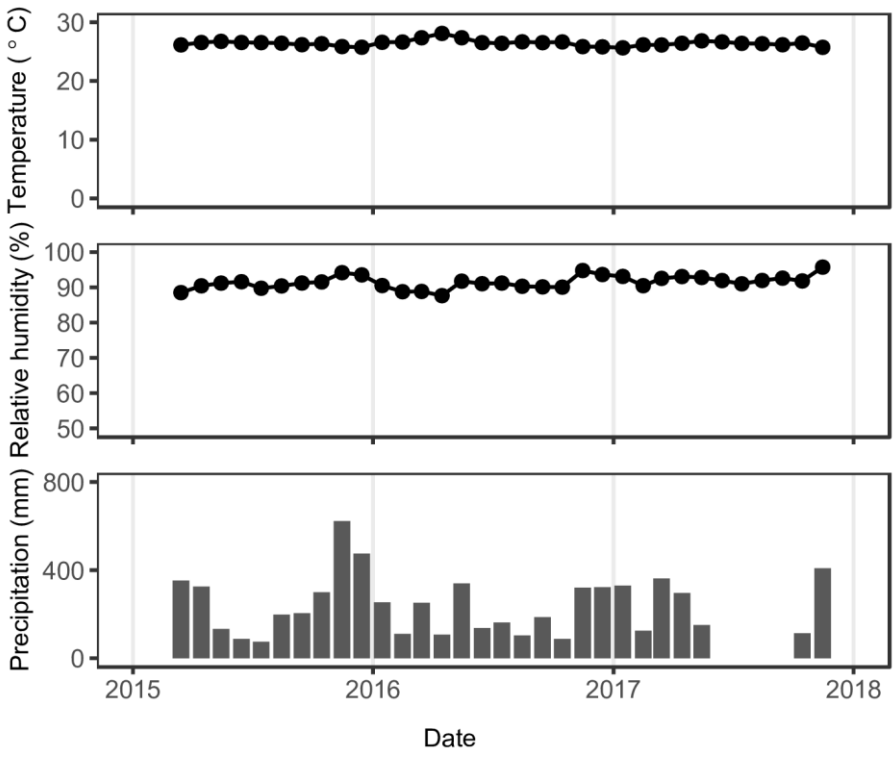

Fig. 5.2 Mean temperature, mean relative humidity, and total precipitation in AHFR from March 2015 to November 2017. Precipitation data from June 2017 to September 2017 was not available because of measurement failure.

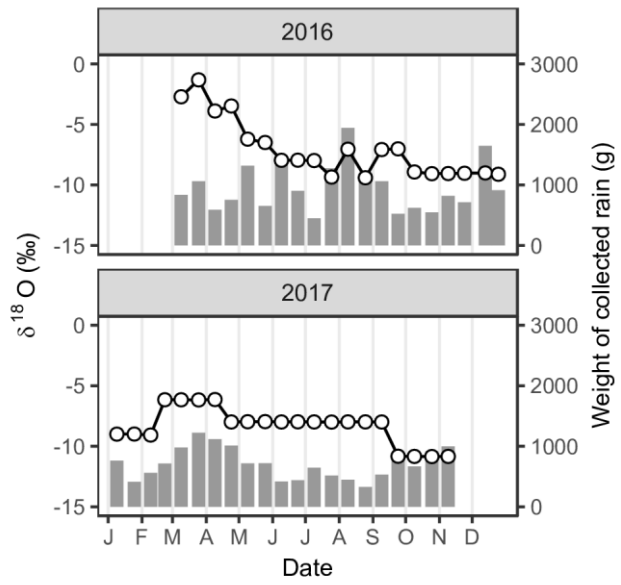

Fig. 5.3 precipitation $\delta^{18}O$ (circle) and weight of collected rain sample (bar) from March 2016 to November 2017 in AHFR. Samples were collected on the 1st and the 16th every month and data are plotted at the middle of each collected period.

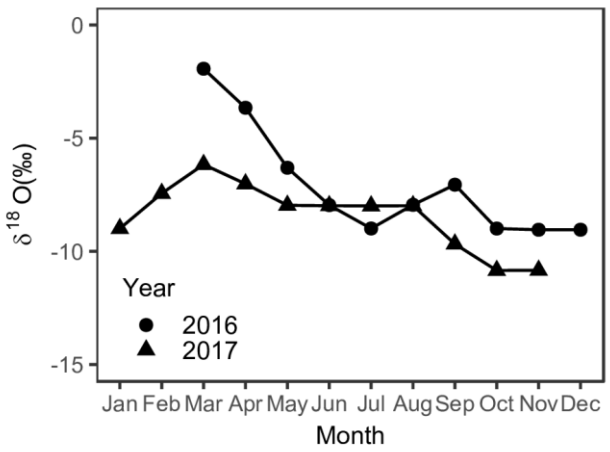

Fig. 5.4 Monthly change of precipitation $\delta^{18}O$ in AHFR. The value of each month is the mean weighted by collected amount.

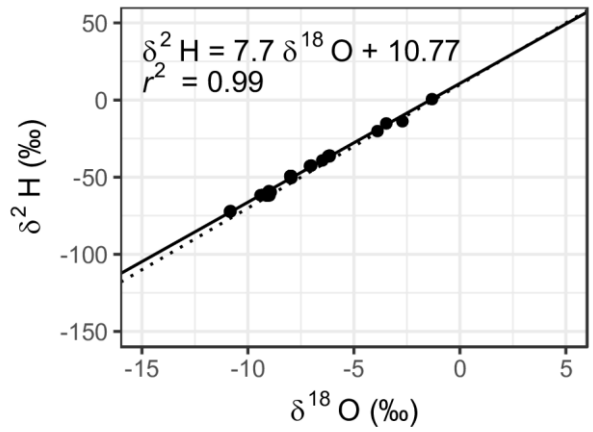

Fig. 5.5 The relationship between δ^2H and δ^{18}O in precipitation in AHFR. A dotted line is the linear regression line ($\delta^2\mathrm{H} = 7.7\,\delta^{18}\mathrm{O} + 10.77$; local meteoric water line) and the solid line is the global meteoric water line ($\delta^2\mathrm{H} = 8\,\delta^{18}\mathrm{O} + 10$)

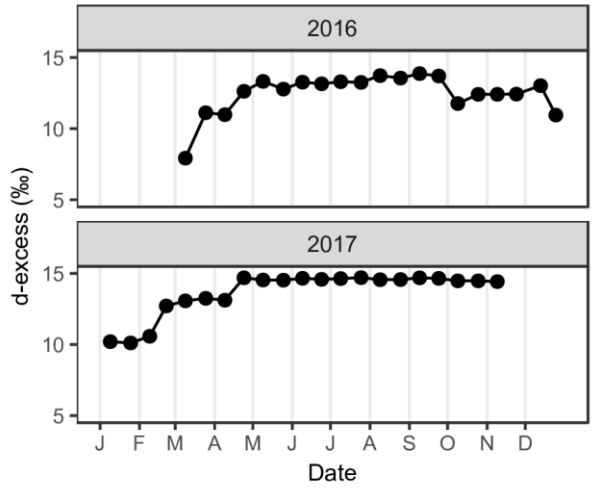

Fig. 5.6 d-excess of rain sample in AHFR from March 2016 to November 2017. Samples were collected on the 1st and the 16th every month and data are plotted at the middle of the each collected period.

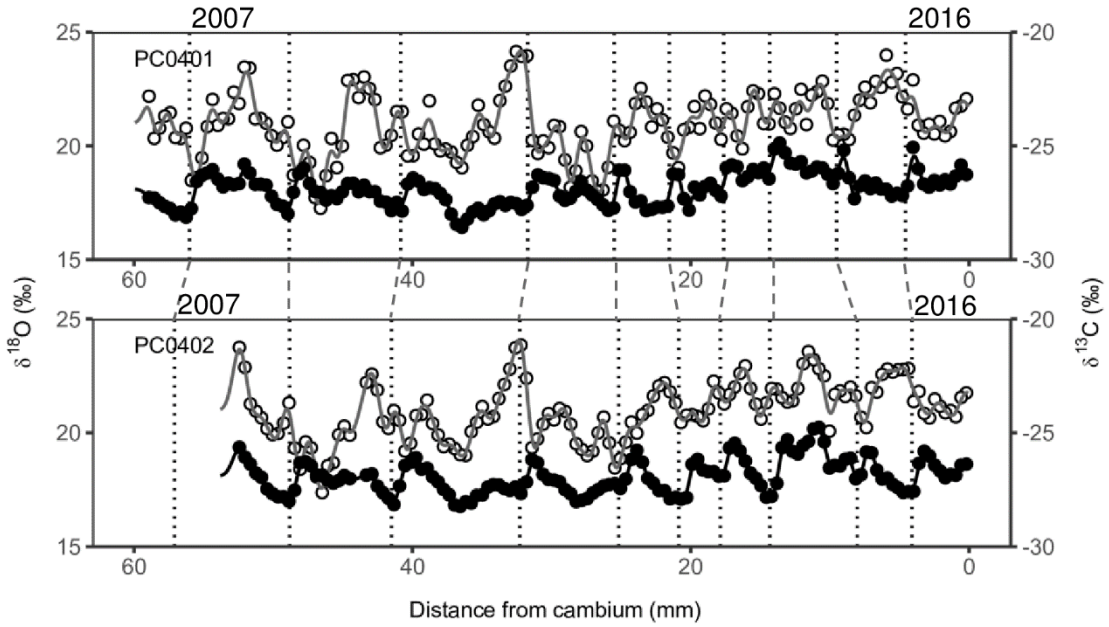

Fig. 5.7 $\delta^{18}O$ (raw: open circle; fitted: gray line) and $\delta^{13}C$ (raw: filled circle; fitted: black line) of *P. canescens* xylem in BHFRIM. Samples were collected on December 2016 and outermost tree ring was produced in 2016. Vertical dotted lines indicate the position of tree ring boundaries.

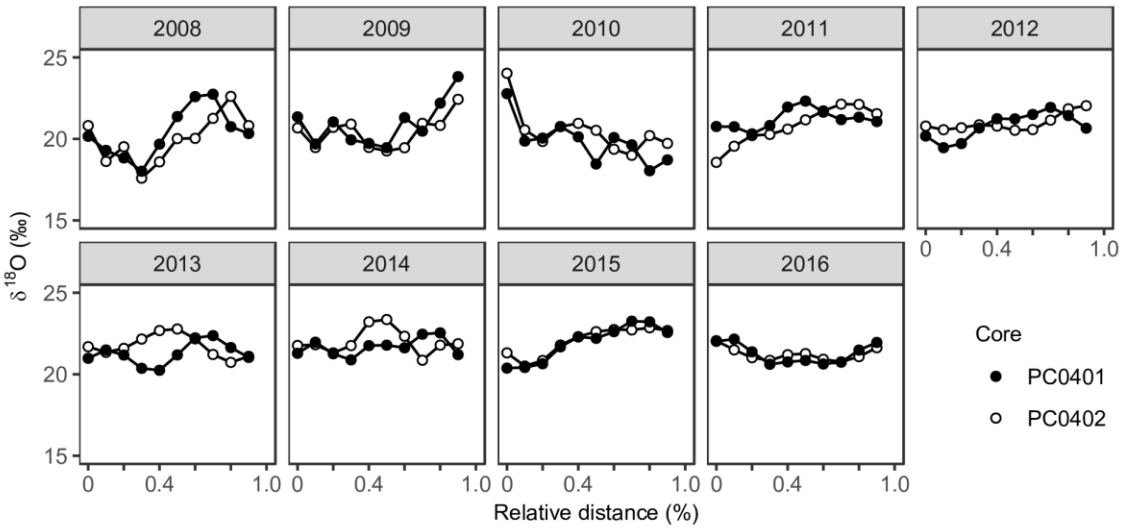

Fig. 5.8 Intra-annual variation of xylem $\delta^{18}O$ in *P. canescens*. Values are plotted against relative distance from the ring boundary.

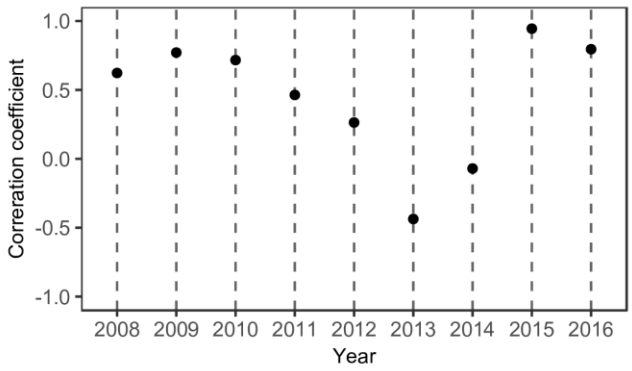

Fig. 5.9 Correlation of intra-annual variation in xylem $\delta^{18}O$ between two cores (PC0401 and PC0402), collected from the same tree of *P. canescens* tree (PC04)

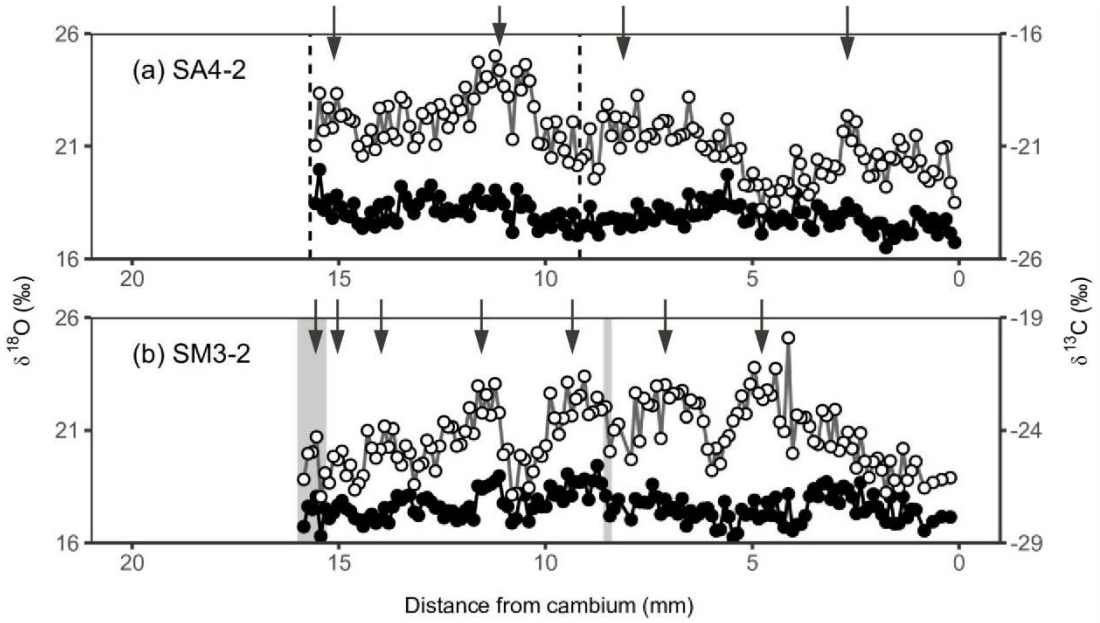

Fig. 5.10 Radial variation of stable carbon (filled circle) and oxygen (open circle) isotope ratio of *Shorea acuminata* (SA4-2) and *Shorea macroptera* (SM3-2) in AHFR. Vertical dashed lines indicate the positions of tissues produced by DC pulse markings (October 2014 and March 2016). The marking positions of SM3-2 (gray shade) were estimated based on other core samples (SM3-1) of the same tree because tissues produced by DC pulse marking were not observed in SM3-2. Black allows indicate positive peaks of $\delta^{18}O$. Samples were collected in December 2017.

Conclusions

In this study, the author discussed the application of $\delta^{18}O$ to tree ring study in tropical region. The conclusions are follows.

The necessity of extracting α-cellulose for xylem $\delta^{18}O$ analysis was tested in Chapter 1. The author concluded that α-cellulose extraction is unnecessary for the purpose of growth ring detection. Xylem $\delta^{18}O$ of bulk sample, not α-cellulose, was analyzed in the following chapter and skipping α-cellulose extraction step greatly reduced the analytical time and labor of $\delta^{18}O$ measurement.

In Chapter 2, whether precipitation $\delta^{18}O$ has a certain annual trend and the trend is recorded in xylem $\delta^{18}O$ was examined using *T. grandis* which forms visible annual rings in seasonally dry forests in northeast Thailand. Precipitation $\delta^{18}O$ has a decreasing trend from spring to summer during research period from 2015 to 2018, and this trend seems to be a typical pattern in northeast Thailand. Xylem $\delta^{18}O$ of *T. grandis* had negative peaks at growth boundaries, and the decreasing part observed in the later growth of each year would reflect the decreasing trend of precipitation $\delta^{18}O$ from spring to summer. Thus, radial cycle of xylem $\delta^{18}O$ could be interpreted as one year's growth of trees in this study site, even if they do not have visible growth rings.

The applicability of high-voltage DC pulse marking was tested for trees without visible growth rings in seasonally dry forests and tropical rainforest in Chapter 3. The sensitivity to the DC pulse marking was different between two sites, and between seasons. DC pulse marking failed to inscribe marks in some trees in the seasonally dry forests, whereas the marking successfully inscribed marks in almost all studied trees in the tropical rainforest. It seems that cambial activity of trees in the tropical rain forest is more active than that in the seasonally dry forest and the difference affected the successful rate of the marking. Affected tissues were similar to those reported in the previous studies in a temperate forest; thin walled wood fiber, deformed ray parenchyma, and crushed vessel. In addition to these, cell deposit was observed in trees in the tropical rainforest. Reaction to DC pulse marking would be various depending on species; for example, traumatic resin canals in *Shorea* spp.. It is necessary to examine suitable condition and species for DC pulse marking.

Growth ring detection using xylem $\delta^{18}O$ variation was tested for trees without visible growth ring in seasonally dry forests in Chapter 4. Assuming that seasonal variation of precipitation $\delta^{18}O$ was recorded in trees grown in the same site in the same way, growth boundaries of trees without visible ring were detectable from xylem $\delta^{18}O$ variation and the result was not contradicted to the result of DC pulse marking. As a tree ring proxy, $\delta^{18}O$ would be reliable in this region, but more case study is needed.

Trees in a tropical rainforest have more complex xylem $\delta^{18}O$ pattern compared to those in seasonally dry forest probably because poor seasonality in precipitation and source water $\delta^{18}O$ (Chapter 5). Although radial variation of xylem $\delta^{18}O$ was similar in *P. canescense*, long-term observation about climate, source water, and phenology is needed to apply seasonal variation of xylem $\delta^{18}O$ to growth ring detection.

There are several methods for growth ring detection, but none of them are applicable globally. Xylem $\delta^{18}O$ has have valuable information for tree ring research both in temperate and tropical regions.

However, to interpret the information adequately, other information as anatomy or phenology is indispensable. Combining plural methods based on different discipline and accumulated knowledge on climate and forest will develop the dendrochronology in tropics.

Acknowledgments

The author would like to express his deepest gratitude to Assoc. Prof. Naoki Okada (Kyoto University) for his inestimable comments and suggestions throughout this study. Special thanks also go to Prof. Akira Osawa (Kyoto University) whose comments made enormous contribution to this study. The author extends special thanks to Prof. Keiji Takabe (Kyoto University) and Prof. Yoshiko Kosugi (Kyoto University) who assumed the examiner for this thesis.

The author wishes to sincerely thank Dr. Amir Affan Bin Abdul Azim (University Putra Malaysia), Dr. Masaki Sano (Waseda University / Research Institute for Humanity and Nature), Prof. Takeshi Nakatsuka (Research Institute for Humanity and Nature) who gave him invaluable comments and warm encouragements,

The author is grateful to Mr. Taksin Artchawakom, Dr. Surachit Waengsothrn (Sakaerat Environmental Research Station) for allowing him to conduct field research and providing great support.

The stable isotope analysis was greatly assisted by Dr. Shinta Ohashi (Forest and Forestry Products and Research Institute), Dr. Shiho Yabusaki, Dr. Akane Tsushima (Research Institute for Humanity and Nature). The field experiments were greatly assisted by many staff of Sakaerat Environmental Research Station.

The author is also grateful to Assist. Prof. Masako Dannoura, Dr. Mioko Ataka, and all the members who shared precious time in the Forest Utilization Seminar.

Finally, the author would like to thank the Japan Society for the Promotion of Science (JSPS) for a grant that made it possible to complete this study.

References

Abdul Azim AA, Okada N. 2014. Occurrence and anatomical features of growth rings in tropical rainforest trees in Peninsular Malaysia: a preliminary study. *Tropics* 23: 15–31. doi: 10.3759/tropics.23.15

Barbour MM, Andrews TJ, Farquhar GD. 2001. Correlations between oxygen isotope ratios of wood constituents of *Quercus* and *Pinus* samples from around the world. *Functional Plant Biology* 28: 335–348. doi: 10.1071/PP00083

Battipaglia G, Jäggi M, Saurer M, Siegwolf RTW, Cotrufo MF. 2008. Climatic sensitivity of $\delta^{18}O$ in the wood and cellulose of tree rings: Results from a mixed stand of *Acer pseudoplatanus* L. and *Fagus sylvatica* L. *Palaeogeography, Palaeoclimatology, Palaeoecology* 261: 193–202. doi: 10.1016/j.palaeo.2008.01.020

Bégin C, Gingras M, Savard MM, Marion J, Nicault A, Bégin Y. 2015. Assessing tree-ring carbon and oxygen stable isotopes for climate reconstruction in the Canadian northeastern boreal forest. *Palaeogeography, Palaeoclimatology, Palaeoecology* 423: 91–101. doi: 10.1016/j.palaeo.2015.01.021

Bhattacharyya A, Yadav RR, Borgaonkar HP, Pant GB. 1992. Growth-ring analysis of Indian tropical trees: dendroclimatic potential. Curr. Sci. 62:736–741.

Cheesman AW, Cernusak LA, Meinzer F. 2017. Infidelity in the outback: Climate signal recorded in $\Delta^{18}O$ of leaf but not branch cellulose of eucalypts across an Australian aridity gradient. *Tree Physiology* 37: 554–564. doi: 10.1093/treephys/tpw121

Colombaroli D, Cherubini P, De Ridder M, Saurer M, Toirambe B, Zweifel N, Beeckman H. 2016. Stable carbon and oxygen isotopes in tree rings show physiological responses of Pericopsis elata to precipitation in the Congo Basin. *Journal of Tropical Ecology* 1–13. doi: 10.1017/S0266467416000134

Cullen LE, Grierson PF. 2006. Is cellulose extraction necessary for developing stable carbon and oxygen isotopes chronologies from *Callitris glaucophylla*? *Palaeogeography, Palaeoclimatology, Palaeoecology* 236: 206–216. doi: 10.1016/j.palaeo.2005.11.003

Cullen LE, Macfarlane C. 2005. Comparison of cellulose extraction methods for analysis of stable-isotope ratios of carbon and oxygen in plant material. *Tree physiology* 25: 563–69.

Dansgaard W. 1964. Stable isotopes in precipitation. Tellus. doi: 10.3402/tellusa.v16i4.8993

Gardner S, Sidisunthorn P, Anusarnsunthorn V. 2000. A field guide to forest trees of northern Thailand. Kobfai Publishing Project, Bangkok

Gazis C, Feng X. 2004. A stable isotope study of soil water: evidence for mixing and preferential flow paths. *Geoderma* 119: 97–111. doi: 10.1016/S0016-7061(03)00243-X

Gori Y, Wehrens R, Greule M, Keppler F, Ziller L, La Porta N, Camin F. 2013. Carbon, hydrogen and oxygen stable isotope ratios of whole wood, cellulose and lignin methoxyl groups of *Picea abies* as climate proxies. *Rapid Communications in Mass Spectrometry* 27: 265–275. doi: 10.1002/rcm.6446

Harada M, Watanabe Y, Nakatsuka T, Tazuru Mizuno S, Horikawa Y, Sugiyama J, Tsuda T, Tagami T. 2014. Alpha-cellulose extraction procedure for the tropical tree sungkai (*Peronema canescens* Jack)

by using an improved vessel for reliable paleoclimate reconstruction. *Geochemical Journal* 48: 299–307. doi: 10.2343/geochemj.2.0306

Harada M, Watanabe Y, Nakatsuka T, Tazuru-Mizuno S, Horikawa Y, Subiyanto B, Sugiyama J, Tsuda T, Tagami T. 2017. Assessment of sungkai tree-ring $\delta^{18}O$ proxy for paleoclimate reconstruction in western Java, Indonesia. *Quaternary International* 432: 33–38. doi: 10.1016/j.quaint.2015.03.038

He Y, Pang H, Theakstone WH, Zhang Z, Lu A, Gu J. 2006. Isotopic variations in precipitation at Bangkok and their climatological significance. *Hydrological Processes* 20: 2873–2884. doi: 10.1002/hyp.6139

Helle G, Schleser GH. 2004. Beyond CO_2-fixation by Rubisco - an interpretation of $^{13}C/^{12}C$ variations in tree rings from novel intra-seasonal studies on broad-leaf trees. *Plant, Cell and Environment* 27: 367–380. doi: 10.1111/j.0016-8025.2003.01159.x

Hietz P, Horsky M, Prohaska T, Lang I, Grabner M. 2015. High-resolution densitometry and elemental analysis of tropical wood. *Trees* 29: 487–497. doi: 10.1007/s00468-014-1126-7

Huang GH, Liang KN, Zhou ZZ, Xu JM, Ma HM. 2015. Genetic variation and origin of teak (*Tectona grandis* L.f.) native and introduced provenances. *Silvae Genetica* 64: 33–46. doi: 10.1515/sg-2015-0003

IAEA/WMO. 2016. *Global network of isotopes in precipitation. The GNIP Database*. http://www.iaea.org/water. (accessed 2016 June 16).

Imagawa H. 1985. Marking Method by Electrical Stimulation for Studying Xylem Formation IV： Occurring Area of the Crushed Tracheids. *Research bulletin of the Hokkaido University Forests* 42: p585-594.

Imagawa H, Ishida S. 1981. New Marking Method by Electrical Stimulation for Studying Xylem Formation. *Research bulletin of the Hokkaido University Forests* 38: 241–248.

Imagawa H, Ishida S. 1983. New Marking Method by Electrical Stimulation for Studying Xylem Formation II： Application to Broad-leaved Trees. *Research bulletin of the Hokkaido University Forests* 40: 387–395.

Ingraham NL. 1998. Chapter 3 - Isotopic Variations in Precipitation. In: Kendall C, McDonnell JJ (eds) *Isotope Tracers in Catchment Hydrology*. Elsevier, Amsterdam, 87–118.

Ishida A, Yamazaki J-Y, Harayama H, Yazaki K, Ladpala P, Nakano T, Adachi M, Yoshimura K, Panuthai S, Staporn D, Maeda T, Maruta E, Diloksumpun S, Puangchit L. 2014. Photoprotection of evergreen and drought-deciduous tree leaves to overcome the dry season in monsoonal tropical dry forests in Thailand. *Tree Physiology* 34: 15–28. doi: 10.1093/treephys/tpt107

Johnstone JA, Roden JS, Dawson TE. 2013. Oxygen and carbon stable isotopes in coast redwood tree rings respond to spring and summer climate signals. *Journal of Geophysical Research: Biogeosciences* 118: 1438–1450. doi: 10.1002/jgrg.20111

Kagawa A, Sano M, Nakatsuka T, Ikeda T, Kubo S. 2015. An optimized method for stable isotope analysis of tree rings by extracting cellulose directly from cross-sectional laths. *Chemical Geology* 393–394: 16–25. doi: 10.1016/j.chemgeo.2014.11.019

Krepkowski J, Gebrekirstos A, Shibistova O, Bräuning A. 2013. Stable carbon isotope labeling reveals different carry-over effects between functional types of tropical trees in an Ethiopian mountain forest. *New phytologist* 199: 441–51. doi: 10.1111/nph.12266

Kurokawa H, Yoshida T, Nakamura T, Lai J, Nakashizuka T. 2003. The age of tropical rain-forest canopy species, Borneo ironwood (Eusideroxylon zwageri), determined by ^{14}C dating. *Journal of Tropical Ecology* 19: 1–7. doi: 10.1017/S0266467403003018

Liu X, Zeng X, Leavitt SW, Wang W, An W, Xu G, Sun W, Wang Y, Qin D, Ren J. 2013. A 400-year tree-ring $\delta^{18}O$ chronology for the southeastern Tibetan Plateau: Implications for inferring variations of the regional hydroclimate. *Global and Planetary Change* 104: 23–33. doi: 10.1016/j.gloplacha.2013.02.005

Loader NJ, Robertson I, Barker AC, Switsur VR, Waterhouse JS. 1997. An improved technique for the batch processing of small wholewood samples to α-cellulose. *Chemical Geology* 136: 313–317. doi: 10.1016/S0009-2541(96)00133-7

Loader NJ, Robertson I, McCarroll D. 2003. Comparison of stable carbon isotope ratios in the whole wood, cellulose and lignin of oak tree-rings. *Palaeogeography, Palaeoclimatology, Palaeoecology* 196: 395–407. doi: 10.1016/S0031-0182(03)00466-8

Managave SR, Sheshshayee MS, Bhattacharyya A, Ramesh R. 2011. Intra-annual variations of teak cellulose $\delta^{18}O$ in Kerala, India: Implications to the reconstruction of past summer and winter monsoon rains. *Climate Dynamics* 37: 555–567. doi: 10.1007/s00382-010-0917-9

Managave SR, Sheshshayee MS, Borgaonkar HP, Ramesh R. 2010. Intra-annual oxygen isotope variations in central Indian teak cellulose: Possibility of improved resolution for past monsoon reconstruction. *Current Science* 98: 930–937.

Marryanna L, Kosugi Y, Itoh M, Noguchi S, Takanashi S, Katsuyama M, Tani M, Siti-Aisah S. 2017. Temporal Variation In The Stable Isotopes In Precipitation Related To The Rainfall Pattern In A Tropical Rainforest In Peninsular Malaysia. *JOURNAL OF TROPICAL FOREST SECIENCE* 29: 349–362. doi: 10.26525/jtfs2017.29.3.349362

McCarroll D, Loader NJ. 2004. Stable isotopes in tree rings. *Quaternary Science Reviews* 23: 771–801. doi: 10.1016/j.quascirev.2003.06.017

Mischel M, Esper J, Keppler F, Greule M, Werner W. 2015. $\delta^{2}H$, $\delta^{13}C$ and $\delta^{18}O$ from whole wood, α-cellulose and lignin methoxyl groups in *Pinus sylvestris* : a multi-parameter approach. *Isotopes in Environmental and Health Studies* 51: 553–568. doi: 10.1080/10256016.2015.1056181

Muangsong C, Cai B, Pumijumnong N, Hu C, Lei G. 2016. Intra-seasonal variability of teak tree-ring cellulose $\delta^{18}O$ from northwestern Thailand: A potential proxy of Thailand summer monsoon rainfall. *The Holocene* 26: 1397–1405. doi: 10.1177/0959683616640045

Nabeshima E, Nakatsuka T, Kagawa A, Hiura T, Funada R. 2018. Seasonal changes of δD and $\delta^{18}O$ in tree-ring cellulose of Quercus crispula suggest a change in post-photosynthetic processes during earlywood growth. *Tree Physiology* 1–12. doi: 10.1093/treephys/tpy068

Nakai W, Okada N, Sano M, Nakatsuka T. 2018. Sample preparation of ring-less tropical trees for $\delta^{18}O$

measurement in isotope dendrochronology. *Tropics* 27: 49–58. doi: https://doi.org/10.3759/tropics.MS17-09

Nakatsuka T, Ohnishi K, Hara T, Sumida A, Mitsuishi D, Kurita N, Uemura S. 2004. Oxygen and carbon isotopic ratios of tree-ring cellulose in a conifer-hardwood mixed forest in northern Japan. *Geochemical Journal* 38: 77–88.

National Climatic Data Center. 2017. *Climate Date Online*. https://www.ncdc.noaa.gov/cdo-web/. (accessed 2017 March 24).

Nobuchi T, Ogata Y, Siripatanadilok S. 1995. Seasonal characteristics of wood formation in Hopea odorata and Shorea henryana. *IAWA journal* 16: 361–369.

Ogata K, Fujii T, Abe H, Baas P. 2008. Identification of the timbers of Southeast Asia and the Western Pacific. Kaiseisha Press

Ohashi S, Durgante FM, Kagawa A, Kajimoto T, Trumbore SE, Xu X, Ishizuka M, Higuchi N. 2016. Seasonal variations in the stable oxygen isotope ratio of wood cellulose reveal annual rings of trees in a Central Amazon terra firme forest. *Oecologia* 180: 685–696. doi: 10.1007/s00442-015-3509-x

Ohashi S, Okada N, Abdul Azim AA, Siripatanadilok S, Veenin T, Yahya AZ, Nobuchi T. 2014. Vessel feature changes as a tool for detecting annual rings in tropical trees. *Trees* 28: 137–149. doi: 10.1007/s00468-013-0936-3

Ohashi S, Okada N, Nobuchi T, Siripatanadilok S, Veenin T. 2009. Detecting invisible growth rings of trees in seasonally dry forests in Thailand: isotopic and wood anatomical approaches. *Trees* 23: 813–822. doi: 10.1007/s00468-009-0322-3

Palakit K, Siripattanadilok S, Duangsathaporn K. 2012. False ring occurrences and their identification in teak (*Tectona grandis*) in north-eastern Thailand. *Journal of Tropical Forest Science* 24: 387–398.

Pedregosa F, Varoquaux G, Gramfort A, Michel V, Thirion B, Grisel O, Blondel M, Prettenhofer P, Weiss R, Dubourg V, Vanderplas J, Passos A, Cournapeau D, Brucher M, Perrot M, Duchesnay E. 2011. Scikit-learn: Machine Learning in Python. *Journal of Machine Learning Research* 12: 2825–2830.

Pettersen RC. 1984. The Chemical Composition of Wood. In: Rowell R (ed) *The chemistry of solid wood*. American Chemical Society, Washington, 57–126.

Pons TL, Helle G. 2011. Identification of anatomically non-distinct annual rings in tropical trees using stable isotopes. *Trees* 25: 83–93. doi: 10.1007/s00468-010-0527-5

Poussart PF, Evans MN, Schrag DP. 2004. Resolving seasonality in tropical trees: multi-decade, high-resolution oxygen and carbon isotope records from Indonesia and Thailand. *Earth and Planetary Science Letters* 218: 301–316. doi: 10.1016/S0012-821X(03)00638-1

Poussart PF, Schrag D. 2005. Seasonally resolved stable isotope chronologies from northern Thailand deciduous trees. *Earth and Planetary Science Letters* 235: 752–765. doi: 10.1016/j.epsl.2005.05.012

Poussart PM, Myneni SCB, Lanzirotti A. 2006. Tropical dendrochemistry: A novel approach to estimate age and growth from ringless trees. *Geophysical Research Letters* 33: L17711. doi: 10.1029/2006GL026929

Pumijumnong N, Eckstein D, Sass U. 1995. Tree-Ring Research on Tectona Grandis in Northern Thailand.

IAWA Journal 16: 385–392. doi: 10.1163/22941932-90001428

Ram S, Borgaonkar HP, Sikder AB. 2008. Tree-ring analysis of teak (*Tectona grandis* L.F.) in central India and its relationship with rainfall and moisture index. *Journal of Earth System Science* 117: 637–645. doi: 10.1007/s12040-008-0058-2

Roden JS, Lin G, Ehleringer JR. 2000. A mechanistic model for interpretation of hydrogen and oxygen isotope ratios in tree-ring cellulose. *Geochimica et Cosmochimica Acta* 64: 21–35. doi: 10.1016/S0016-7037(99)00195-7

Rozendaal DM a., Zuidema P a. 2011. Dendroecology in the tropics: a review. *Trees* 25: 3–16. doi: 10.1007/s00468-010-0480-3

Sakaerat Environmental Research Station. 2016. *Meteorological Information of Sakaerat Environmental Research Station*. http://sakaeratsers.weebly.com/358636573629361736413621362936403605364036093636361836173623636360736183634.html. (accessed 2016 September 27).

Sakaerat Environmental Research Station. 2018. *Meteorological Information of Sakaerat Environmental Research Station*. http://sakaeratsers.weebly.com/358636573629361736413621362936403605364036093636361836173623636360736183634.html. (accessed 2018 December 12).

Sano M, Xu C, Nakatsuka T. 2012. A 300-year Vietnam hydroclimate and ENSO variability record reconstructed from tree ring $\delta^{18}O$. *Journal of Geophysical Research: Atmospheres* 117: D12115. doi: 10.1029/2012JD017749

Sass U, Killmann W, Eckstein D. 1995. Wood formation in two species of Dipterocarpaceae in peninsular Malaysia. *IAWA journal* 16: 371–384.

Schollaen K, Heinrich I, Neuwirth B, Krusic PJ, D'Arrigo RD, Karyanto O, Helle G. 2013. Multiple tree-ring chronologies (ring width, $\delta^{13}C$ and $\delta^{18}O$) reveal dry and rainy season signals of rainfall in Indonesia. *Quaternary Science Reviews* 73: 170–181. doi: 10.1016/j.quascirev.2013.05.018

Shiokura T. 1989. A Method to Measure Radial Incremenf in Tropical Trees. *IAWA Journal* 10: 147–154.

Stahle D., Mushove P., Cleaveland M., Roig F, Haynes G. 1999. Management implications of annual growth rings in Pterocarpus angolensis from Zimbabwe. *Forest Ecology and Management* 124: 217–229. doi: 10.1016/S0378-1127(99)00075-4

Szymczak S, Joachimski MM, Bräuning A, Hetzer T, Kuhlemann J. 2011. Comparison of whole wood and cellulose carbon and oxygen isotope series from *Pinus nigra* ssp. *laricio* (Corsica/France). *Dendrochronologia* 29: 219–226. doi: 10.1016/j.dendro.2011.04.001

Tayasu I, Hirasawa R, Ogawa NO, Ohkouchi N, Yamada K. 2011. New organic reference materials for carbon- and nitrogen-stable isotope ratio measurements provided by Center for Ecological Research, Kyoto University, and Institute of Biogeosciences, Japan Agency for Marine-Earth Science and Technology. *Limnology* 12: 261–266. doi: 10.1007/s10201-011-0345-5

Verheyden A, Helle G, Schleser GH, Dehairs F, Beeckman H, Koedam N. 2004. Annual cyclicity in high-resolution stable carbon and oxygen isotope ratios in the wood of the mangrove tree *Rhizophora*

mucronata. *Plant, Cell and Environment* 27: 1525–1536. doi: 10.1111/j.1365-3040.2004.01258.x

Weigt RB, Bräunlich S, Zimmermann L, Saurer M, Grams TEE, Dietrich H-P, Siegwolf RTW, Nikolova PS. 2015. Comparison of $\delta^{18}O$ and $\delta^{13}C$ values between tree-ring whole wood and cellulose in five species growing under two different site conditions. *Rapid Communications in Mass Spectrometry* 29: 2233–2244. doi: 10.1002/rcm.7388

Wilson AT, Grinsted MJ. 1977. $^{12}C/^{13}C$ in cellulose and lignin as palaeothermometers. *Nature* 265: 133–135. doi: 10.1038/265133a0

Wolter KE. 1968. Notes: A New Method for Marking Xylem Growth. *Forest Science* 14: 102–104.

Worbes M. 2002. One hundred years of tree-ring research in the tropics – a brief history and an outlook to future challenges. *Dendrochronologia* 20: 217–231. doi: 10.1078/1125-7865-00018

Worbes M. 1995. How to measure growth dynamics in tropical trees a review. *IAWA Journal* 16: 337–351.

Worbes M. 1999. Annual growth rings, rainfall-dependent growth and long-term growth patterns of tropical trees from the Caparo Forest Reserve in Venezuela. *Journal of Ecology* 87: 391–403. doi: 10.1046/j.1365-2745.1999.00361.x